Discovery, Synthesis and Biological Evaluation of Small-Molecule Inhibitors of Toll-like Receptor Signaling Pathways

by

Shuting Zhang

M.S., Beijing Normal University, China, 2009
B.S., Beijing Normal University, China, 2006

A thesis submitted to the

Faculty of the Graduate School of the

University of Colorado in partial fulfillment

of the requirement for the degree of

Doctor of Philosophy

Department of Chemistry & Biochemistry

2014

This thesis entitled:
Discovery, Synthesis and Biological Evaluation of Small-Molecule Inhibitors of Toll-like Receptor Signaling Pathways
written by Shuting Zhang
has been approved for the Department of Chemistry & Biochemistry

_____
Dr. Hang H. Yin

_____
Dr. Zhongping Tan

Date_____

The final copy of this thesis has been examined by the signatories, and we find that both the content and the form meet acceptable presentation standards of scholarly work in the above mentioned discipline.

Abstract

Zhang, Shuting

(Ph.D., Department of Chemistry & Biochemistry)

Discovery, Synthesis and Biological Evaluation of Small-Molecule Inhibitors of Toll-like Receptor Signaling Pathways

Thesis directed by Professor Hang Hubert Yin

Toll-like receptors (TLRs) are essential to the innate immune system. These receptors help drive inflammatory responses, host defense, and adaptive immune responses upon detection of invading microorganisms. Small molecules capable of targeting TLR signaling are of considerable interest as potential therapeutic agents for the treatment of human inflammatory diseases and cancers that are caused by dysregulation of TLR signaling. The goal of this doctoral dissertation research is to identify small-molecule modulators of TLR signaling via high-throughput screening (HTS) approach followed by structure-activity relationship (SAR) studies.

Chapter 1 is an overview of the current knowledge of TLRs, including their structures and functions, signaling pathways, as well as their roles in inflammatory diseases and cancer. The current status of TLR agonists and antagonists in clinical studies is also summarized.

Chapter 2 focuses on the development of a new family of TLR4 signaling inhibitors, identified from a cell-based screening. A series of arylidene malonate analogs were synthesized and assayed in murine macrophages for their inhibitory activity against LPS-induced nitric oxide (NO) production. The lead compound, **1** (**NCI126224**), was found to suppress LPS-induced production of nuclear factor-kappaB (NF-κB), tumor necrosis factor (TNF-α), interleukin-1β (IL-1β), and nitric oxide (NO) in the nanomolar to low micromolar range.

Chapter 3 describes a high-throughput compound library screening to identify novel TLR8 signaling antagonists. The Maybridge Hitfinder library of 14,400 compounds was screened using SEAP reporter cells expressing TLR8. The screen yielded thirteen novel TLR8 signaling specific inhibitors. Structure-activity relationship investigation and biological evaluation were mainly focused on one hit **40-D4** with a pyrazolo[1,5-*a*]pyrimidine scaffold. Two lead compounds, **8m** and **4m**, were identified with nanomolar potencies inhibiting TLR8 signaling. Further biological evaluation indicates that **8m** specifically inhibits TLR8 signaling without affecting other TLRs. **8m** also suppresses TLR8 induced proinflammatory cytokine and cytokine mRNA levels. These finding suggests that these compounds may have therapeutic applications in the treatment of TLR8-related inflammatory diseases.

Chapter 4 described a study which utilized both *in silico* and cell-based screening to identify agonists and antagonists of TLR5 signaling. One potential TLR5 signaling inhibitor was identified from cell-based HTS.

Chapter 5 summarizes the major findings of this dissertation research, illustrates the potential of the identified small-molecule suppressors, and explores future research directions for understanding the mechanism of these TLR inhibitors.

To my beloved family

Acknowledgments

This dissertation marks the end of a major educational journey that I started more than twenty years ago. Therefore, it is an important milestone in my life. I owe a huge debt of gratitude to many people who warmly helped and supported me in different ways during my PhD study in Boulder.

I would like to express my sincere gratitude to my advisor Dr. Hang Hubert Yin for taking me as his student, and patiently guiding me. I am grateful for his support, excellent mentorship, direction, encouragement, and tireless patience with me throughout the years' PhD training in his laboratory.

I sincerely thank my doctoral committee members Dr. Linda Watkins, Dr. Xuedong Liu, Dr. Xiang Wang and Dr. Zhongping Tan for kindly agreeing to serve on my dissertation committee. Their helpful comments and discussions were essential for the completion of my thesis.

I am grateful to the technical support from all the staff members in CU Boulder. I thank Dr. Wei Wang in the High-Throughput Screening Core Facility, Dr. Richard Shoemaker in the NMR Facility and Theresa Nahreini in Cell Culture Facility for their help with the instruments and training.

All the current and former Yin lab members have contributed greatly to my personal and professional time in CU. The group has been a source of friendship as well as good advices and collaborations. Especially thank Dr. Xiaohui Wang, Dr. Kui Cheng, and Dr. Lei Zhang for their valuable discussion, sharing their knowledge with me and help in my research that benefits me a lot. My thanks also go to other previous and current group members. It was my great pleasure to know and work with you all.

I would like to thank the Department of Chemistry and Biochemistry, University of Colorado Boulder, my fellowship from China Scholarship Council and the funding from National Institute of Health, and the National Science Foundation for supporting my research.

Last but not least, I would like to thank my parents, my late father Haofeng Zhang and my mother Jingqin Yin, for their love, support and encouragement throughout my whole life. It was my father's wish to see me with a doctorate degree, if he were still alive, he would be very proud. I also would like to thank my little brother Xinpeng Zhang for supporting me and believing in me.

Contents

List of Tables

Table

List of Figures

Figure

List of Schemes

Scheme

List of Abbreviations

Å	Angstrom
APC	antigen presenting cells
aq	aqueous
Boc	*tert*-butyloxycarbonyl
$CHCl_3$	chloroform
COX-2	cyclooxygenase-2
DAMP	damage-associated molecular pattern
DCM	dichloromethane
DD	death domain
DMEM	Dulbecco's modified eagle's medium
DMF	dimethylformamide
DMF-DMA	dimethylformamide dimethylacetal
DMSO	dimethyl sulfoxide
EBV	Epstein-Barr virus
ECD	ectdomain
ELISA	enzyme-linked immunosorbent assay
FBS	fetal bovine serum
FP	fluorescence polarization
Glide	grid-based ligand docking with energetics

HEK	human embryonic kidney
HPLC	high pressure liquid chromatography
HTS	high throughput screening
HTVS	high-throughput virtual screening
IBD	inflammatory bowel disease
IC_{50}	half maximal inhibitory concentration
IL-1β	interleukin-1beta
iNOS	inducible nitric oxide synthase
IRAK4	interleukin-1 receptor-associated kinase 4
IRFs	IFN regulatory factors
Kd	dissociation constant
kD	kilodalton
LPS	lipopolysaccharide
LRR	leucine-rich repeat
M	molar
MAL	MyD88-adaptor-like
MAPKs	mitogen-activated protein kinases
MCP-1	monocyte chemoattractant protein 1
*m*CPBA	*meta*-chloroperoxybenzoic acid
MD-2	myeloid differentiation factor 2
min	minutes
MLA	Monophosphoryl lipid A

mol	mole
MyD88	myeloid differentiation factor 88
NaCl	sodium chloride
NaOH	sodium hydroxide
NF-κB	nuclear factor κB
nm	nanometer
NO	nitric oxide
NOD	nucleotide-binding oligomerization proteins
PAMP	pathogen-associated molecular pattern
PBS	phosphate buffered saline
PDB	protein data bank
pDCs	plasmacytoid dendritic cells
PRR	pattern-recognition receptor
RIP1	receptor-interacting protein kinase 1
RMS	root mean square
RMSD	root mean square deviation
RPMI	Roswell Park Memorial Institute
RT-PCR	real-time polymerase chain reaction
SAR	structure-activity relationship
SEAP	Secreted embryonic alkaline phosphatase
SLE	systemic lupus erythematosus
SNP	single-nucleotide polymorphism

SP	standard precision
ssRNA	single-stranded RNA
THF	tetrahydrofuran
TIR	Toll-IL-1R (Interleukin-1-Receptor)
TLC	thin-layer chromatography
TLR	toll-like receptors
TMD	transmembrane domain
TNF-α	tumor necrosis factor-α
TRAF6	TNF receptor-associated factor 6
TRAM	TRIF-related adaptor molecule
TRIF	TIR-domain-containing adaptor protein inducing IFNβ
XP	extra precision

CHAPTER 1

Introduction

1. 1 Innate and adaptive immunity

The immune system is an intact network of cells, tissues, organs and cytokines that work together to protect the body against infection and to eliminate diseases from the host. The immune system is typically divided into two categories –innate and adaptive systems, determined by the speed and specificity of the reaction.[1]

The adaptive immune responses are carried out by lymphocytes. There are two classes of such responses, antibody responses and cell-mediated immune responses, and they are carried out by B lymphocytes and T lymphocytes, respectively. In antibody responses, the antigen activated B cells produce antibodies. The antibodies circulate in the blood stream, permeate other body fluids and bind specifically to pathogens and foreign antigens. Antibody binding inactivates viruses or bacterial toxins by blocking their ability to bind to receptors on the surface of the host cells.

In cell-mediated immune responses, activated T cells attack antigens directly, and destroy diseased and invading cells. The adaptive responses are specific to the particular pathogen that induced them and provide long lasting protection, however,

it takes from 4 to 7 days for them to develop. In this time period, the dangerous organisms could overwhelm the host.[2]

In contrast, the innate immune responses are not pathogen-specific, but they occur more rapidly and stronger to combat the invade threats. Innate immunity provides the first line of host defense against the invading pathogens; it recognizes microorganisms via a limited number of germline-encoded pattern-recognition receptors (PRRs). There are several classes of PRRs including toll-like receptors (TLRs), nucleotide-binding oligomerization proteins (NODs), and mannose receptors. PRRs are activated by structurally conserved pathogen-associated molecular patterns (PAMPs) present in invading microorganisms or by damage-associated molecular patterns (DAMPs) exposed on the surface of, or secreted/released by dying, stressed or injured cells. In most cases, PAMPs recognition by PRRs trigger proinflammatory and antimicrobial responses by activating a multitude of intracellular signaling pathways including adaptor molecules, kinases, and transcription factors. PPR-induced signal transduction pathways eventually result in the expression of proinflammatory cytokines, chemokines, antiviral molecules, and cell-adhering molecules, which together arrange the early host response to the invading microorganisms. Among all the PRRs, the family of TLRs was the first PRRs to be identified, and is also the most extensively studied.[3]

1.2 Toll-like receptors

Toll-like receptors are a class of type I transmembrane PRRs characterized by N-terminal leucine-rich repeats (LRRs) and a transmembrane region followed by a cytoplasmic Toll/IL-1R homology (TIR) domain. The TLR family is a major component of innate immunity; it plays a crucial role in host cell's recognition and response to microbial pathogens. It is reported that TLRs also recognize endogenous ligands, such as DAMPs and induce inflammatory responses in many pathological processes that release DAMPs as a result of cell necrosis and tissue remodeling.[4-6] Thus, the innate immune system is activated by both TLR recognition of PAMPs and DAMPs released after tissue injury or cellular stress.[7]

1.2.1 TLR structures and ligands

To date, 13 murine and 10 human TLRs have been identified;[8] TLR1 to TLR9 are conserved in both species. However, certain TLRs found in humans are not present in all mammals.[9] For example, a gene-encoding analogue to TLR10 in humans is present in mice, but appears to have been damaged by retroviral insertion.[10] On the other hand, TLR11, 12 and 13 are functional in mice, but none of them are present in humans.[11-12]

TLRs are not only expressed in innate immune cells, like monocytes, microglia, and macrophages, but also in non-immune cells including lymphocytes, epithelial cells, and cancer cells.

Table 1-1. Description of the Toll-like receptors family (based on ref. 13-17)

Receptor	Location	Ligand	Origin of the Ligand	Adaptor
1 (with TLR2)	cell membrane	triacyl lipoprotein, modulin	gram positive bacteria	MyD88/ TIRAP
2 (with TLR1 or TLR6)	cell membrane	lipoprotein	gram positive bacteria, fungi, viruses, parasites, self	MyD88/ TIRAP
3	endolysosomal	double-stranded RNA	viruses	TRIF
4	cell membrane endolysosomal	LPS	gram negative bacteria, viruses, self	MyD88/ TIRAP, TRIF/TRAM
5	cell membrane	flagellin	flagellated bacteria	MyD88
6 (with TLR2)	cell membrane	diacyl lipoprotein	gram positive bacteria, viruses, fungi	MyD88/ TIRAP
7	endolysosomal	single-stranded RNA, imidazoquinoline, loxoribine, bropirimine	viruses, bacteria, synthetic compounds	MyD88
8	endolysosomal	single-stranded RNA, imidazoquinoline	viruses, bacteria, synthetic compounds	MyD88
9	Endolysosomal	CpG-DNA	bacteria, viruses, fungi	MyD88
10 (with TLR2)	cell membrane	lipopeptide (prediction)		MyD88
11	endolysosomal	flagellin, profilin	uropathogenic bacteria, profilin-like molecule	MyD88
12	endolysosomal	profilin	parasites	MyD88
13	endolysosomal	23S RNA	bacteria	MyD88

TLRs are localized in distinct cellular compartments. For example, TLR1, TLR2, TLR4, TLR5, TLR6, and TLR11 are located on the cell membrane, whereas TLR3, TLR7, TLR8, TLR9, TLR11, TLR12, and TLR13 are expressed in intracellular vesicles such as the endosome and ER.[18] The Toll-like receptor family

recognizes specific patterns of microbial components and their signal transduction requires different adaptor proteins (**Table 1-1**).

Members of TLR family share a common structure: a leucine-rich repeat (LRR) ectodomain (ECD), a helical transmembrane domain and an intracellular Toll/IL-1 receptor homology (TIR) signaling domain. The N-terminal extracellular ectodomain contains 16-28 LRRs with horseshoe-like shapes that are responsible for the detection and interaction with PAMPs. The LRR module is typically 22-29 residues in length, and contains a conserved "LxxLxLxxN" motif, as well as a variable part.[19-20] In three dimensions, all the LRRs have a common horseshoe-like shape, the hydrophobic core, which is formed by conserved leucines and hydrophobic residues in the variable regions, extends throughout the entire protein. Each LRR protein consists of a concave surface, a convex surface, an ascending lateral surface that consists of loops connecting the ß strand to the convex surface, and a descending lateral surface on the opposite side.[21] In the solved TLR-ligand structures, ligand binding occurs most often in the ascending lateral surface of the TLR-ECD.[19] The C-terminal ends of the TLR ectodomains continue with a typical stretch of approximately 20 uncharged, mostly hydrophobic residues that comprise the protein's transmembrane domain (TMD). The role of the TMD in TLR signaling is still unclear, however its importance for the TLR activation was demonstrated in recent studies. Deletion of the ECD and TIR of TLR4 from the TMD can inhibit its signaling and that TLR4 constructs with the deleted ECD are still constitutively active.[22] Our group has reported that the isolated TMDs of all the TLRs showed

strong homotypic interaction in bacterial membranes and suggested that this short hydrophobic region could play a pivotal role in the dimerization and function of TLRs.[23]

The cytoplasmic tails of the TLR family members end with a highly conserved Toll/Interleukin-1 receptor (TIR) domain. The TIR domain is a key signaling domain for both TLRs and IL-1 receptors, and it requires cytosolic adaptor proteins for downstream signaling.[24] Similar to the TLRs, the adaptor proteins are conserved in many species.[25] TLR signaling involves a family of five adaptor proteins, known as myeloid differentiation factor 88 (MyD88), MyD88-adaptor-like (MAL; also known as TIRAP), TIR-domain-containing adaptor protein inducing IFNß (TRIF; also known as TICAM1), TRIF-related adaptor molecule (TRAM; also known as TICAM2) and sterile-alpha and armadillo-motif containing protein (SARM).[26-27] Most TLRs signal through MyD88, except for TLR3 which signals through TRIF, and TLR4, which signals through both MyD88 and TRIF.[28] TLRs located on the plasma membrane require MAL or TRAM to signal through MyD88 or TRIF respectively.[19, 29] The binding of ligands to the extracellular domains of TLRs induces the dimerization of the receptors (Heterodimerization: TLR2-TLR1, TLR2-TLR6, TLR1/2-TLR10,[30] TLR11-TLR12;[31] Homodimerization: TLR3, TLR4, TLR5, TLR7, TLR8, TLR9, TLR10,[30] TLR11, TLR12 and TLR13), triggers the recruitment of specific adaptor proteins to the intracellular TIR domain, and initiates downstream signaling. The adaptor proteins also contain TIR domains. The TIR-TIR interactions between receptor-receptor, receptor-adaptor, and adaptor-adaptor are important for

signaling.[32]

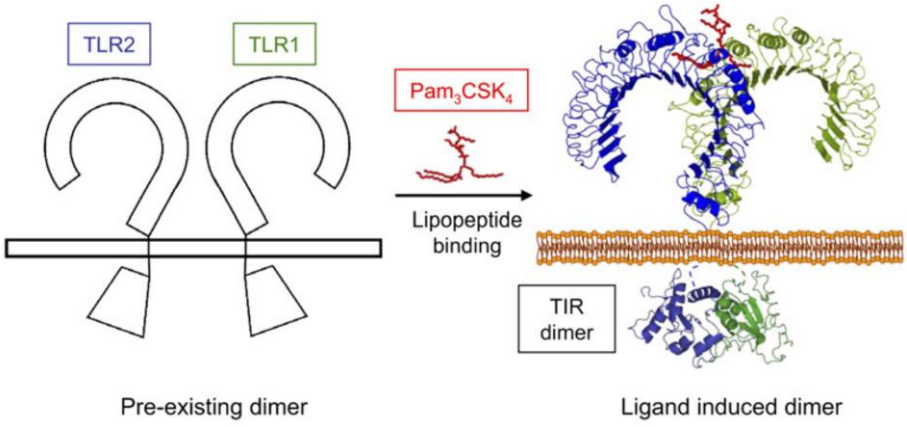

Figure 1-1. Model of ligand-induced dimerization of full-length TLR1/TLR2. Reprinted from *Cell*, Vol. 130, Mi Sun Jin *et al*, Crystal structure of the TLR1-TLR2 heterodimer induced by binding of a tri-acylated lipopeptide, 1071-1082, Copyright 2007, with permission from Elsevier.

The structure of typical ligand-induced TLR dimer is shown in **Figure 1-1**. A number of crystal structures of these TLR-ligand complexes have been solved and are as follows: TLR4-MD2- *E. coli* LPS,[33] TLR3-dsRNA,[34] TLR1-TLR2-triacylated lipopeptide,[35] TLR2-TLR6-diacylated lipopeptide,[36] TLR5-Flagellin,[37] and TLR8-CL097.[38]

In these "m"-shaped complexes, the C termini of the extracellular domains of the TLRs converge in the middle, which suggests the hypothesis that the dimerization of the extracellular domains likewise forces the intracellular TIR domains to dimerize, and thus initiate the signaling by recruiting intracellular adaptor proteins. Several types of m-shaped TLR ligand-binding ectodomains examples are shown in **Figure1-2**.[38]

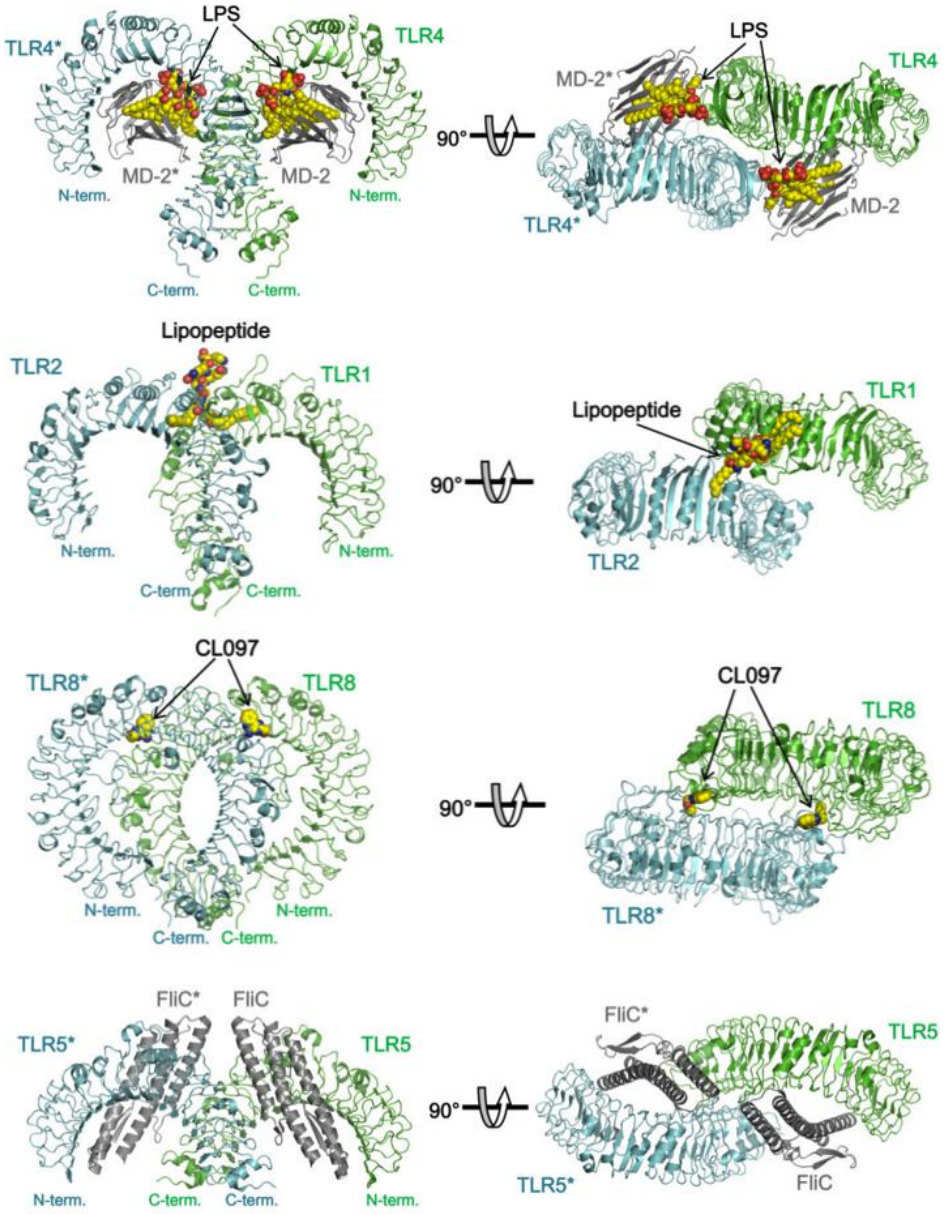

Figure 1-2. The "m" shaped TLR dimers induced by binding of ligands. Front (left panels) and top (right panels) view of the ligand-bound dimer structures of TLR4/MD-2/LPS, TLR1/TLR2/lipopeptide, TLR8/CL097 and TLR5/Flagellin. From Tanji, H. and co-authors, 2013: Structural reorganization of the toll-like receptor 8 dimer induced by agonistic ligands. Science **339**, 1426-1429. Reprinted with permission from AAAS.

Hydrophobic ligands of TLR1, TLR2 and TLR4 interact with the internal protein pockets of the receptors. Flagellin binds directly to the lateral surfaces of

TLR5 in a symmetrical arrangement, while the small molecule TLR8 ligand binds to the dimerization interface of TLR8. For TLR1/2, 2/6, 3, 4 and 5, their solved structures demonstrate that they exist as a monomer in solution and the dimerization takes place only upon ligand binding. Conversely, TLR8 exists as preformed inactive dimers that subsequently change conformation upon ligand binding. For these TLRs, the resulting ligand-induced dimerization subsequently triggers a proinflammatory response to invading pathogens.

1.2.2 TLR downstream signaling pathways

To date, two main TLR signaling pathways are known: the MyD88-dependent signaling pathway and the TRIF-dependent signaling pathway.[39] TLR-induced responses are mainly mediated by three major downstream signaling pathways: nuclear factor κB (NF-κB), mitogen-activated protein kinases (MAPKs), and IFN regulatory factors (IRFs). Whereas NF-κB and MAPKs play central roles in the stimulation of proinflammatory responses, IRFs are essential for induction of IFN production.[40-41] The MyD88-dependent pathway acts via NF-κB to induce proinflammatory cytokines such as interleukin-1beta (IL-1ß) and tumor necrosis factor-α (TNF-α), while the TRIF-dependent pathway proceeds via type I interferons to increase the expression of interferon-inducible genes. Studies have indicated that some features of these pathways are cell type-specific, which define their different immunological properties. For example, plasmacytoid dendritic cells (pDCs) and inflammatory monocytes have unique signaling pathways that regulate the

antiviral responses that are probably absent in other cell types, such as conventional dendritic cells (cDC) and macrophages.[42-43]

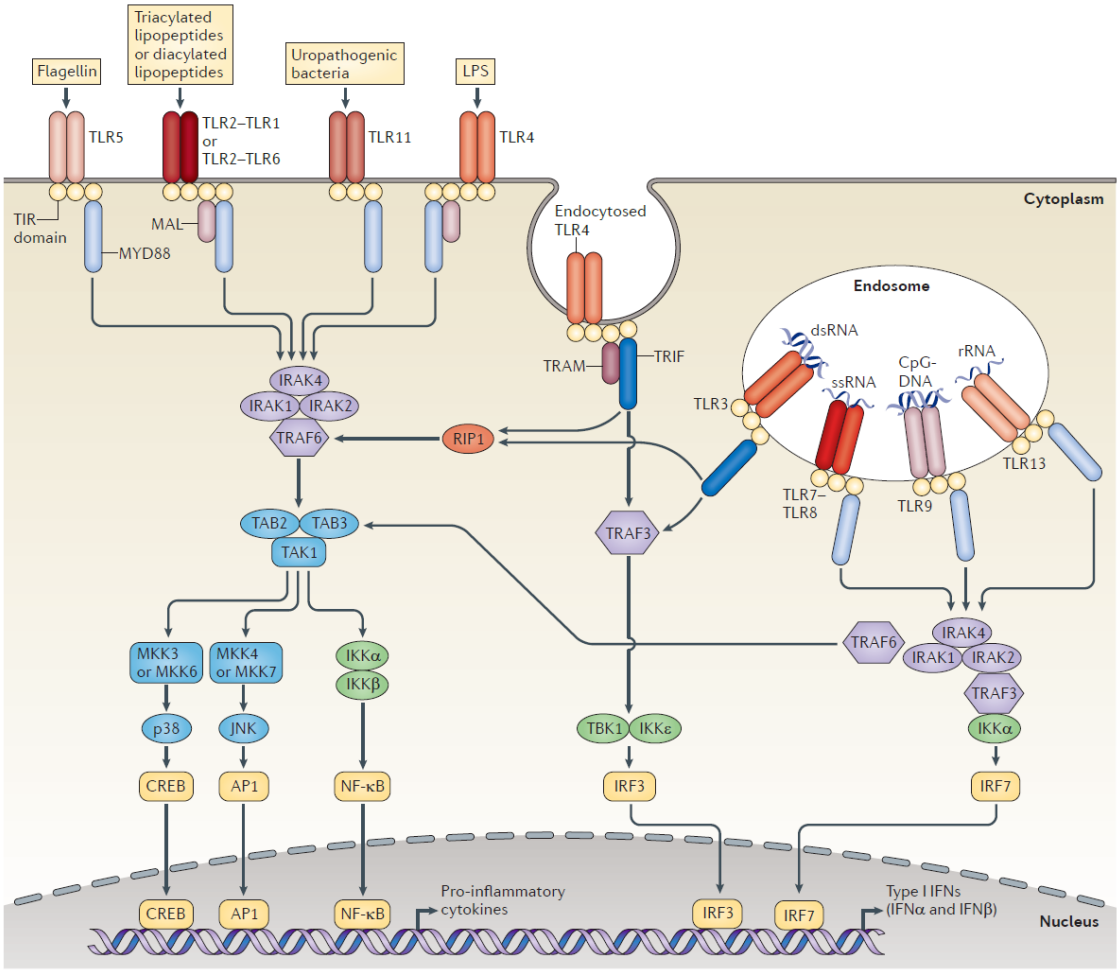

Figure 1-3. Mammalian TLR signaling pathway. Reprinted by permission from Macmillan Publishers Ltd: *Nature Reviews Immunology* 13: 453-460, copyright 2013.

MyD88-dependent pathway

TLR-mediated responses are controlled mainly by the MyD88-dependent pathway, which is used by all the TLRs except TLR3.[44] Activation of the MyD88-dependent pathway results in rapid NF-κB activation and release of proinflammatory cytokines such as TNF-α, IL-1ß, IL-6, and chemokines like

monocyte chemoattractant protein 1 (MCP-1), macrophage inflammatory protein 3α (MIP-3α) and IL-8 (**Figure 1-3**).[45]

Upon specific ligand binding, activated TLRs recruit the adaptor protein MyD88 via their TIR domain. MyD88 then binds to the death domain (DD) of the interleukin-1 receptor-associated kinase 4 (IRAK4) through homotypic interactions, which sequentially activates, through phosphorylation, the other IRAKs, such as IRAK1 and IRAK2. Upon release from MyD88, the phosphorylated IRAKs activate the TNF receptor-associated factor 6 (TRAF6), an E3 ligase that catalyzes the synthesis of polyubiquitin linked to Lys63 (K63) on target proteins, including TRAF6 itself and IRAK1, in conjunction with the dimeric E2 ubiquitin-conjugating enzymes Ubc13 and Uev1A.[39] The K63-linked polyubiquitin chains then bind to the novel zinc finger-type ubiquitin-binding domain of transforming growth factor ß-activated kinase 1 (TAK1)-binding proteins 2 and 3 (TAB2 and TAB3), the regulatory components of the kinase TAK1 complex, to activate TAK1.[46]

The K63-linked polyubiquitin chains also bind to an essential regulatory component of the IκB kinase IKK complex that is required for NF-κB activation. A TAK1-IKK complex forms, which allows TAK1 to phosphorylate IKKß through its close proximity to the IKK complex. This, in turn, leads to NF-κB nuclear translocation and activation via phosphorylation, polyubiquitination, and degradation of IκBα proteins.[14]

TAK1 is also responsible for the activation of MAPKs, such as extracellular signal-regulated kinase (ERK), the c-jun N terminal kinase (JNK) and p38 by

inducing the phosphorylation (rather than ubiquitination) of MAPK kinases, which then activate various transcription factors including activating protein (AP)-1 that regulates distinct proinflammatory gene expression.[14] Furthermore, TLR1, 2, 4 and 6 recruit another TIR-containing adaptor, the TIR-associated protein (TIRAP) (also known as MyD88-adaptor-like (MAL)), and that serves as a linker adaptor to recruit MyD88 to the TLRs.[47]

Activation of the MyD88-dependent pathway also induces many transcriptional regulators, and some of them have critical roles in modulating NF-κB-dependent transcription. For example, IκB protein IκBζ functions as an inducible coactivator for the NF-κB p50 subunit to facilitate IL-6 and IL-12p40 production.[48] Another protein, IκB-NS suppresses the induction of both IL-6 and TNF-α by modulating the DNA-binding activity of the NF-κB p65 subunit.[49]

TRIF-dependent signaling pathway

The TIR-domain-containing adaptor inducing IFN-ß (TRIF) dependent pathway (also commonly called the MyD88-independent pathway) was discovered at a later time when MyD88 deficient cells showed the induction of the type I IFN response and a delayed NF-κB activation when stimulated with LPS.[50-51] This suggested that MyD88-independent signaling can be activated downstream of TLR. Activation of the TRIF-dependent pathway boosts both the primary MyD88-dependent pathway response,[52-53] and induces expression of type 1 interferon (IFN-ß) and IFN-α.[54]

TRIF recruits TRAF6 and activates TAK1 for NF-κB activation, probably

through ubiquitination-dependent mechanisms similar to those of the MyD88-dependent pathway.[39] After stimulation by a TLR3 agonist, TRIF also recruits the receptor-interacting protein kinase 1 (RIP1) by interacting with a complex composed of the tumor necrosis factor receptor type 1-associated death domain protein (TRADD) and the FAS-associated death domain containing protein (FADD).[55] RIP1 undergoes ubiquitination that permits activation of TAK1, which in turns activates NF-κB and AP-1.[14] Collectively, TRIF forms a multiprotein signal with TRAF6 and RIP1 for the activation of TAK1, which activates NF-κB and MARK pathway.

In addition, TRIF activation also leads to upregulation of IRF3 and IFN-ß transcpription.[56] TRIF interacts with TRAF3 to activate TANK-binding kinase 1 (TBK-1) and the inducible IκB kinase (IKKi), which catalyzes the C-terminal phosphorylation of TRF3, leading to its homodimerization and inducing its nuclear translocation.[39]

1.2.3 TLRs in disease

The significance of individual TLRs in protecting against infectious diseases by activating/mediating the innate immune signaling has been demonstrated clearly. However, it has been also known that TLRs are implicated as contributors to the severity of numerous diseases. Through the underlying mechanisms that are largely unknown, TLR-mediated inflammatory signaling functions as double-edged sword: both protecting the host from infection or damaging and promoting

immunological pathogenesis.[57] Dysregulation of TLR signaling results in over-exuberant inflammation, which has severe consequences, such as organ damage or the emergence of autoimmune diseases.[58] On the other hand, to avoid harmful inflammation, cells acquire tolerance and become significantly less responsive to prolonged stimulation. This contributes clinically to immunosuppression related morbidity and mortality associated with many chronic inflammatory diseases such as sepsis, asthma, and cancer (**Table 1-2**).[57-58]

Infectious and inflammatory diseases

Recent studies have demonstrated that the role of TLRs in orchestrating an inflammatory cascade can trigger immune and inflammatory diseases. TLR7 and TLR9 have important roles in development of systemic autoimmune diseases.[59] It is reported that the inhibition of TLR7 and/or TLR9 signaling might be a useful

Table 1-2. TLRs in different human diseases (based on ref. 60, 61, 62)

TLR	Disease association
TLR1/2, TLR2/6	Lyme disease, atherosclerosis, asthma, ischemia/reperfusion, diabetes, malaria, hepatitis B (HBV), human immunodeficiency virus (HIV), chlamydia, influenza, cancer
TLR3	HIV, human papillomavirus (HPV), influenza, cancer
TLR4	atherosclerosis, asthma, ischemia/reperfusion, diabetes, rheumatoid arthritis, sepsis, Alzheimer's disease. Parkinson's disease, HBV, Legionnaires' disease, HIV, HPV, melanoma, malaria, influenza, cancer
TLR5	Crohn's disease, malaria, HPV, influenza, cancer
TLR7, TLR8	primary tumors, cutaneous metastases, chronic lymphocyte leukemia, HPV, Herpes simplex virus (HSV), leishmania, cancer
TLR9	asthma, allergy, systemic lupus erythematosus (SLE), HIV, HBV, HPV, malaria, influenza, melanoma, cancer

therapeutic strategy for the treatment of SLE and related systemic autoimmune diseases.[63] An increasing amount of clinical data reveals that TLR mutations and dysfunction are the contributing factors in the maintenance of inflammatory bowel disease (IBD).[64] IBD, classified as Crohn' disease or ulcerative colitis, is caused by a dysregulated mucosal immune response.[65] In active IBD, TLR3 is significantly down-regulated in active Crohn' disease but not in ulcerative colitis, while TLR4 is unregulated in both conditions. TLR5 also participates in this disease due to the high concentration of flagellin-specific antibody in the serum of patients.[66] Recently, TLR8 has also been identified as a key player in autoimmune inflammation in humans.[62] The study showed that TLR8 is overexpressed in patients with systemic arthritis and suggested that the signaling through this receptor may play a role in the disease pathogenesis.[62] Recent studies have demonstrated TLR2 and TLR4 to be significant in the pathogenesis of autoimmune diseases including rheumatoid arthritis (RA), systemic lupus erythematosus (SLE), systemic sclerosis, Sjogren's syndrome, psoriasis, multiple sclerosis, and autoimmune diabetes.[67]

Studies on the incidence of infectious disease in people with single-nucleotide polymorphism (SNP) in TLRs demonstrate that these minor changes can produce a subtle but specific disturbed TLR-related response that are associated with increased susceptibility to infections and autoimmune diseases in human.[68] The first polymorphic variation to be described in TLRs was in TLR4, in which D229G and T339I substitution were reported to decrease the interaction of the receptor with LPS and to increase the susceptibility of patients to sepsis due to infection

with Gram-negative bacteria.[69] Another example is the two polymorphisms in the extracellular region of the TLR3: one caused by a substitution of adenine for thymine at 952 bp (N284I) and the other by a substitution of thymine for cytosine at 1335 bp (L412F). Both modify the response of TLR3 and reduce the activity of NF-κB. It is speculated that functional polymorphisms of TLR3 predispose individuals to increased susceptibility to viral infections and cancers associated with viral infections and also to diseases associated with inflammatory responses.[70] Also, in the case of the adaptor protein TIRAP, the polymorphism (C558T) is associated with an increased susceptibility to meningeal tuberculousis,[71] while a different substitution (S180L) has protective effect against the development of invasive pneumococcal disease, bacteraemia, malaria and tuberculosis.[72]

Cancer

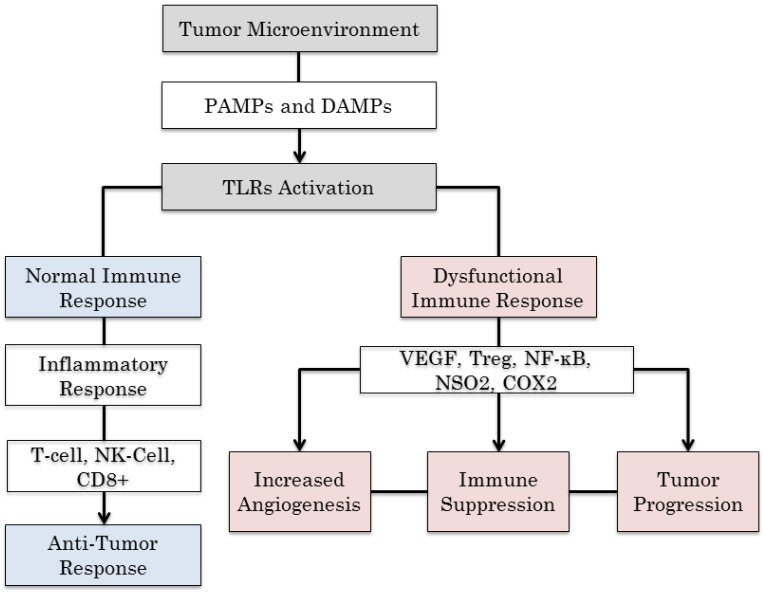

Figure 1-4. TLR activation by PAMPs and DAMPs act as double-edged sword in cancer. Reproduced with modification from Nader Husseinzadeh, Sara Madison Davenport [75] with permission from Elsevier.

Infection, chronic irritation and inflammation have been linked to cancer development. Some examples are infections of *H. pylori* that can develop gastric carcinoma,[73] or the association of the Epstein-Barr virus (EBV) hematologic.[74] The relationship between inflammation and cancer is complicated: inflammation either has tumor progression or tumor suppression effects, depending on the type of inflammation. TLRs play a critical role in the initiation of innate immune responses against invading pathogens, proinflammatory cytokine production and development of adaptive immune response. In addition to the protective role of TLRs against infectious pathogens, they may also contribute to tumor progression and host immune responses. The complex interactions between PAMP/DAMP, tumor cells and immune cells can promote the tumor progression or develop antitumor effect through TLR signaling. Thus, TLR activation acts as a double-edged sword in cancer (**Figure 1-4**).[57]

In the early 18th century, Deidier reported that infection in cancer patients can have positive effect on remission of malignant disease, making the first inference that microbial products could have anticancer effects.[76] At the end of 19th century, William Coley observed that repeated injections of a mixture of bacterial toxins (later identified as LPS) could serve as an efficient antitumor agent.[77] Since then, numerous studies have been conducted to investigate the effects of LPS on tumors. Several studies on tumor cell lines showed that TLR4 activation has an anti-tumor effect and a TLR4 agonist has been successfully used as a therapeutic agent in many types of malignancies, including cervical cancer, gastric cancer and

squamous cell carcinoma.[78] It is also reported that TLR2 plays a protective role against the development of colitis-associated colorectal cancer in a mouse model and Poly (I: C)-triggered TLR3 signaling causes apoptosis of human breast and prostate cancer cells.[79-80] However, not all the TLR activations have antitumor effects.

Table 1-3. Expression of TLRs in various tumor cells and tissue (based on ref. 5, 57, 81)

TLRs	Expressing cancer cells and tissues
TLR1	colon cancer, multiple myeloma cells
TLR2	colon cancer, gastric cancer, hepatocellular carcinoma, ovarian carcinoma, laryngeal carcinoma, intestinal adenocarcinoma, oral squamous cell carcinoma
TLR3	breast cancer, melanoma, colon cancer, hepatocellular carcinoma, laryngeal carcinoma, ovarian carcinoma, prostate carcinoma, esophageal squamous cell carcinoma, human neuroblastoma cells, cervical carcinoma, nasopharyngeal and lung carcinoma
TLR4	breast cancer, colon cancer, melanoma, gastric cancer, hepatocellular carcinoma, ovarian cancer, prostate carcinoma, laryngeal carcinoma, lung carcinoma, gastric cancer, adrencortial carcinoma, bladder cancer
TLR5	breast cancer, gastric cancer, cervical squamous cell carcinoma, intestinal adenocarcinoma, ovarian carcinoma, colon cancer
TLR6	hepatocellular carcinoma
TLR7	multiple myeloma cells, lung carcinoma, colorectal carcinoma, chronic lymphocytic leukemia
TLR8	lung carcinoma, colorectal carcinoma
TLR9	breast cancer, gastric cancer, prostate cancer, hepatocellular carcinoma, cervical squamous cell carcinoma, glioma, multiple myeloma cells, esophageal squamous cell carcinoma, lung carcinoma, renal cell carcinoma, ovarian cancer

Functional TLRs have been shown to express in a variety of tumor cells (**Table 1-3**) where they help shape the inflammatory profile of the tumor environment. The accumulating evidence indicates that TLR-related inflammation

and the downstream production of molecules arising from TLR activation in tumor cells can promote tumorigenisis, tumor progression and tumor invasion. These tumor growth-promoting processes occur particularly through the NF-κB signaling pathway. TLR4 is over-expressed in human and mouse inflammation-associated colorectal neoplasia and TLR4-deficient mice are markedly protected form colon carcinogenesis, suggesting that TLR4 signaling is critical for colon cancer progression in chronic colitis.[82] The elevated expression of TLR5 and TLR9 on the surface of cervical epithelial cells was reported to contribute to cervical cancer progression.[83] It is also revealed that TLR7 and TLR8 are expressed in human lung cancer *in situ* and in human lung tumor cell lines. Triggering with TLR7 or TLR8 agonists led to NF-κB activation, upregulated expression of the antiapoptotic protein Bcl-2, increased tumor cell survival, and chemoresistance.[84] In 2006, Merrell and colleagues concluded that synthetic CpG nucleotides activated TLR9 signaling induced invasion of breast cancer cells through secretion of matrix metalloproteinases.[85] Numerous reports concerning activation of different TLRs inducing tumor invasion have been published afterwards. Invasion has been reported with activation of TLR2, TLR4 or TLR9 in breast cancer cells.[86-87] TLR5 activation induced invasion of adenocarcinoma cells of the human salivary gland.[88]

1.2.4 TLRs as therapeutic targets

There is now a significant amount of evidence for the involvement of TLRs in multiple pathologic conditions.[89] The development of therapeutics targeting either the TLR themselves or the signals they generate is proving to be of great

interest. There is now sufficient evidence surrounding certain TLRs to justify them as therapeutical targets. These validation criteria includes: expression in disease, activation leading to enhanced disease, protection of TLR-knockout mice from disease, and association with disease susceptibility by single nucleotide polymorphism in the genes coding TLRs or their adaptors. Moreover, inflammatory cytokines such as TNF and IL-6, which are produced as a consequence of the activation of TLRs, have been proven to be excellent targets for inflammatory diseases such as rheumatoid arthritis. Targeting TLRs can regulate the pathway activation at an earlier point and therefore are also likely to prevent the induction of many immune and inflammatory proteins. This can, in turn, lead to a reduction in disease severity. In the recent past, a significant amount of research has been carried out aiming to develop TLR drugs that are either agonists to rectify aberrant and/or inadequate immune response, or antagonists to inhibit overactivation. Both TLR agonists and antagonists are potential drug candidates.

Drugs or candidates stimulating TLR

TLR agonists possess remarkable properties, particularly with regard to dendritic cell activation, inducing proinflammatory cytokine production and promoting a cytotoxic immune response. Experimental models and clinical studies chave shown that TLR agonists can act as immunologic adjuvants for use in vaccines against infectious diseases, allergies, and cancer immunotherapy (**Table 1-4**).[90-91] TLR3, TLR4 and TLR9 agonists have been shown to improve a number of vaccines, examples of which are those against HBV, influenza, malaria, and

anthrax, as well as some types of cancer. Monophosphoryl lipid A (MPL) (**Figure 1-5**), a derivative of *Salmonella minnesota* LPS that acts as a potent agonist of TLR4, has been authorized by the FDA for use within the formulation of Cervarix®, a vaccine against human papillomavirus type (HPV) 16 and 18. HPV16 and HPV18 are the causative agents of approximately 70% of cervical carcinoma cases.[92] TLR7/TLR8 agonists are less developed as adjuvants but are already used with success in topical cancer immunotherapy.

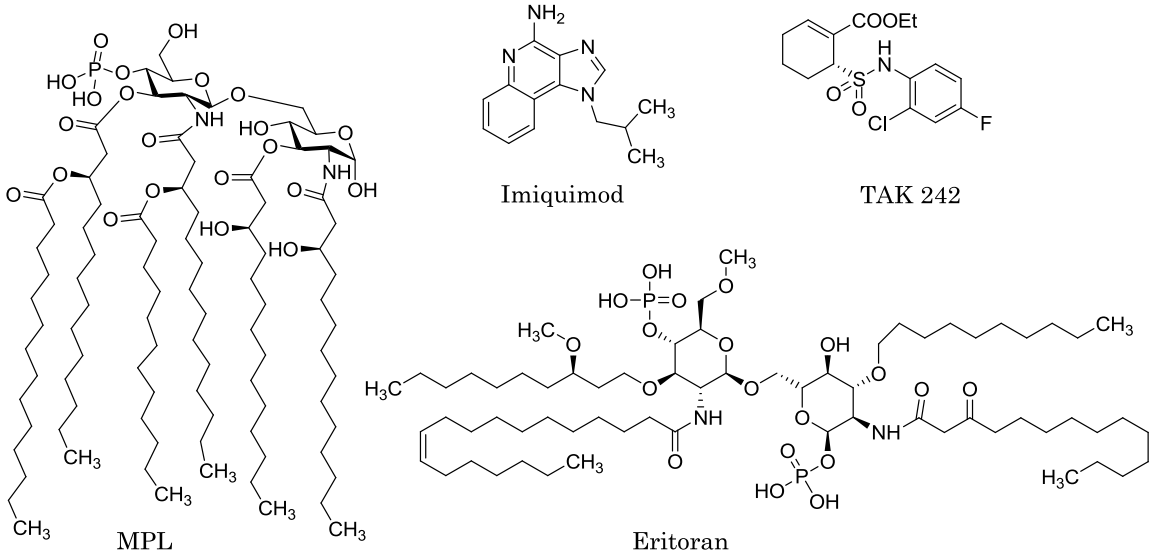

Figure 1-5. Examples of small molecule TLR agonist or antagonist structures.

Imiquimod (Aldara™) (**Figure 1-5**), which acts through TLR7-MyD88 dependent pathway to induce TNF-α, IFN-α and other proinflammatory cytokines, was approved for the treatment of genital warts, actinic keratosis and superficial basal cell carcinoma.[93] CBLB502, a pharmacologically optimized derivative of Salmonella flagellin, is a clinical-stage investigational drug with potential application as a cancer treatment.[94] Additionally there is substantial interest in combining TLR agonists with traditional vaccines to enhance immunogenicity and

efficacy. *In vitro* and *in vivo* studies have found that certain combinations of TLR agonists can synergistically improve vaccine efficacy.[95-96]

Table 1-4. Developmental status of TLR targeted agonists (based on ref 91, 97-98)

Compound	Company	Indications	Target	Drug Class	Clinical Status
SMP-105	Dainippon Sumitomo Pharma	cancer	TLR2	autoclaved mycobacteria	preclinical
OM174	OM Pharma	solid tumor	TLR2/4	lipidA derivative	phase I completed
Pollinex Quattro	Allergy Therapeutics	allergy	TLR4	MPL plus pollen	phase III
CBLB502	Cleveland Biolabs Inc.	ischemic renal failure, cancer	TLR5	flagellin	preclinical
VAX125	Vaxlnnate	influenza	TLR5	flagellin and hemagglutinin	phase II completed
ANA773	Anadys Pharmaceuticals	cancer, Hepatitis C	TLR7	ssRNA molecule	phase I completed
Imiquimod	3M Pharmaceuticals	keratosis, papillomavirus infection	TLR7	Small molecule	approved
AZD8848	Astra Zeneca	allergy, asthma	TLR7	ssRNA based molecule	phase II completed
VTX1463	VentiRx Pharmaceuticals	allergy	TLR8	ssRNA based molecule	phase I
Resiquimod	3M Pharmaceuticals	Hepatitis C ingection, herpes	TLR7/8	ssRNA molecule	suspended in phase II and III
DIMS0150	InDex Pharmaceuticals	ulcerative colitis	TLR9	CpG oligonucleotide	phase III completed
HEPLISAV	Dynavx Technologies	Hepatitis B	TLR9	Hapatitis B antigen	phase III completed
Agatolimod	Pifzer	cancer	TLR9	CpG oligonucleotide	phase II
IMO2134	Idera Pharmaceuticals	allergy, asthma	TLR9	CpG oligonucleotide	phase I completed

Drugs or candidates inhibiting TLR

Overactivation or dysregulation of TLR signaling pathways contributes to diverse pathogenesis of autoimmune, chronic inflammatory, and infectious diseases. Therefore TLR signaling and subsequent function must be under tight negative

regulation to prevent unwanted or prolonged stimulation, which might be harmful for the host. It has been reported that negative regulation of TLRs had also been attempted in clinical studies.[99] Therapies involving the synthetic molecule inhibitors of TLR4, TAK242 (a cyclohexene derivative) (**Figure 1-5**) and Eritoran (a synthetic lipid A analogue) (**Figure 1-5**) were tested in patients with severe sepsis in as early as 2005 and 2007 respectively.[100] However, they ultimately had only marginal inhibitory effects,[101-103] possibly because they were administered at a late time point in the disease course. The identification of a new TLR4 specific inhibitor to serve as a novel therapeutic is still an urgent need in the field of inflammatory diseases. Another clinical trial checking the efficacy and safety of TAK-242 in patients with sepsis-induced cardiovascular and respiratory failure has also been terminated. IMO-8400, which is Idera's lead clinical candidate, is a synthetic DNA-based antagonist of TLR7, 8 and 9 in clinical development for the treatment of autoimmune diseases, including psoriasis, lupus, and arthritis.[104] OPN-305, a first-in-class antibody that specifically targets and blocks TLR2 was shown to efficiently minimize the sequelae of ischemia/reperfusion injury by tempering the innate immune response following reperfusion.[105] Numerous early-stage therapeutics targeting specific inhibitions of TLRs and their signaling networks are in development (**Table 1-5**).[90-91] Concerns will always be raised over targeting molecules with critical roles within the immune system. The desired therapeutic treatment for autoimmune and inflammatory diseases would provide an

inhibitor with good efficacy, a favorable toxicity profile, simple administration, and a relatively lower production cost than current biological therapies.

Table 1-5. Developmental status of TLR targeted antagonists (based on ref. 60, 91, 97)

Compound	Company	Indications	Target	Drug Class	Clinical Status
OPN305 **OPN401**	Opsona Therapeutics	heart ischemia, delayed graft function, rheumatoid arthritis	TLR2	antibody	phase I preclinical
1A6	Novlmmune	colitis	TLR4	antibody	precilnical
Eritoran	Eisai Pharmaceuticals	sepsis	TLR4	synthetic lipodisaccharide	suspended in Phase III
TAK242	Takeda	Sepsis	TLR4	small molecule	suspended in phase III
NI0101	Novlmmune	acute and chronic inflammation	TLR4	monoclonal antibody	currently recruiting
AV441	Avigen	chronic pain, withdrawal	TLR4	Small molecule	phase II
IMO3100	Idera Pharmaceutical	systemic lupus Erythematosus, rheumatoid arthritis, multiple sclerosis psoriasis	TLR7/9	CpG oligonucleotide	phase II
IMO8400	Idera Pharmaceutical	systemic lupus erythematosus	TLR7/8/9	CpG oligonucleotide	currently recruiting
DV1079	Dynavax Technologies	systemic lupus erythematosus, HIV	TLR7/9	CpG oligonucleotide	phase I
CPG52364	Pfizer	systemic lupus erythematosus	TLR7/8/9	quinazoline derivative	phase I

TLRs play an important role in either promoting or suppressing disease progression in different inflammatory diseases and cancer. Both effective agonists and antagonists of TLRs have potential as therapeutic agents for the pathogenesis of disease process. Despite the fact that some nucleic acid and protein-based TLR

signaling regulators have reached clinical applications, very few small-molecule modules have been successful in clinical use. For drug development, small molecules have the advantage of the potential for high receptor activity, oral bioavailability, cell permeability, enhanced metabolic stability, and cost effective large-scale manufacturing. Therefore, the identification of new small molecule TLR agonists and antagonists that can serve as novel therapeutics is still an urgent need. The goal of my doctoral research is to identify small molecules capable of suppressing or activating a distinct TLR, potentially as new therapies for the treatment of TLR-related diseases.

1.3 Reference

1. Parkin, J.; Cohen, B., An overview of the immune system. *Lancet* **2001,** *357* (9270), 1777-89.
2. Akira, S.; Takeda, K.; Kaisho, T., Toll-like receptors: critical proteins linking innate and acquired immunity. *Nat. Immunol.* **2001,** *2* (8), 675-80.
3. Broz, P.; Monack, D. M., Newly described pattern recognition receptors team up against intracellular pathogens. *Nat. Rev. Immunol.* **2013,** *13* (8), 551-65.
4. Imai, Y.; Kuba, K.; Neely, G. G.; Yaghubian-Malhami, R.; Perkmann, T.; van Loo, G.; Ermolaeva, M.; Veldhuizen, R.; Leung, Y. H.; Wang, H.; Liu, H.; Sun, Y.; Pasparakis, M.; Kopf, M.; Mech, C.; Bavari, S.; Peiris, J. S.; Slutsky, A. S.; Akira, S.; Hultqvist, M.; Holmdahl, R.; Nicholls, J.; Jiang, C.; Binder, C. J.; Penninger, J. M., Identification of oxidative stress and Toll-like receptor 4 signaling as a key pathway of acute lung injury. *Cell* **2008,** *133* (2), 235-49.
5. So, E. Y.; Ouchi, T., The application of Toll like receptors for cancer therapy. *Int. J. Biol. Sci.* **2010,** *6* (7), 675-81.
6. West, X. Z.; Malinin, N. L.; Merkulova, A. A.; Tischenko, M.; Kerr, B. A.; Borden, E. C.; Podrez, E. A.; Salomon, R. G.; Byzova, T. V., Oxidative stress induces angiogenesis by activating TLR2 with novel endogenous ligands. *Nature* **2010,** *467* (7318), 972-6.
7. Piccinini, A. M.; Midwood, K. S., DAMPening inflammation by modulating TLR signalling. *Mediators of inflammation* **2010,** *2010*.
8. Siednienko, J.; Miggin, S. M., Expression analysis of the Toll-like receptors in human peripheral blood mononuclear cells. *Methods Mol. Biol.* **2009,** *517*, 3-14.

9. Dar, A. A.; Patil, R. S.; Chiplunkar, S. V., Insights into the Relationship between Toll Like Receptors and Gamma Delta T Cell Responses. *Front. Immunol.* **2014,** *5*, 366.
10. Kawai, T.; Akira, S., The roles of TLRs, RLRs and NLRs in pathogen recognition. *Int. Immunol.* **2009,** *21* (4), 317-37.
11. Roach, J. C.; Glusman, G.; Rowen, L.; Kaur, A.; Purcell, M. K.; Smith, K. D.; Hood, L. E.; Aderem, A., The evolution of vertebrate Toll-like receptors. *Proc. Natl. Acad. Sci. U. S. A.* **2005,** *102* (27), 9577-82.
12. Ariffin, J. K.; Sweet, M. J., Differences in the repertoire, regulation and function of Toll-like Receptors and inflammasome-forming Nod-like Receptors between human and mouse. *Curr. Opin. Microbiol.* **2013,** *16* (3), 303-10.
13. Takeuchi, O.; Akira, S., Pattern Recognition Receptors and Inflammation. *Cell* **2010,** *140* (6), 805-20.
14. Vandevenne, P.; Sadzot-Delvaux, C.; Piette, J., Innate immune response and viral interference strategies developed by human herpesviruses. *Biochem. Pharmacol.* **2010,** *80* (12), 1955-72.
15. Manavalan, B.; Basith, S.; Choi, S., Similar Structures but Different Roles - An Updated Perspective on TLR Structures. *Front. Physiol.* **2011,** *2*, 41.
16. Koblansky, A. A.; Jankovic, D.; Oh, H.; Hieny, S.; Sungnak, W.; Mathur, R.; Hayden, M. S.; Akira, S.; Sher, A.; Ghosh, S., Recognition of Profilin by Toll-like Receptor 12 Is Critical for Host Resistance to Toxoplasma gondii. *Immunity* **2013,** *38* (1), 119-30.
17. Oldenburg, M.; Kruger, A.; Ferstl, R.; Kaufmann, A.; Nees, G.; Sigmund, A.; Bathke, B.; Lauterbach, H.; Suter, M.; Dreher, S.; Koedel, U.; Akira, S.; Kawai, T.; Buer, J.; Wagner, H.; Bauer, S.; Hochrein, H.; Kirschning, C. J., TLR13 Recognizes Bacterial 23S rRNA Devoid of Erythromycin Resistance-Forming Modification. *Science* **2012,** *337* (6098), 1111-5.
18. Dar, A. A.; Patil, R. S.; Chiplunkar, S. V., Insights into the realtionship between toll like receptors and gamma delta T cell responses. *Frontiers in immunology* **2014,** *5*.
19. Botos, I.; Segal, D. M.; Davies, D. R., The structural biology of Toll-like receptors. *Structure* **2011,** *19* (4), 447-59.
20. Jin, M. S.; Lee, J. O., Structures of the toll-like receptor family and its ligand complexes. *Immunity* **2008,** *29* (2), 182-91.
21. Bella, J.; Hindle, K. L.; McEwan, P. A.; Lovell, S. C., The leucine-rich repeat structure. *Cell. Mol. Life Sci.* **2008,** *65* (15), 2307-33.
22. Panter, G.; Jerala, R., The ectodomain of the Toll-like receptor 4 prevents constitutive receptor activation. *J. Biol. Chem.* **2011,** *286* (26), 23334-44.
23. Godfroy, J. I., 3rd; Roostan, M.; Moroz, Y. S.; Korendovych, I. V.; Yin, H., Isolated Toll-like receptor transmembrane domains are capable of oligomerization. *PloS one* **2012,** *7* (11), e48875.
24. Gay, N. J.; Keith, F. J., Drosophila Toll and IL-1 receptor. *Nature* **1991,** *351* (6325), 355-6.

25. Sodergren, E.; Weinstock, G. M.; Davidson, E. H., The genome of the sea urchin Strongylocentrotus purpuratus. *Science* **2006,** *314* (5801), 941-52.
26. O'Neill, L. A.; Bowie, A. G., The family of five: TIR-domain-containing adaptors in Toll-like receptor signalling. *Nat. Rev. Immunol* **2007,** *7* (5), 353-64.
27. Watters, T. M.; Kenny, E. F.; O'Neill, L. A., Structure, function and regulation of the Toll/IL-1 receptor adaptor proteins. *Immunol. Cell Biol.* **2007,** *85* (6), 411-9.
28. Hua, Z.; Hou, B., TLR signaling in B-cell development and activation. *Cell. Mol. Immunol.* **2013,** *10* (2), 103-6.
29. Beutler, B. A., TLRs and innate immunity. *Blood* **2009,** *113* (7), 1399-407.
30. Verma, R.; Jung, J. H.; Kim, J. Y., 1,25-Dihydroxyvitamin D3 up-regulates TLR10 while down-regulating TLR2, 4, and 5 in human monocyte THP-1. *J. Steroid Biochem. Mol. Biol.* **2014,** *141*, 1-6.
31. Koblansky, A. A.; Jankovic, D.; Oh, H.; Hieny, S.; Sungnak, W.; Mathur, R.; Hayden, M. S.; Akira, S.; Sher, A.; Ghosh, S., Recognition of profilin by Toll-like receptor 12 is critical for host resistance to Toxoplasma gondii. *Immunity* **2013,** *38* (1), 119-30.
32. Dasu, M. R.; Rivkah Isseroff, R., Toll-Like Receptors in Wound Healing: Location, Accessibility, and Timing. *J. Invest. Dermatol.* **2012,** *132* (8), 1955-8.
33. Park, B. S.; Song, D. H.; Kim, H. M.; Choi, B. S.; Lee, H.; Lee, J. O., The structural basis of lipopolysaccharide recognition by the TLR4-MD-2 complex. *Nature* **2009,** *458* (7242), 1191-5.
34. Choe, J.; Kelker, M. S.; Wilson, I. A., Crystal structure of human toll-like receptor 3 (TLR3) ectodomain. *Science* **2005,** *309* (5734), 581-5.
35. Jin, M. S.; Kim, S. E.; Heo, J. Y.; Lee, M. E.; Kim, H. M.; Paik, S. G.; Lee, H.; Lee, J. O., Crystal structure of the TLR1-TLR2 heterodimer induced by binding of a tri-acylated lipopeptide. *Cell* **2007,** *130* (6), 1071-82.
36. Kang, J. Y.; Nan, X.; Jin, M. S.; Youn, S. J.; Ryu, Y. H.; Mah, S.; Han, S. H.; Lee, H.; Paik, S. G.; Lee, J. O., Recognition of lipopeptide patterns by Toll-like receptor 2-Toll-like receptor 6 heterodimer. *Immunity* **2009,** *31* (6), 873-84.
37. Yoon, S. I.; Kurnasov, O.; Natarajan, V.; Hong, M.; Gudkov, A. V.; Osterman, A. L.; Wilson, I. A., Structural basis of TLR5-flagellin recognition and signaling. *Science* **2012,** *335* (6070), 859-64.
38. Tanji, H.; Ohto, U.; Shibata, T.; Miyake, K.; Shimizu, T., Structural reorganization of the Toll-like receptor 8 dimer induced by agonistic ligands. *Science* **2013,** *339* (6126), 1426-29.
39. Kawai, T.; Akira, S., The role of pattern-recognition receptors in innate immunity: update on Toll-like receptors. *Nat. Immunol.* **2010,** *11* (5), 373-84.
40. Akira, S.; Takeda, K., Toll-like receptor signalling. *Nat. Rev. Immunol.* **2004,** *4* (7), 499-511.
41. Kawai, T.; Akira, S., Signaling to NF-kappaB by Toll-like receptors. *Trends Mol. Med.* **2007,** *13* (11), 460-9.

42. Barbalat, R.; Lau, L.; Locksley, R. M.; Barton, G. M., Toll-like receptor 2 on inflammatory monocytes induces type I interferon in response to viral but not bacterial ligands. *Nat. Immunol.* **2009,** *10* (11), 1200-7.
43. Kawai, T.; Akira, S., Innate immune recognition of viral infection. *Nat. Immunol.* **2006,** *7* (2), 131-7.
44. Mogensen, T. H., Pathogen recognition and inflammatory signaling in innate immune defenses. *Clin. Microbiol. Rev.* **2009,** *22* (2), 240-73.
45. Broad, A.; Kirby, J. A.; Jones, D. E.; Applied, I.; Transplantation Research, G., Toll-like receptor interactions: tolerance of MyD88-dependent cytokines but enhancement of MyD88-independent interferon-beta production. *Immunology* **2007,** *120* (1), 103-11.
46. Bhoj, V. G.; Chen, Z. J., Ubiquitylation in innate and adaptive immunity. *Nature* **2009,** *458* (7237), 430-7.
47. Lin, S. C.; Lo, Y. C.; Wu, H., Helical assembly in the MyD88-IRAK4-IRAK2 complex in TLR/IL-1R signalling. *Nature* **2010,** *465* (7300), 885-90.
48. Yamamoto, M.; Yamazaki, S.; Uematsu, S.; Sato, S.; Hemmi, H.; Hoshino, K.; Kaisho, T.; Kuwata, H.; Takeuchi, O.; Takeshige, K.; Saitoh, T.; Yamaoka, S.; Yamamoto, N.; Yamamoto, S.; Muta, T.; Takeda, K.; Akira, S., Regulation of Toll/IL-1-receptor-mediated gene expression by the inducible nuclear protein IkappaBzeta. *Nature* **2004,** *430* (6996), 218-22.
49. Kuwata, H.; Matsumoto, M.; Atarashi, K.; Morishita, H.; Hirotani, T.; Koga, R.; Takeda, K., IkappaBNS inhibits induction of a subset of Toll-like receptor-dependent genes and limits inflammation. *Immunity* **2006,** *24* (1), 41-51.
50. Kaisho, T.; Takeuchi, O.; Kawai, T.; Hoshino, K.; Akira, S., Endotoxin-induced maturation of MyD88-deficient dendritic cells. *J. Immunol.* **2001,** *166* (9), 5688-94.
51. Kawai, T.; Takeuchi, O.; Fujita, T.; Inoue, J.; Muhlradt, P. F.; Sato, S.; Hoshino, K.; Akira, S., Lipopolysaccharide stimulates the MyD88-independent pathway and results in activation of IFN-regulatory factor 3 and the expression of a subset of lipopolysaccharide-inducible genes. *J. Immunol.* **2001,** *167* (10), 5887-94.
52. Gohda, J.; Matsumura, T.; Inoue, J., Cutting edge: TNFR-associated factor (TRAF) 6 is essential for MyD88-dependent pathway but not toll/IL-1 receptor domain-containing adaptor-inducing IFN-beta (TRIF)-dependent pathway in TLR signaling. *J. Immunol.* **2004,** *173* (5), 2913-7.
53. Cusson-Hermance, N.; Khurana, S.; Lee, T. H.; Fitzgerald, K. A.; Kelliher, M. A., Rip1 mediates the Trif-dependent toll-like receptor 3- and 4-induced NF-{kappa}B activation but does not contribute to interferon regulatory factor 3 activation. *J. Bio. Chem.* **2005,** *280* (44), 36560-6.
54. Honda, K.; Taniguchi, T., IRFs: master regulators of signalling by Toll-like receptors and cytosolic pattern-recognition receptors. *Nat. Rev. Immunol.***2006,** *6* (9), 644-58.
55. Chen, N. J.; Chio, II; Lin, W. J.; Duncan, G.; Chau, H.; Katz, D.; Huang, H. L.; Pike, K. A.; Hao, Z.; Su, Y. W.; Yamamoto, K.; de Pooter, R. F.; Zuniga-Pflucker, J. C.; Wakeham, A.; Yeh, W. C.; Mak, T. W., Beyond tumor necrosis factor receptor:

TRADD signaling in toll-like receptors. *Proc. Natl. Acad. Sci. U. S. A.* **2008,** *105* (34), 12429-34.
56. Hacker, H.; Tseng, P. H.; Karin, M., Expanding TRAF function: TRAF3 as a tri-faced immune regulator. *Nat. Rev. Immunol.* **2011,** *11* (7), 457-68.
57. Basith, S.; Manavalan, B.; Yoo, T. H.; Kim, S. G.; Choi, S., Roles of toll-like receptors in cancer: a double-edged sword for defense and offense. *Arch. Pharmacal Res.* **2012,** *35* (8), 1297-316.
58. Lamagna, C.; Scapini, P.; van Ziffle, J. A.; DeFranco, A. L.; Lowell, C. A., Hyperactivated MyD88 signaling in dendritic cells, through specific deletion of Lyn kinase, causes severe autoimmunity and inflammation. *Proc. Natl. Acad. Sci. U. S. A.* **2013,** *110* (35), E3311-20.
59. Pradhan, V. D.; Das, S.; Surve, P.; Ghosh, K., Toll-like receptors in autoimmunity with special reference to systemic lupus erythematosus. *Indian J. Hum. Genet.* **2012,** *18* (2), 155-60.
60. O'Neill, L. A. J.; Bryant, C. E.; Doyle, S. L., Therapeutic Targeting of Toll-Like Receptors for Infectious and Inflammatory Diseases and Cancer. *Pharmacol. Rev.* **2009,** *61* (2), 177-197.
61. Maisonneuve, C.; Bertholet, S.; Philpott, D. J.; De Gregorio, E., Unleashing the potential of NOD- and Toll-like agonists as vaccine adjuvants. *Proc. Natl. Acad. Sci. U. S. A.* **2014,** *111* (34), 12294-12299.
62. Guiducci, C.; Gong, M.; Cepika, A. M.; Xu, Z.; Tripodo, C.; Bennett, L.; Crain, C.; Quartier, P.; Cush, J. J.; Pascual, V.; Coffman, R. L.; Barrat, F. J., RNA recognition by human TLR8 can lead to autoimmune inflammation. *J. Exp. Med.* **2013,** *210* (13), 2903-19.
63. Marshak-Rothstein, A., Toll-like receptors in systemic autoimmune disease. *Nat. Rev. Immunol.* **2006,** *6* (11), 823-35.
64. Cario, E., Toll-like receptors in inflammatory bowel diseases: a decade later. *Inflammatory Bowel Dis.* **2010,** *16* (9), 1583-97.
65. Shih, D. Q.; Targan, S. R., Insights into IBD Pathogenesis. *Curr. Gastroenterol. Rep.* **2009,** *11* (6), 473-80.
66. Yamamoto-Furusho, J. K.; Podolsky, D. K., Innate immunity in inflammatory bowel disease. *World J. Gastroenterol.* **2007,** *13* (42), 5577-80.
67. Liu, Y.; Yin, H.; Zhao, M.; Lu, Q., TLR2 and TLR4 in Autoimmune Diseases: a Comprehensive Review. *Clin. Rev. Allergy Immunol.* **2014,** *47* (2), 136-47.
68. Trejo-de la, O. A.; Hernandez-Sancen, P.; Maldonado-Bernal, C., Relevance of single-nucleotide polymorphisms in human TLR genes to infectious and inflammatory diseases and cancer. *Genes Immun.* **2014,** *15* (4), 199-209.
69. Arbour, N. C.; Lorenz, E.; Schutte, B. C.; Zabner, J.; Kline, J. N.; Jones, M.; Frees, K.; Watt, J. L.; Schwartz, D. A., TLR4 mutations are associated with endotoxin hyporesponsiveness in humans. *Nat. Genet.* **2000,** *25* (2), 187-91.
70. Ranjith-Kumar, C. T.; Miller, W.; Sun, J.; Xiong, J.; Santos, J.; Yarbrough, I.; Lamb, R. J.; Mills, J.; Duffy, K. E.; Hoose, S.; Cunningham, M.; Holzenburg, A.; Mbow, M. L.; Sarisky, R. T.; Kao, C. C., Effects of single nucleotide polymorphisms

on Toll-like receptor 3 activity and expression in cultured cells. *J. Biol. Chem.* **2007,** *282* (24), 17696-705.
71. Hawn, T. R.; Dunstan, S. J.; Thwaites, G. E.; Simmons, C. P.; Thuong, N. T.; Lan, N. T.; Quy, H. T.; Chau, T. T.; Hieu, N. T.; Rodrigues, S.; Janer, M.; Zhao, L. P.; Hien, T. T.; Farrar, J. J.; Aderem, A., A polymorphism in Toll-interleukin 1 receptor domain containing adaptor protein is associated with susceptibility to meningeal tuberculosis. *J. Infect. Dis.* **2006,** *194* (8), 1127-34.
72. Khor, C. C.; Chapman, S. J.; Vannberg, F. O.; Dunne, A.; Murphy, C.; Ling, E. Y.; Frodsham, A. J.; Walley, A. J.; Kyrieleis, O.; Khan, A.; Aucan, C.; Segal, S.; Moore, C. E.; Knox, K.; Campbell, S. J.; Lienhardt, C.; Scott, A.; Aaby, P.; Sow, O. Y.; Grignani, R. T.; Sillah, J.; Sirugo, G.; Peshu, N.; Williams, T. N.; Maitland, K.; Davies, R. J.; Kwiatkowski, D. P.; Day, N. P.; Yala, D.; Crook, D. W.; Marsh, K.; Berkley, J. A.; O'Neill, L. A.; Hill, A. V., A Mal functional variant is associated with protection against invasive pneumococcal disease, bacteremia, malaria and tuberculosis. *Nat. Genet.* **2007,** *39* (4), 523-8.
73. Romero-Gallo, J.; Harris, E. J.; Krishna, U.; Washington, M. K.; Perez-Perez, G. I.; Peek, R. M., Jr., Effect of Helicobacter pylori eradication on gastric carcinogenesis. *Lab. Invest.* **2008,** *88* (3), 328-36.
74. Thorley-Lawson, D. A.; Gross, A., Persistence of the Epstein-Barr virus and the origins of associated lymphomas. *N. Engl. J. Med.* **2004,** *350* (13), 1328-37.
75. Husseinzadeh, N.; Davenport, S. M., Role of Toll-like receptors in cervical, endometrial and ovarian cancers: A review. *Gynecol. Oncol.* **2014**.
76. Garay, R. P.; Viens, P.; Bauer, J.; Normier, G.; Bardou, M.; Jeannin, J. F.; Chiavaroli, C., Cancer relapse under chemotherapy: why TLR2/4 receptor agonists can help. *Eur. J. Pharmacol.* **2007,** *563* (1-3), 1-17.
77. Coley, W. B., The treatment of malignant tumors by repeated inoculations of erysipelas. With a report of ten original cases. 1893. *Clin. Orthop. Relat. Res.* **1991,** (262), 3-11.
78. Oblak, A.; Jerala, R., Toll-like receptor 4 activation in cancer progression and therapy. *Clin. Dev. Immunol.* **2011,** *2011*, 609579.
79. Lowe, E. L.; Crother, T. R.; Rabizadeh, S.; Hu, B.; Wang, H.; Chen, S.; Shimada, K.; Wong, M. H.; Michelsen, K. S.; Arditi, M., Toll-like receptor 2 signaling protects mice from tumor development in a mouse model of colitis-induced cancer. *PloS one* **2010,** *5* (9), e13027.
80. Harashima, N.; Minami, T.; Uemura, H.; Harada, M., Transfection of poly(I:C) can induce reactive oxygen species-triggered apoptosis and interferon-beta-mediated growth arrest in human renal cell carcinoma cells via innate adjuvant receptors and the 2-5A system. *Mol. Cancer* **2014,** *13*, 217.
81. Sato, Y.; Goto, Y.; Narita, N.; Hoon, D. S., Cancer Cells Expressing Toll-like Receptors and the Tumor Microenvironment. *Cancer Microenviron.* **2009,** *2 Suppl 1*, 205-14.
82. Fukata, M.; Chen, A.; Vamadevan, A. S.; Cohen, J.; Breglio, K.; Krishnareddy, S.; Hsu, D.; Xu, R.; Harpaz, N.; Dannenberg, A. J.; Subbaramaiah, K.; Cooper, H. S.;

Itzkowitz, S. H.; Abreu, M. T., Toll-like receptor-4 promotes the development of colitis-associated colorectal tumors. *Gastroenterol.* **2007,** *133* (6), 1869-81.
83. Kim, W. Y.; Lee, J. W.; Choi, J. J.; Choi, C. H.; Kim, T. J.; Kim, B. G.; Song, S. Y.; Bae, D. S., Increased expression of Toll-like receptor 5 during progression of cervical neoplasia. *Int. J. Gynecol. Cancer* **2008,** *18* (2), 300-5.
84. Cherfils-Vicini, J.; Platonova, S.; Gillard, M.; Laurans, L.; Validire, P.; Caliandro, R.; Magdeleinat, P.; Mami-Chouaib, F.; Dieu-Nosjean, M. C.; Fridman, W. H.; Damotte, D.; Sautes-Fridman, C.; Cremer, I., Triggering of TLR7 and TLR8 expressed by human lung cancer cells induces cell survival and chemoresistance. *J. Clin. Invest.* **2010,** *120* (4), 1285-97.
85. Merrell, M. A.; Ilvesaro, J. M.; Lehtonen, N.; Sorsa, T.; Gehrs, B.; Rosenthal, E.; Chen, D.; Shackley, B.; Harris, K. W.; Selander, K. S., Toll-like receptor 9 agonists promote cellular invasion by increasing matrix metalloproteinase activity. *Mol. Cancer Res.* **2006,** *4* (7), 437-47.
86. Xie, W.; Wang, Y.; Huang, Y.; Yang, H.; Wang, J.; Hu, Z., Toll-like receptor 2 mediates invasion via activating NF-kappaB in MDA-MB-231 breast cancer cells. *Biochem. Biophys. Res. Commun.* **2009,** *379* (4), 1027-32.
87. Liao, S. J.; Zhou, Y. H.; Yuan, Y.; Li, D.; Wu, F. H.; Wang, Q.; Zhu, J. H.; Yan, B.; Wei, J. J.; Zhang, G. M.; Feng, Z. H., Triggering of Toll-like receptor 4 on metastatic breast cancer cells promotes alphavbeta3-mediated adhesion and invasive migration. *Breast Cancer Res. Treat.* **2012,** *133* (3), 853-63.
88. Park, J. H.; Yoon, H. E.; Kim, D. J.; Kim, S. A.; Ahn, S. G.; Yoon, J. H., Toll-like receptor 5 activation promotes migration and invasion of salivary gland adenocarcinoma. *J. Oral Pathol. Med.* **2011,** *40* (2), 187-93.
89. Cook, D. N.; Pisetsky, D. S.; Schwartz, D. A., Toll-like receptors in the pathogenesis of human disease. *Nat. Immunol.* **2004,** *5* (10), 975-9.
90. Basith, S.; Manavalan, B.; Lee, G.; Kim, S. G.; Choi, S., Toll-like receptor modulators: a patent review (2006-2010). *Expert Opin. Ther. Pat.* **2011,** *21* (6), 927-944.
91. Hennessy, E. J.; Parker, A. E.; O'Neill, L. A. J., Targeting Toll-like receptors: emerging therapeutics? *Nat. Rev. Drug Discovery* **2010,** *9* (4), 293-307.
92. Vacchelli, E.; Galluzzi, L.; Eggermont, A.; Fridman, W. H.; Galon, J.; Sautes-Fridman, C.; Tartour, E.; Zitvogel, L.; Kroemer, G., Trial watch: FDA-approved Toll-like receptor agonists for cancer therapy. *Oncoimmunology* **2012,** *1* (6), 894-907.
93. Novak, N.; Yu, C. F.; Bieber, T.; Allam, J. P., Toll-like receptor 7 agonists and skin. *Drug News Perspect.* **2008,** *21* (3), 158-65.
94. Ding, X.; Bian, G.; Leigh, N. D.; Qiu, J.; McCarthy, P. L.; Liu, H.; Aygun-Sunar, S.; Burdelya, L. G.; Gudkov, A. V.; Cao, X., A TLR5 agonist enhances CD8(+) T cell-mediated graft-versus-tumor effect without exacerbating graft-versus-host disease. *J. Immunol.* **2012,** *189* (10), 4719-27.
95. Orr, M. T.; Beebe, E. A.; Hudson, T. E.; Moon, J. J.; Fox, C. B.; Reed, S. G.; Coler, R. N., A dual TLR agonist adjuvant enhances the immunogenicity and protective efficacy of the tuberculosis vaccine antigen ID93. *PloS one* **2014,** *9* (1), e83884.

96. Zhu, Q.; Egelston, C.; Vivekanandhan, A.; Uematsu, S.; Akira, S.; Klinman, D. M.; Belyakov, I. M.; Berzofsky, J. A., Toll-like receptor ligands synergize through distinct dendritic cell pathways to induce T cell responses: implications for vaccines. *Proc. Natl. Acad. Sci. U. S. A.* **2008,** *105* (42), 16260-5.
97. Connolly, D. J.; O'Neill, L. A., New developments in Toll-like receptor targeted therapeutics. *Curr. Opin. Pharmacol.* **2012,** *12* (4), 510-8.
98. Engel, A. L.; Holt, G. E.; Lu, H., The pharmacokinetics of Toll-like receptor agonists and the impact on the immune system. *Expert Rev. Clin. Pharmacol. 2011, 4 (2), 275-89.*
99. O'Neill, L. A. J.; Golenbock, D.; Bowie, A. G., The history of Toll-like receptors - redefining innate immunity. *Nat. Rev. Immunol.* **2013,** *13* (6), 453-60.
100. Barochia, A.; Solomon, S.; Cui, X.; Natanson, C.; Eichacker, P. Q., Eritoran tetrasodium (E5564) treatment for sepsis: review of preclinical and clinical studies. *Expert Opin. Drug Metab. Toxicol.* **2011,** *7* (4), 479-94.
101. Kalil, A. C.; LaRosa, S. P.; Gogate, J.; Lynn, M.; Opal, S. M.; Eritoran Sepsis Study, G., Influence of severity of illness on the effects of eritoran tetrasodium (E5564) and on other therapies for severe sepsis. *Shock* **2011,** *36* (4), 327-31.
102. Bennett-Guerrero, E.; Grocott, H. P.; Levy, J. H.; Stierer, K. A.; Hogue, C. W.; Cheung, A. T.; Newman, M. F.; Carter, A. A.; Rossignol, D. P.; Collard, C. D., A phase II, double-blind, placebo-controlled, ascending-dose study of Eritoran (E5564), a lipid A antagonist, in patients undergoing cardiac surgery with cardiopulmonary bypass. *Anesth. Analg.* **2007,** *104* (2), 378-83.
103. Rice, T. W.; Wheeler, A. P.; Bernard, G. R.; Vincent, J. L.; Angus, D. C.; Aikawa, N.; Demeyer, I.; Sainati, S.; Amlot, N.; Cao, C.; Ii, M.; Matsuda, H.; Mouri, K.; Cohen, J., A randomized, double-blind, placebo-controlled trial of TAK-242 for the treatment of severe sepsis. *Crit. Care Med.* **2010,** *38* (8), 1685-94.
104. Kandimalla, E. R.; Bhagat, L.; Wang, D.; Yu, D.; Sullivan, T.; La Monica, N.; Agrawal, S., Design, synthesis and biological evaluation of novel antagonist compounds of Toll-like receptors 7, 8 and 9. *Nucleic Acids Res.* **2013,** *41* (6), 3947-61.
105. Reilly, M.; Miller, R. M.; Thomson, M. H.; Patris, V.; Ryle, P.; McLoughlin, L.; Mutch, P.; Gilboy, P.; Miller, C.; Broekema, M.; Keogh, B.; McCormack, W.; van de Wetering de Rooij, J., Randomized, double-blind, placebo-controlled, dose-escalating phase I, healthy subjects study of intravenous OPN-305, a humanized anti-TLR2 antibody. *Clin. Pharmacol. Ther.* **2013,** *94* (5), 593-600.

CHARPTER 2

Selection, synthesis, and anti-inflammatory evaluation of the arylidene malonate derivatives as TLR4 signaling inhibitor

Reformatted from the manuscript published under the same name of Selection, synthesis, and anti-inflammatory evaluation of the arylidene malonate derivatives as TLR4 signaling inhibitor. *Bioorg Med Chem* **2012**, 20, 6073-6079, co-authored with Cheng, K., Wang, X., and Yin, H.

2.1 Introduction

The first line of defense in host protection against invading microbial pathogens is the innate immune system, where the TLRs play a critical role.[1] TLRs function to detect and respond to a series of structurally conserved molecules known as PAMPs. Response to PAMPs by TLRs leads to the up-regulation of pro-inflammatory cytokines and mediators, initiating the innate immune response. The first identified and most well studied TLR is TLR4, which recognizes lipopolysaccharide (LPS) or endotoxin, a major component of the outer membrane of gram-negative bacteria.[2-4] LPS-induced TLR4 signal transduction requires the association of the accessory protein myeloid differentiation factor 2 (MD-2) to TLR4. Binding of LPS to the large hydrophobic pocket on the MD-2 surface induces the homodimerization of two copies of the MD-2-TLR4-LPS complex.[5]

This homodimerization diverges to result in the activation of either myeloid

differentiation primary-response gene 88 (MyD88)-dependent, or Toll/interleukin-1 receptor domain-containing adaptor inducing IFN-ß (TRIF)-dependent signaling.[6] MyD88-dependent signaling induces NF-κB activation as an inflammatory response. Under normal circumstances, NF-κB remains sequestered in the cytoplasm as an inactive complex by a family of inhibitory proteins known as IκBs.[7] Upon binding to MD-2 in the presence of LPS, TLR4 initiates a series of phosphorylation events resulting in the phosphorylation of the cytoplasmic IκBs. These phosphorylated IκBs then undergo ubiquitylation and subsequent degradation by the proteasome, resulting in the translocation of NF-κB into the nucleus.[8,9] Nuclear NF-κB promotes transcription of various proinflammatory cytokines including inducible nitric oxide synthase (iNOS), cyclooxygenase-2 (COX-2), tumor necrosis factor (TNF)-α, interleukin-1ß (IL-1ß), and IL-6.[10, 11] In contrast, TRIF-dependent signaling activates interferon regulatory factor 3 (IRF3), which induces type I interferon (IFN) expression.[12, 13]

Although LPS-induced proinflammatory cytokine production initiates the host defense against injury and infection,[14, 15] the dysregulation of TLR4 signaling contributes to an array of acute and chronic human diseases such as septic shock, inflammatory arthritis, atherosclerosis, and cancer.[16-18] Its involvement in human disease makes the TLR4 signaling pathway an important therapeutic target.[19] In fact, several TLR4 signaling inhibitors have already been investigated as potential anti-sepsis drugs. The most advanced of these, TAK242 and Eritoran,[20, 21] were successful in pre-clinical trials but both failed in Phase III clinical trials due to lack

of efficacy.[22,23] Therefore, the identification of new TLR4 signaling inhibitors which serve as novel therapeutics is still an urgent need.

In the present study, we identified a group of novel TLR4 signaling inhibitors, developed from our initial lead 2-(2-nitrobenzylidene) malonate (**1**), and investigated their structure-activity relationship. Further, we examined the inhibitory effects of **1** on downstream NF-κB activation to elucidate the mechanism of its inhibitory effects.

2.2 Results and discussion

2.2.1 Screening for TLR4 signaling inhibitors

We interrogated the 1,363-member Diversity Set II library from the National Cancer Institute (NCI) for inhibition of LPS-induced NO production using murine macrophage RAW 264.7 cells as previously reported.[24] This library consists of small molecules that were selected from the larger 140,000-compound NCI library on the basis of availability, purity, and other diversity criteria. After the preliminary screening, a total of 6 compounds were identified that showed >80% inhibitory activity at a concentration of 1.0 μM. To ensure that the observed inhibition was not due to cell proliferation inhibition, we used the previously established WST-1 toxicity assay to determine the cytotoxicity of the 6 selected hits.[25] Only one compound, NCI126224 (**1**, **Scheme 2-1**) based on an arylidene malonate scaffold did not show significant toxicity up to 10.0 μM, prompting us to focus on this scaffold for further investigation.

2.2.2. Structure-activity relationship studies of the arylidene malonate derivatives

Next, we performed structure-activity relationship (SAR) studies of the selected hit compound, **1**, to identify the key structural features essential for inhibitory activity. The representative synthetic route for **1-21** is shown in **Scheme 2-1**.

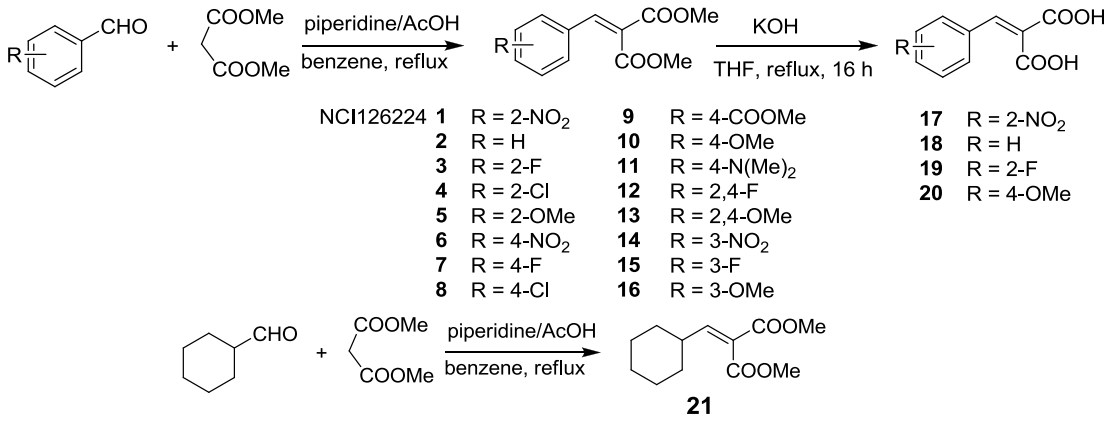

Scheme 2-1. Generic synthesis route of compounds **1-21**.

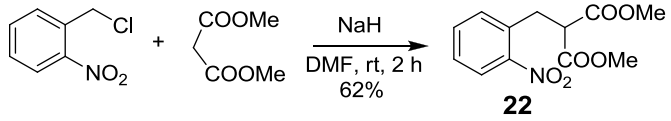

Scheme 2-2. Synthesis of compound **22**.

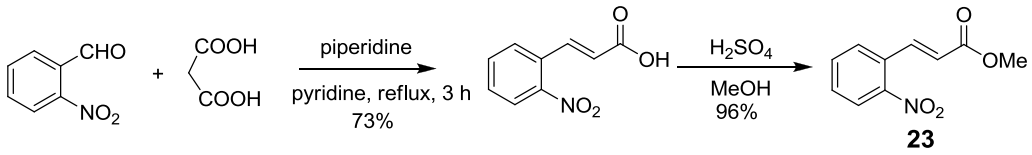

Scheme 2-3. Synthesis of compound **23.**

Commercially available dimethyl malonate underwent a piperidine-catalyzed Knoevenagel condensation with various aldehydes, affording **1-16** and **21** in good yields. Then, the resultant Compounds **1-3** and **10** were converted to the corresponding diacids, **17-20**, by hydrolysis with potassium hydroxide. Dimethyl

malonate was treated with sodium hydride, then 2-nitrobenzyl chloride to give the fully saturated analog **22** (**Scheme 2-2**). Compound **23** was obtained from the condensation of 2-nitrobenzaldehyde and malonic acid followed by methyl-esterification (**Scheme 2-3**).

Table 2-1. Inhibitory effects of the arylidene malontate derivatives on LPS-induced NO production in RAW 264.7 macrophage cells.

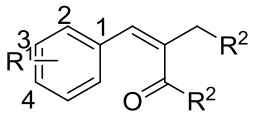

1-20

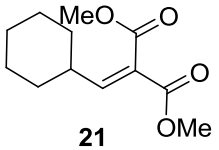

21

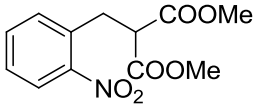

22

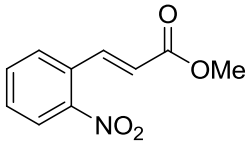

23

	R^1	R^2	IC_{50} (μM)
1 (NCI126224)	2-NO_2	OMe	0.31 ± 0.03
2	H	OMe	0.82 ± 0.08
3	2-F	OMe	0.33 ± 0.14
4	2-Cl	OMe	0.82 ± 0.15
5	2-OMe	OMe	0.74 ± 0.26
6	4-NO_2	OMe	0.82 ± 0.04
7	4-F	OMe	0.71 ± 0.14
8	4-Cl	OMe	1.54 ± 0.22
9	4-COOMe	OMe	1.33 ± 0.05
10	4-OMe	OMe	1.24 ± 0.12
11	4-$N(Me)_2$	OMe	3.11 ± 0.26
12	2,4-F	OMe	0.42 ± 0.08
13	2,4-OMe	OMe	0.82 ± 0.27
14	3-NO_2	OMe	2.13 ± 0.26
15	3-F	OMe	2.53 ± 0.31
16	3-OMe	OMe	3.72 ± 0.36
17	2-NO_2	OH	0.52 ± 0.12
18	2-F	OH	0.41 ± 0.16
19	H	OH	0.93 ± 0.07
20	4-OMe	OH	1.44 ± 0.18
21			78.2 ± 1.6
22			> 100
23			4.53 ± 0.36

These synthesized compounds were then evaluated for their inhibitory activities against LPS-induced NO production in RAW 264.7 cells. As shown in **Table 2-1**, 12 compounds exhibited submicromolar IC_{50} values for inhibition of LPS-induced NO production in RAW 264.7 cells. As a comparison, their inhibitory activities were significantly higher than the widely used anti-inflammatory agent, curcumin (IC_{50} =6 μM).[21] To study the influence of the α, ß-double bond, reduced analog (**22**) of **1** was evaluated. The reduction of the α, ß-double bond resulted in a complete loss of inhibitory activity (IC_{50}>100 μM), so compound **22** was used as the negative control in the subsequent biological evaluations. This demonstrates that the presence of Michael acceptor maybe essential for its TLR4 signaling inhibitory activity. This property is consistent with TAK242, a known TLR inhibitor that covalently bind to Cys747 in TLR4 via a Michael reaction.[26]

Covalent inhibitors are rarely considered when initiating a target-directed drug discovery project due to safety concerns. Nonetheless, a relatively potent inhibitor may render an activity window that allows useful applications of specifically regulating the TLR4-mediated inflammation response. Furthermore, the recent revived interests of covalent drugs also suggest that such molecules could still serve as promising drug candidates in principle.[27] **Figure 2-1A** showed a representative dose-response analysis of **1** to assess the IC_{50} values for inhibition of LPS-induced NO production in the RAW 264.7 cells in comparison with **22**. The results showed that **1** potently blocked LPS-induced NO production with an IC_{50} of 0.31±0.03 μM. By contrast, compound **22** showed negligible inhibition at the tested concentrations.

Replacement of the phenyl ring with a cyclohexyl ring (**21**) resulted in reduced activity. Additionally, the monoester (**23**) was less potent than the corresponding diester (**1**). The effect of the arylidene malonate pharmacophore on TLR4 signaling was also investigated with regard to the electronic properties of phenyl substituent. As shown in **Table 2-1**, the *ortho*-substituted arylidene malonates (**1**, **3**, **5**) were remarkably more potent than their *meta*-substituted counterparts (**14**, **15**, **16**). The corresponding *para*-substituted analogs (**6**, **7**, **10**) were slightly less potent than the *ortho*-substituted analogs. Further SAR studies revealed that the presence of a strong electron-withdrawing group on the 2-position of the benzene ring remarkably increased the inhibitory activity. This suggests that the electron deficiency aromatic ring is critical for compound efficacy. When the nitro group at the 2-position was replaced with fluorine (**3**), no significant inhibitory potency change was observed. By contrast, the introduction of a methoxy group to the 2-position (**5**) led to a decreased inhibitory activity. With the absence of any substituent on the benzene ring (**2**) the activity decreased by greater than 2-fold. It was also determined that the malonic acid derivatives (**17-20**) were less active than the corresponding ester analogs (R_2=methoxy group). Nevertheless, these di-acid derivatives were still effective TLR4 signaling inhibitors with IC_{50} values in the low micromolar range. Taken together, these results suggest that arylidene malontate derivatives present a consistent SAR and small modifications of its core significantly affect its inhibitory potency, implying a near optimal recognition of its potential target.

2.2.3 Effect of **1** on downstream NF-κB activation

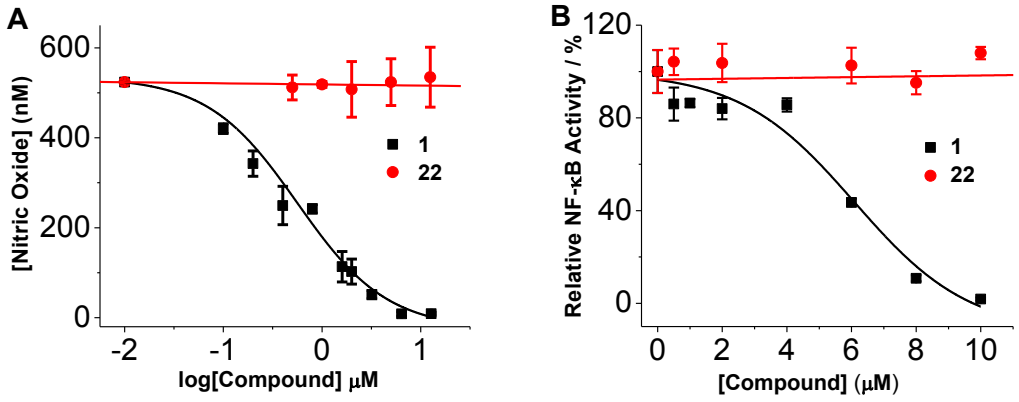

Figure 2-1. Inhibitory effect of **1** and **22** on LPS-induced NO production and NF-κB activation: (A) Representative dose-dependent inhibitory response of the arylidene malonate analogs on LPS-induced NO production in RAW 264.7 macrophage cells. (B) Effects of **1** and the negative control, **22**, on LPS-induced activation of NF-κB using a NF-κB dual luciferase reporter assay in BV-2 microglial cells.

Induction of the TLR4 signaling pathway stimulates the activation of NF-κB through both the MyD88- and TRIF-dependent pathways. NF-κB activation upregulates iNOS, resulting in elevated production of NO. To determine whether the inhibition of NO production by **1** is due to the suppression of NF-κB activation, an NF-κB luciferase reporter gene assay was performed. NF-κB dual-luciferase reporter in BV-2 cells, a widely used microglial cell line expressing various TLR receptors,[28] were incubated with LPS (200 ng/mL) in the absence or presence of **1** or the negative control, compound **22**, for 24 h. NF-κB reporter activity was increased by 45-fold after LPS treatment and this increase was diminished in cells treated with **1** in a dose-dependent manner (**Figure 2-1B**). The IC_{50} value obtained for **1** was 5.92 ± 0.14 μM. By contrast, the inactive compound, **22,** did not alter the LPS-

induced NF-κB activation at concentrations up to 10 μM. This result suggests that **1** inhibits the TLR4 signaling pathway upstream of NF-κB activation, which is in a good agreement with its inhibitory activity of the NO production.

2.2.4 Effect of **1** on downstream cytokines production

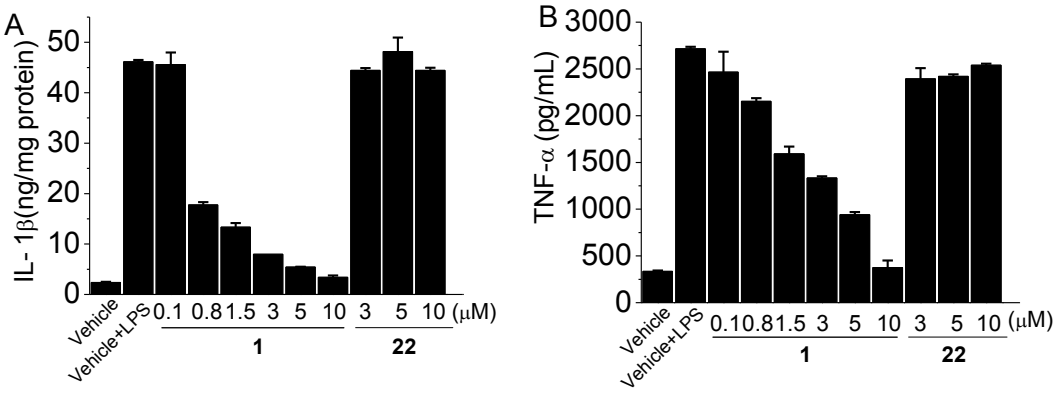

Figure 2-2. Inhibitory effect of **1** and **22** on LPS-induced cytokines production: (A) Dose-dependence effects of **1** and **22** on LPS-induced IL-1ß production in the RAW 264.7 cells. (B) Dose-dependence effects of **1** and **22** on the LPS-induced TNF-α production in the RAW 264.7 cells.

LPS-induced TLR4 activation results in an increased production of the proinflammatory cytokines, IL-1ß and TNF-α. To further understand the mechanism of TLR4 signaling inhibition by **1**, we examined its effect on LPS-induced production of two cytokines, IL-1ß and TNF-α, in macrophages using a previously developed ELISA assay.[29] LPS treatment resulted in the production of significant elevation of the IL-1ß and TNF-α levels compared to vehicle treated cells, reaching a maximum of approximately 20-fold and 10-fold after 24 h, respectively. LPS-induced IL-1ß production in macrophages was potently inhibited by **1** in a dose-dependent manner, with an IC_{50} value of 0.42 ± 0.15 μM (**Figure 2-2A**).

Similarly, LPS-induced TNF-α production was decreased in the presence of **1**, with a measured IC_{50} value of 1.54 ± 0.17 μM (**Figure 2-2B**). By contrast, the inactive compound **22** did not affect the production of either IL-1ß or TNF-α. Thus, **1** can efficiently block the LPS-induced production of several different cytokines in macrophages, which is in good agreement with our observations of its activities in NO and NF-κB inhibition.

2.2.5. Selectivity and specificity of **1**

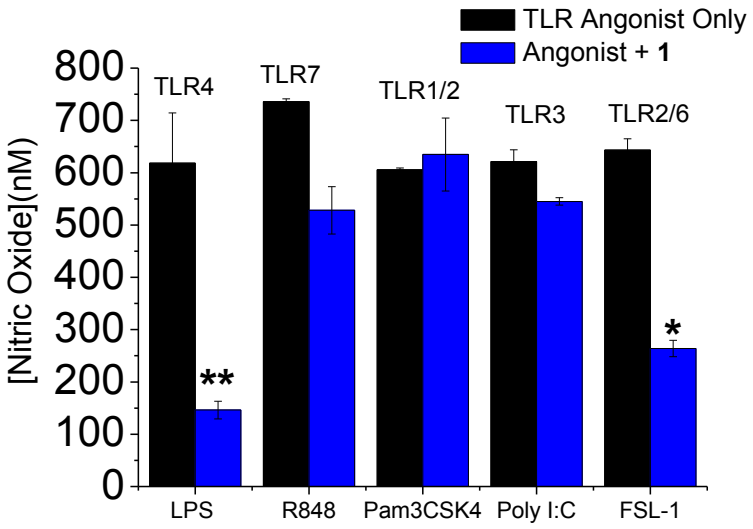

Figure 2-3. Inhibitory effects of **1** on the NO production induced by various TLR-specific ligands in RAW 264.7 cells. LPS (lipopolysaccharide), R848 {4-amino-2-(ethoxymethyl)-R, R-dimethyl-1H-imidazo [4, 5-c] quinoline-1-ethanol}, Pam_3CSK_4 {N-palmitoyl-S-[2,3-bis(palmitoyloxy)-(2R,S)-propyl]-[R]-cysteinyl-[S]-seryl-[S]-lysyl-[S]-lysyl-[S]-lysyl-[S]-lysine·3HCl}, poly(I:C) (polyriboinosinic:polyribocytidylic acid), and FSL-1[(S,R)-(2,3-bispalmitoyloxypropyl)-Cys-Gly-Asp-Pro-Lys-His-Pro-Lys-Ser-Phe], were used to selectively activate TLR4, TLR7, TLR2/1, TLR3, and TLR2/6, respectively, in the presence or absence of 0.6 μM **1**. Data present the mean values (±SD) of 3 separate experiments, each performed in triplication (significance vs. LPS alone treated group, **P<0.01; significance vs. FSL-1 alone treated group, *P<0.01).

As previously discussed, a potential pitfall for **1** is its specificity due to its ability

to serve as a Michael acceptor. In order to determine if **1** selectively inhibits the TLR4 signaling, the effects of **1** on other murine analogous TLRs were investigated using a previously reported method with RAW 264.7 macrophage cells that can be activated by different TLR-specific ligands.[30] At a concentration of 0.6 μM, **1** showed negligible inhibition to TLR1/TLR2, TLR3, or TLR7/8, suggesting that **1** is TLR4-specific (**Figure 2-3**). Interestingly, it reduced the signal *via* the TLR2/TLR6 heterodimer for reasons yet to be identified (see further discussion *vide infra*).

2.2.6 Molecular docking of **1** to the TLR4-MD-2 interface

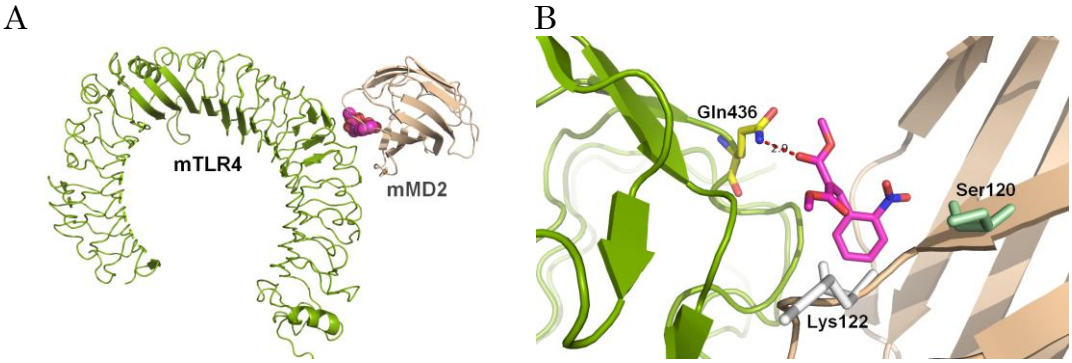

Figure 2-4. Molecular docking of **1** to the TLR4-MD-2 complex. (A) Docking simulation of **1** to the crystal structure of the human TLR4-MD-2 complex was performed using *Glide 5.6*. Molecular modeling of **1** in the LPS-binding site of the TLR4-MD-2 complex is represented as **1** by the magenta sphere; TLR4 is shown in green ribbon and MD-2 in light orange ribbon. (B) A close-up view of the predicted interaction between **1** and the LPS-binding site of the TLR4-MD-2 complex. TLR4 is shown in green and MD-2 in light orange.

Based on the evidence that **1** inhibits the TLR4 signaling pathway but also affects the TLR2/TLR6 signaling pathway, we speculated that a potential binding mode for **1** is that it might disrupt the TLR4 signaling by interacting with MD-2, complex as TLR4 and TLR2 are the only TLRs that have been reported to require

an accessory protein, MD-2, to initiate their signaling.[31] It would be conceivable that an inhibitor that targets the MD-2 interface with TLR4 or TLR2/6 might selectively block TLR2 and TLR4 over other TLRs. To further explore this hypothesis, a computational docking search was carried out to determine if there is a desired binding mode of **1** to the TLR4/MD-2 protein interface (TLR2/MD-2 structure remains unsolved). As shown in **Figure 2-4**, in the most energetically favorable predicted binding mode, **1** was found to fit into the LPS-binding site of TLR4-MD-2 complex exhibiting close contacts with Gln436 of TLR4, as well as Lys122 and Ser120 in the Phe126 loop of MD-2. The entire structure of **1** was buried inside the LPS-binding pocket where the carbonyl group could form a hydrogen bond with the Gln436 residue on the TLR4 surface. Interestingly, the hydrophilic residues in the Phe126 loop of MD-2 and the Gln436 residue on TLR4 are known to be important for the interaction between LPS and TLR4-MD-2. These docking results implied a possible binding mode of **1** as a disruptor of the TLR4-MD-2 protein-protein interactions.

In summary, we have identified, synthesized and evaluated a series of arylidene malonate analogs as TLR4 signaling inhibitors. SAR studies have determined the important structural requirements for the high potency observed with the lead compound, **1**. Furthermore, **1** was found to inhibit LPS-mediated NF-κB activation and the cytokine production of IL-1ß and TNF-α. A possible mechanism of **1** targeting the TLR4-MD-2 interface was proposed.

2.3 Materials and methods

2.3.1 Chemistry

Chemicals were purchased from Sigma Aldrich Chemical Co. TLC was performed on glass plates precoated by silica gel with visualization by UV-light. ^{1}H NMR and ^{13}C NMR spectra were recorded on a Bruker 300 MHz or 400 MHz instrument and were referenced internally to the residual solvent peak. A compound library consisting of 1,364 compounds was obtained from the National Cancer Institute Development Therapeutics Program repository (http://www.dtp.nci.nih.gov/index.html).

Compound **22** and **23** were prepared by following the literature procedures (**Scheme 2-2**, **2-3**).[32, 33] The preparation of alkylidene and arylidene malonates (**1-16, 21**) is through Knoevenagel condensation of malonates and carbonyl compounds. The synthetic sequence is outlined in **Scheme 2-1**. A mixture of aldehyde (3.5 mmole), dimethyl malonate (3.5 mmole), acetic acid (10 µL) and piperidine (20 µL) in benzene (1.5mL) was heated under reflux with azeotropic removal of water overnight. Benzene was removed by rotavapor, the residue was diluted with ethyl acetate (20 mL), washed with 10 percent hydrochloric acid, saturated sodium bicarbonate and brine. The organic layer was dried over anhydrous sodium sulfate, concentrated in vacuo and the residue was purified by silica chromatography to provide pure product.

As shown in **Scheme 2-1**, the diester (2 mmol) was dissolved in methanol (1.5 mL) and treated with a solution of KOH (0.23 g, 4 mmol) in water (1 mL), and the mixture was diluted with a minimum volume of THF to provide for its homogeneity.

The reaction was heated under reflux for 16 h and concentrated in vacuo. This residue was dissolved in a minimum of water, and extracted with Et_2O. The aqueous layer was acidified with 17.5% hydrochloric acid to pH 3-4 and extracted with Et_2O. The ethereal extract was washed with water, dried over anhydrous sodium sulfate and evaporated. Products were purified by recrystallization or by precipitating them with hexane from the ethereal solution.

Dimethyl 2-(2-nitrobenzylidene)malonate **1:** yield: 75%. ^{1}H NMR (300 MHz, $CDCl_3$) δ 8.25 – 8.22 (m, 2H), 7.76 – 7.53 (m, 2H), 7.44 – 7.41 (m, 1H), 3.90 (s, 3H), 3.62 (s, 3H).

Dimethyl 2-benzylidenemalonate **2**: yield: 86%. ^{1}H NMR (300 MHz, $CDCl_3$) δ 8.09 (s, 1H), 7.48 – 7.29 (m, 4H), 7.28 – 7.23 (m, 1H), 3.89 (s, 3H), 3.77 (s, 3H).

Dimethyl 2-(2-fluorobenzylidene) malonate **3**: yield: 89%. ^{1}H NMR (300 MHz, $CDCl_3$) δ 7.96 (s, 1H), 7.45 – 7.37 (m, 2H), 7.19 – 7.09 (m, 2H), 3.88 (s, 3H), 3.84 (s, 3H).

Dimethyl 2-(2-chlorobenzylidene) malonate **4**: yield: 73%. ^{1}H NMR (300 MHz, $CDCl_3$) δ 8.09 (s, 1H), 7.47 – 7.34 (m, 3H), 7.33 – 7.27 (m, 1H), 3.89 (s, 3H), 3.77 (s, 3H).

Dimethyl 2-(2-methoxybenzylidene) malonate **5**: yield: 66%. ^{1}H NMR (300 MHz, $CDCl_3$) δ 8.13 (s, 1H), 7.42 - 7.33 (m, 2H), 6.97 - 6.90 (m, 2H), 3.87 (s, 3H), 3.86 (s, 3H), 3.80 (s, 3H).

Dimethyl 2-(4-nitrobenzylidene) malonate **6**: yield: 79%. ^{1}H NMR (300 MHz, $CDCl_3$) δ 8.29 – 8.24 (m, 2H), 7.82 (s, 1H), 7.63 – 7.58 (m, 2H), 3.90 (s, 3H), 3.86 (s, 3H).

Dimethyl 2-(4-fluorobenzylidene) malonate **7**: yield: 74%. ^{1}H NMR (300 MHz, $CDCl_3$) δ 7.74 (s, 1H), 7.50 – 7.38 (m, 2H), 7.09 (m, 2H), 3.86 (s, 3H), 3.86 (s, 3H).

Dimethyl 2-(4-chlorobenzylidene) malonate **8**: yield: 83%. ^{1}H NMR (300 MHz, $CDCl_3$) δ 7.73 (s, 1H), 7.37 (s, 4H), 3.86 (s, 3H), 3.86 (s, 3H).

Dimethyl 2-(4-(methoxycarbonyl)benzylidene) malonate **9**: yield:71%. ^{1}H NMR (300 MHz, $CDCl_3$) δ 8.04 (d, J = 8.3 Hz, 2H), 7.79 (s, 1H), 7.48 (d, J = 8.3 Hz, 2H), 3.92 (s, 3H), 3.86 (s, 3H), 3.83 (s, 3H).

Dimethyl 2-(4-methoxybenzylidene) malonate **10**: yield: 66%. ^{1}H NMR (300 MHz, $CDCl_3$) δ 7.72 (s, 1H), 7.39 (d, J = 6.8 Hz, 2H), 6.90 (d, J = 6.8 Hz, 2H), 3.87 (s, 3H), 3.84 (s, 6H).

Dimethyl 2-(4-(dimethylamino)benzylidene)malonate **11**: yield: 63%. ^{1}H NMR (300 MHz, $CDCl_3$) δ 7.69 (s, 1H), 7.35 (dd, J = 9.1, 0.4 Hz, 2H), 6.65 (d, J = 9.0 Hz, 2H), 3.90 (s, 3H), 3.83 (s, 3H), 3.05 (s, 6H).

Dimethyl 2-(2.4-difluorobenzylidene) malonate **12**: yield: 85%. ^{1}H NMR (300 MHz, $CDCl_3$) δ 7.86 (s, 1H), 7.52 – 7.33 (m, 1H), 6.96 – 6.78 (m, 2H), 3.86 (s, 3H), 3.83 (s, 3H). ^{13}C NMR (101 MHz, $CDCl_3$) δ166.43 (s), 164.28 (dd, J_{CF} = 253.0, 12.0 Hz), 164.09 (s), 161.39 (dd, J_{CF} = 256.2, 12.2 Hz), 134.44 (dd, J_{CF} = 4.6, 1.2 Hz), 130.48 (dd, J_{CF} = 10.1, 3.6 Hz), 127.13 (s), 117.57 (dd, J_{CF} = 12.5, 4.0 Hz), 112.05 (dd, J_{CF} = 21.7, 3.7 Hz), 104.54 (t, J_{CF} = 25.6 Hz), 52.78 (s), 52.68 (s). MS (ESI^{+}) m/z: 279.0 (M+Na), 257.1 (M+H^{+}).

Dimethyl 2-(2.4-dimethoxybenzylidene) malonate **13**: yield: 75%. ^{1}H NMR (300 MHz, $CDCl_3$) δ 8.09 (s, 1H), 7.32 (d, J = 8.5 Hz, 1H), 6.50 – 6.44 (m, 2H), 3.86 (s, 3H), 3.85 (s, 3H), 3.84 (s, 3H), 3.83 (s, 3H).

Dimethyl 2-(3-nitrobenzylidene) malonate **14**: yield: 69%. ^{1}H NMR (400 MHz, $CDCl_3$) δ 8.38 – 8.31 (m, 1H), 8.31 – 8.25 (m, 1H), 7.82 (s, 1H), 7.78 – 7.74 (m, 1H), 7.65 – 7.59 (m, 1H), 3.92 (s, 3H), 3.91 (s, 3H).

Dimethyl 2-(3-fluorobenzylidene) malonate **15**: yield: 73%. ^{1}H NMR (400 MHz, $CDCl_3$) δ 7.73 (s, 1H), 7.41 – 7.34 (m, 1H), 7.25 – 7.19 (m, 1H), 7.17 – 7.07 (m, 2H), 3.87 (s, 6H).

Dimethyl 2-(3-methoxybenzylidene) malonate **16**: yield: 85%. ^{1}H NMR (400 MHz, $CDCl_3$) δ 7.77 (s, 1H), 7.36 – 7.29 (m, 1H), 7.07 – 7.01 (m, 1H), 7.01 – 6.92 (m, 2H), 3.87 (s, 6H), 3.83 (s, 3H).

2-(2-nitrobenzylidene)malonic acid **17**: yield: 52%. ^{1}H NMR (400 MHz, DMSO-d_6) δ 8.24 – 8.15 (m, 1H), 7.93 (s, 1H), 7.84 – 7.79 (m, 1H), 7.72 – 7.67 (m, 1H), 7.54 – 7.51 (m, 1H).

2-benzylidene malonic acid **18**: yield: 55%. ^{1}H NMR (400 MHz, DMSO-d_6) δ 7.63 – 7.55 (m, 2H), 7.54 (s, 1H), 7.48 – 7.42 (m, 3H).

2-(2-fluorobenzylidene)malonic acid **19**: yield: 46%. ^{1}H NMR (400 MHz, DMSO-d_6) δ 7.62 (s, 1H), 7.61 – 7.56 (m, 1H), 7.54 – 7.48 (m, 1H), 7.35 – 7.26 (m, 2H).

2-(4-methoxybenzylidene) malonic acid **20**: yield: 54%. ^{1}H NMR (400 MHz, DMSO-d_6) δ 7.78 (s, 1H), 7.50 – 7.46 (m, 1H), 7.46 – 7.41 (m, 1H), 7.14 – 7.07 (m, 1H), 7.01 – 6.96 (m, 1H).

Dimethyl 2-(cyclohexylmethylene) malonate **21**: yield: 88%. ^{1}H NMR (300 MHz, $CDCl_3$) δ 6.86 (d, *J* = 10.5 Hz, 1H), 3.84 (s, 3H), 3.78 (s, 3H), 2.39 (dd, *J* = 10.8, 3.3 Hz, 1H), 1.79 – 1.63 (m, 5H), 1.37 – 1.11 (m, 5H).

Dimethyl 2-(2-nitrobenzyl) malonate **22**: yield: 62%. ^{1}H NMR (300 MHz, $CDCl_3$) δ 8.04-8.01 (m, 1H), 7.58 – 7.53 (m, 1H), 7.47 – 7.37 (m, 2H), 3.94 (t, *J* = 7.6 Hz, 1H), 3.72 (s, 6H), 3.53 (d, *J* = 7.6 Hz, 2H).

(E)-methyl 3-(2-nitrophenyl) acrylate **23**: ^{1}H NMR (300 MHz, $CDCl_3$) δ 8.14 (d, *J* = 15.8 Hz, 1H), 8.09 – 8.04 (m, 1H), 7.69 – 7.64 (m, 2H), 7.60 – 7.54 (m, 1H), 6.39 (d, *J* = 15.8 Hz, 1H), 3.85 (s, 3H).

2.3.2 Cell culture and inhibitor treatment

Each compound is dissolved at a concentration of 10 mM in DMSO. Murine macrophage RAW 264.7 (American Type Culture Collection, Rockville, MD) were routinely cultured at 37℃ in a humidified 5% CO_2 atmosphere in RPMI 1640 supplemented with 10% fetal bovine serum, penicillin (100 units/mL), and streptomycin sulfate (100 μg/mL). Cells placed in a 96-well plate at a density of 7×10^6 cells/well were incubated for 24 h. Cultured cells were treated with vehicle (control) and various concentrations of compound and then stimulated with 20 ng/mL of LPS for 24 h.

2.3.3 Cell viability assay

Cell viability was determined by (4-[3-(4-iodophenyl)-2-(4- nitrophenyl)-. 2H-5-

tetrazolio]-1, 3-benzene disulfonate, WST-1) assay using Clontech premixed WST-1 cell proliferation reagent according to the manufacturer's instructions. Briefly, cells were inoculated at a density of 2×10^4 cells/well into 96-well plate and cultured at 37℃ for 24 h. The culture medium was replaced with 100 μL serum free medium and cultured cells were treated with vehicle (control) and various concentrations of compound. After 24 h, 10 μL premixed WST-1 solution was added to each well. After incubation at 37℃ for 30 minutes, the absorbance at 490 nm was measured using a microplate reader.

2.3.4 Measurement of NO

RAW 264.7 cells were placed in a 96-well plate at a density of 7.5×10^6 cells/well and incubated for 24 h. On the treatment day, media was removed and replaced with RPMI 1640 medium. Cultured cells were treated with vehicle or various concentration of compound then stimulated with 20 ng/mL LPS for 24 h. The nitrite concentration in the cultured media was measured as an indicator of NO secretion. Culture media (100 μL) were mixed with 10 μL of 2, 3-diaminonaphthalene (0.05 mg/mL in 0.62 M aqueous HCl solution). After 15 min incubation in the dark, 5 μL of a 3 M aqueous NaOH solution was added to each well. Then, absorbance of the mixture at 450 nm was measured with a microplate reader.

2.3.5 Screening for NO production inhibitors

For screening of the 1364-compound NCI Diversity Set II library, the murine

macrophage RAW 264.7 based nitric oxide (NO) assay was used. The library compounds (final concentration were 10 μM) were added in duplicate. Hits were qualified as compounds that reduced LPS-induced nitric oxide (NO) production by 90% or more at a concentration of 10 μM. The inhibition rate (%) of NO release was determined using the following formula: Inhibition (%) = (OD450 value of LPS and vehicle treated group–OD450 value of compound treated group)/ (OD450 value of LPS and vehicle treated group-OD450 value of vehicle treated group) ×100. For validation, positive and negative control wells were also include that consisted of LPS-activated cells without inhibitor and LPS-activated cells with TAK242.

To ascertain relative potencies of the most effective hits, we further assessed the activities of the compounds that showed more than 90% inhibition of the NO production at the initial concentration of 10 μM. Secondary screening was performed using the Nitric Oxide assay at a compound concentration of 1 μM in triplicate. Compounds exhibiting the inhibitory by 80% or more were subjected to a toxicity analysis.

2.3.6 TLR specificity test

This assay was performed using the same protocol with "2.3.4 Measurement of NO" as previously described. Instead of LPS, polyriboinosinic:polyribocytidylic acid (Poly(I:C)), FSL-1 ((S,R)-(2,3-bispalmitoyloxypropyl)-Cys-Gly-Asp-Pro-Lys-His-Pro-Lys-Ser-Phe), R848 (4-amino-2-(ethoxymethyl)-α, α-dimethyl-1H-imidazo[4,5-c]quinoline-1-ethanol) and Pam_3CSK_4 (N-palmitoyl-S-[2,3-bis(palmitoyloxy)-(2RS)-

propyl]-[R]-cysteinyl-[S]-seryl-[S]-lysyl-[S]-lysyl-[S]-lysyl-[S]-lysine·3HCl) were used to selectively activate TLR3, TLR2/6, TLR7 and TLR1/2, respectively.

2.3.7 Dual Luciferase report assay

NF-κB dual luciferase reporter BV-2 cells were cultured in DMEM medium supplemented with 10% FBS, penicillin (100 unit/mL), streptomycin (100 μg/mL) and puromycin (3 μg/mL). BV-2 reporter cells were seeded at a density of 1×10^4 cells/well in 96-well plates. After 24 h incubation, medium was changed to Opti-MEM medium supplemented with 0.5% FBS and indicated concentration of compound was added, and then stimulated with 200 ng/mL of LPS. After further 24 h treatment, the NF-κB activity was analyzed by Dual-Glo Luciferase Assay System. The ratio of Firefly luciferase activity to Renilla luciferase activity represents the NF-κB activity.

2.3.8 Measurement of cytokines

RAW 264.7 cells (5×10^5/well) pretreated with or without LPS, followed by treatment with indicated compound in 6-well plates. After 24 h, supernatants were harvested, clarified by centrifugation, and stored at -80℃ prior to analysis. Cells were collected and lysed by mammalian protein extraction reagent (Thermo Scientific, Rockford, IL, USA). Cell lysates were centrifuged at 1.3k rpm for 30 minutes at 4℃, the supernatant were collected and stored at -80℃ prior to analysis. RAW 264.7 cell lysate IL-1β levels and RAW 264.7 cell media TNF-α levels were

determined by enzyme-linked immunosorbent assay (ELISA) (BD Bioscience, San Diego, CA, USA) following the manufacturer's protocol. The total amount of the IL-1ß was normalized to the total protein concentration.

2.3.9 Molecular modeling

Docking stimulation of **1** was carried out using the Glide 5.6 program.[29, 34]and the crystal structure of human TLR4-MD-2-LPS was cited from Protein Data Bank (3FXI).[5] The TLR4-MD-2-LPS complex orientations and conformations were prepared using standard Glide protocol and compound **1** was created with multiple conformational states and all possible rotational orientations.[35] **1** was final docked using standard Glide.

2.4 References:

1. Akira, S.; Uematsu, S.; Takeuchi, O., Pathogen recognition and innate immunity. *Cell* **2006,** *124* (4), 783-801.
2. Akira, S., TLR signaling. *Curr. Top Microbiol. Immunol.* **2006,** *311*, 1-16.
3. Dauphinee, S. M.; Karsan, A., Lipopolysaccharide signaling in endothelial cells. *Lab Invest.* **2006,** *86* (1), 9-22.
4. Raetz, C. R.; Whitfield, C., Lipopolysaccharide endotoxins. *Annu. Rev. Biochem.* **2002,** *71*, 635-700.
5. Park, B. S.; Song, D. H.; Kim, H. M.; Choi, B. S.; Lee, H.; Lee, J. O., The structural basis of lipopolysaccharide recognition by the TLR4-MD-2 complex. *Nature* **2009,** *458* (7242), 1191-U130.
6. Saitoh, S.; Akashi, S.; Yamada, T.; Tanimura, N.; Kobayashi, M.; Konno, K.; Matsumoto, F.; Fukase, K.; Kusumoto, S.; Nagai, Y.; Kusumoto, Y.; Kosugi, A.; Miyake, K., Lipid A antagonist, lipid IVa, is distinct from lipid A in interaction with Toll-like receptor 4 (TLR4)-MD-2 and ligand-induced TLR4 oligomerization. *Int. Immunol.* **2004,** *16* (7), 961-9.
7. Collins, T.; Read, M. A.; Neish, A. S.; Whitley, M. Z.; Thanos, D.; Maniatis, T., Transcriptional regulation of endothelial cell adhesion molecules: NF-kappa B and

cytokine-inducible enhancers. *Faseb J* **1995,** *9* (10), 899-909.
8. Zhang, G.; Ghosh, S., Toll-like receptor-mediated NF-kappaB activation: a phylogenetically conserved paradigm in innate immunity. *J. Clin. Invest.* **2001,** *107* (1), 13-9.
9. Karin, M.; Ben-Neriah, Y., Phosphorylation meets ubiquitination: the control of NF-[kappa]B activity. *Annu. Rev. Immunol.* **2000,** *18*, 621-63.
10. Tian, B.; Brasier, A. R., Identification of a nuclear factor kappa B-dependent gene network. *Recent Prog. Horm. Res.* **2003,** *58*, 95-130.
11. Hawiger, J., Innate immunity and inflammation: a transcriptional paradigm. *Immunol. Res.* **2001,** *23* (2-3), 99-109.
12. Hennessy, E. J.; Parker, A. E.; O'Neill, L. A., Targeting Toll-like receptors: emerging therapeutics? *Nat. Rev. Drug. Discov.* **2010,** *9* (4), 293-307.
13. Guo, L. H.; Schluesener, H. J., The innate immunity of the central nervous system in chronic pain: the role of Toll-like receptors. *Cell Mol. Life Sci.* **2007,** *64* (9), 1128-36.
14. Lucas, S. M.; Rothwell, N. J.; Gibson, R. M., The role of inflammation in CNS injury and disease. *Br. J. Pharmacol.* **2006,** *147 Suppl 1*, S232-40.
15. Friedman, W. J., Cytokines regulate expression of the type 1 interleukin-1 receptor in rat hippocampal neurons and glia. *Exp Neurol* **2001,** *168* (1), 23-31.
16. Rocha, V. Z.; Libby, P., Obesity, inflammation, and atherosclerosis. *Nat. Rev. Cardiol.* **2009,** *6* (6), 399-409.
17. Serhan, C. N.; Savill, J., Resolution of inflammation: the beginning programs the end. *Nat Immunol* **2005,** *6* (12), 1191-7.
18. Carcillo, J. A., Pediatric septic shock and multiple organ failure. *Crit. Care Clin.* **2003,** *19* (3), 413-40, viii.
19. Buchanan, M. M.; Hutchinson, M.; Watkins, L. R.; Yin, H., Toll-like receptor 4 in CNS pathologies. *J. Neurochem.* **2010,** *114* (1), 13-27.
20. Ii, M.; Matsunaga, N.; Hazeki, K.; Nakamura, K.; Takashima, K.; Seya, T.; Hazeki, O.; Kitazaki, T.; Iizawa, Y., A novel cyclohexene derivative, ethyl (6R)-6-[N-(2-Chloro-4-fluorophenyl)sulfamoyl]cyclohex-1-ene-1-carboxylate (TAK-242), selectively inhibits toll-like receptor 4-mediated cytokine production through suppression of intracellular signaling. *Mol. Pharmacol.* **2006,** *69* (4), 1288-95.
21. Mullarkey, M.; Rose, J. R.; Bristol, J.; Kawata, T.; Kimura, A.; Kobayashi, S.; Przetak, M.; Chow, J.; Gusovsky, F.; Christ, W. J.; Rossignol, D. P., Inhibition of endotoxin response by e5564, a novel Toll-like receptor 4-directed endotoxin antagonist. *J. Pharmacol. Exp. Ther.* **2003,** *304* (3), 1093-102.
22. Rice, T. W.; Wheeler, A. P.; Bernard, G. R.; Vincent, J. L.; Angus, D. C.; Aikawa, N.; Demeyer, I.; Sainati, S.; Amlot, N.; Cao, C.; Ii, M.; Matsuda, H.; Mouri, K.; Cohen, J., A randomized, double-blind, placebo-controlled trial of TAK-242 for the treatment of severe sepsis. *Crit. Care Med.* **2010,** *38* (8), 1685-94.
23. Bloomberg Web site. http://www.bloomberg.com/news/2011-01-25/eisai-s-sepsis-drug-eritoran-fails-to-save-more-lives-in-final-stage-study.html. Posted January 25, 2011

24. Nussler, A. K.; Glanemann, M.; Schirmeier, A.; Liu, L.; Nussler, N. C., Fluorometric measurement of nitrite/nitrate by 2,3-diaminonaphthalene. *Nat. Protoc.* **2006,** *1 (*5), 2223-6.
25. Ngamwongsatit, P.; Banada, P. P.; Panbangred, W.; Bhunia, A. K., WST-1-based cell cytotoxicity assay as a substitute for MTT-based assay for rapid detection of toxigenic Bacillus species using CHO cell line. *J. Microbiol. Methods* **2008,** *73 (*3), 211-5.
26. Takashima, K.; Matsunaga, N.; Yoshimatsu, M.; Hazeki, K.; Kaisho, T.; Uekata, M.; Hazeki, O.; Akira, S.; Iizawa, Y.; Ii, M., Analysis of binding site for the novel small-molecule TLR4 signal transduction inhibitor TAK-242 and its therapeutic effect on mouse sepsis model. *Br. J. Pharmacol.* **2009,** *157 (*7), 1250-62.
27. Guterman, L., COVALENT DRUGS FORM LONG-LIVED TIES. Ch*emical & Engineering News Archive* **2011,** *89 (*36), 19-26.
28. Liu, S.; Kielian, T., Microglial activation by Citrobacter koseri is mediated by TLR4- and MyD88-dependent pathways. *J. Immunol* **2009,** *183 (*9), 5537-47.
29. Cheng, K.; Wang, X.; Yin, H., Small-molecule inhibitors of the TLR3/dsRNA complex. *J. Am. Chem. Soc.* **2011,** *133 (*11), 3764-7.
30. Bevan, D. E.; Martinko, A. J.; Loram, L. C.; Stahl, J. A.; Taylor, F. R.; Joshee, S.; Watkins, L. R.; Yin, H., Selection, Preparation, and Evaluation of Small-Molecule Inhibitors of Toll-Like Receptor 4. *ACS Med. Chem. Lett.* **2010,** *1 (*5), 194-198.
31. Dziarski, R.; Gupta, D., Role of MD-2 in TLR2- and TLR4-mediated recognition of Gram-negative and Gram-positive bacteria and activation of chemokine genes. *J. Endotoxin. Res.* **2000,** *6 (*5), 401-5.
32. Adediran, S. A.; Cabaret, D.; Lohier, J. F.; Wakselman, M.; Pratt, R. F., Substituted aryl malonamates as new serine beta-lactamase substrates: structure-activity studies. *Bioorg. Med. Chem.* **2010,** *18 (*1), 282-91.
33. Chang, S.; Yin, S. L.; Wang, J.; Jing, Y. K.; Dong, J. H., Design and synthesis of novel 2-phenylaminopyrimidine (PAP) derivatives and their antiproliferative effects in human chronic myeloid leukemia cells. *Molecules* **2009,** *14 (*10), 4166-79.
34. Glide, version 5.6; Schrödinger, LLC: New York, NY, 2010.
35. Halgren, T. A.; Murphy, R. B.; Friesner, R. A.; Beard, H. S.; Frye, L. L.; Pollard, W. T.; Banks, J. L., Glide: a new approach for rapid, accurate docking and scoring. 2. Enrichment factors in database screening. *J. Med. Chem.* **2004,** *47 (*7), 1750-9.

CHAPTER 3

Discovery, synthesis and optimization of Toll-like Receptor 8 inhibitors with downstream signaling evaluation

3.1 Introduction

The innate immunity response functions as the very first line of defense against pathogenic microorganisms, and has also been implicated in autoimmune-mediated inflammatory diseases. This response is primarily triggered by activating TLRs with molecules of foreign origin, or in the case of immune-mediated inflammatory diseases, with molecules released by damaged host cells. The intracellular TLRs, including TLR3, TLR7, TLR8, and TLR9, are intrinsically capable of detecting different classes of bacterial, viral, and endogenous nucleic acids. TLR3 recognizes dsRNA, TLR7 and 8 are activated by ssRNAs and imidazoquinoline derivatives, whereas TLR9 is activated by unmethylated ssDNA.[1]

There is now considerable emerging evidence that nucleic acids recognition through endosomal TLRs can contribute significantly to the pathogenesis of a variety of autoimmune diseases, such as systemic lupus erythematosus (SLE).[2, 3] SLE patients have circulating DNA- and RNA-containing immune complexes in the blood,[4] which pDCs via endosomal TLR7 and TLR9, inducing proinflammatory

cytokine production and disease development.[2, 3] TLR3 signaling is an essential contributor to the virus-induced autoimmune diseases, such as viral hepatitis, glomerular diseases.[5, 6] Inhibition of endosomal TLR signaling pathways has a great therapeutic potential for the treatment of autoimmune diseases.[7]

In humans, TLR7 and TLR8 are phylogenetically and structurally related. However, differences have been identified between TLR7 and TLR8, in terms of expression pattern among human blood cells,[8] preference for specific bases within the ssRNA ligand,[9] and secondary structure prior to ligand binding.[10, 11] It is reported that activation of human TLR8 by endogenous ligands leads to a different spectrum of inflammatory diseases than the one resulting from activation of TLR7.[12] Based on gene polymorphism studies, TLR8 has been implicated in human inflammatory diseases, including rheumatoid arthritis (RA), antiphospholipid syndrome and inflammatory bowel disease (IBD).[13-15] Additionally, TLR8 signaling promotes RA both in human TLR8 transgenic mice and in human patients.[12] The development of novel small molecules that inhibit TLR8 and the subsequent pro-inflammatory response is a potential approach for treatment of autoimmune diseases.

Despite the potential therapeutic utility, no high throughput screens for synthetic compounds that inhibit TLR8 have been reported. In this chapter, the identification of novel small molecule TLR8 antagonists by HTS of small molecule library is presented. Synthesis was developed to investigate the structure-activity relationships (SAR) of a novel series of pyrazolo[1,5-

a]pyrimidine derivatives as TLR8 antagonists. Further studies indicate that these compounds inhibit mRNA expression levels of several cytokines in HEK-Blue TLR8 cells, and TNF-α production in human monocytes THP-1 cells.

3.2 Results and discussion

3.2.1 High-throughput screening for inhibitors of TLR8 signaling

Compound library

The Maybridge HitFinder library of 14,400 small molecules was chosen to screen for small-molecule inhibitors of TLR8 signaling. The library compounds follow the Lipinski guidelines for "drug-likeness" and have properties that include: no more than 5 hydrogen bond donors, no more than 10 hydrogen acceptors, a molecular weight less than 500, and an octanol-water partition coefficient log P less than 5.[16]

Different controls (both positive and negative) are necessary to obtain meaningful and reliable results from HTS. Triptolide, a small molecule from a Chinese herb, inhibits the NF-κB activity via blocking the association of p65 subunit.[17] With HTS secreted embryonic alkaline phosphatase (SEAP) assay, we used triptolide as positive control due to its good concentration-dependent effects on the NF-κB activation in HEK-Blue TLR cells. Triptolide completely inhibited the NF-κB signal at a concentration of 25 nM, with the IC_{50} value of 50.3 ± 4.5 nM.

Z'-Factor determination

To determine if the TLR8 inhibitor screening is robust enough to distinguish between a positive and negative control, the Z'-factor statistical parameter was determined. The ideal and highest score of a Z'-factor is 1 but a score above 0.5 considered acceptable for HTS. A low Z'-factor, below 0.5 is considered a marginal assay that might not suitable for HTS. For cell-based assays, Z'-factor above 0.5 is considered good. The statistical Z'-factor for high-throughput assays was calculated by using the following formula: [18]

$$Z' = 1 - \frac{3\sigma c_+ + 3\sigma c_-}{|\mu c_+ - \mu c_-|}$$

σ = standard deviation, μ = mean, c+ = Triptolide (25 nM), and c-= 0.4% DMSO

The Z'-factor was determined by dividing a 384 well plate into 3 parts, where the right 32 wells contain medium only, the middle top 176 wells are positive controls and the left 176 wells are negative controls. For the first and second measurements of Z'-factor, the values were 0.57 and 0.71 respectively, indicating the robustness of the HEK-blue TLR8 cell-based screening assay.

Maybridge HitFinder library screening results

As previously described, a robust high-throughput assay using HEK-Blue TLR8 cells to screen for inhibitors of TLR8 signaling was developed. With the help of Dr. Wei Wang and Dr. Xiang Wang in the High-Throughput Screening Core Facility, Maybridge HitFinder library was screened. Both Dr. Wangs provided guidance in using screening instruments and analyzing screening data. The screening protocol is summarized in the flowchart of **Figure 3-1**, and

further details are provided in the experimental section. In the primary HTS, compounds were considered active if they decreased the SEAP levels, indicated by a decrease in absorbance. The positive control triptolide, decreased R848 induced SEAP level by 90% at 25 nM was used to perform the data analysis. For the primary screening and other assays, negative control wells and positive control wells were included on every plate. The data for each library compound was converted into root mean square (RMS) values, and the Z-score of each library compound was calculated based on the distribution of the RMS (**Figure 3-2**). We perform hit selection based on the rank of the compounds' Z-score. The top 150 compounds in the Z-score ranking were considered hits and chosen for confirmation in further studies.

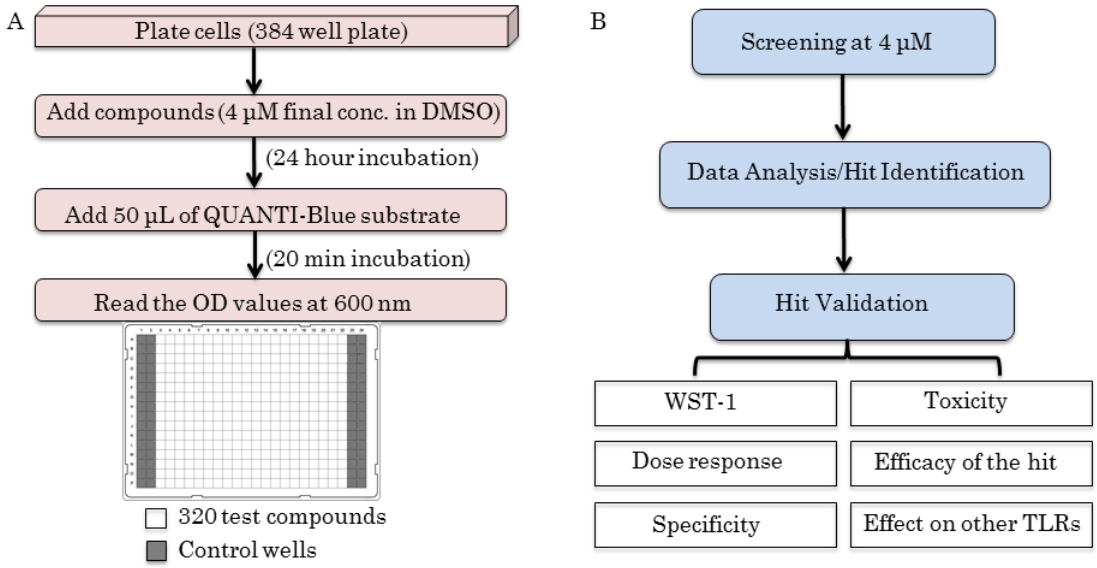

Figure 3-1. Flowcharts illustrating the process of the HTS: A) Step by Step flow chart of the HTS protocol; B) Critical path for the TLR8 inhibitor HTS.

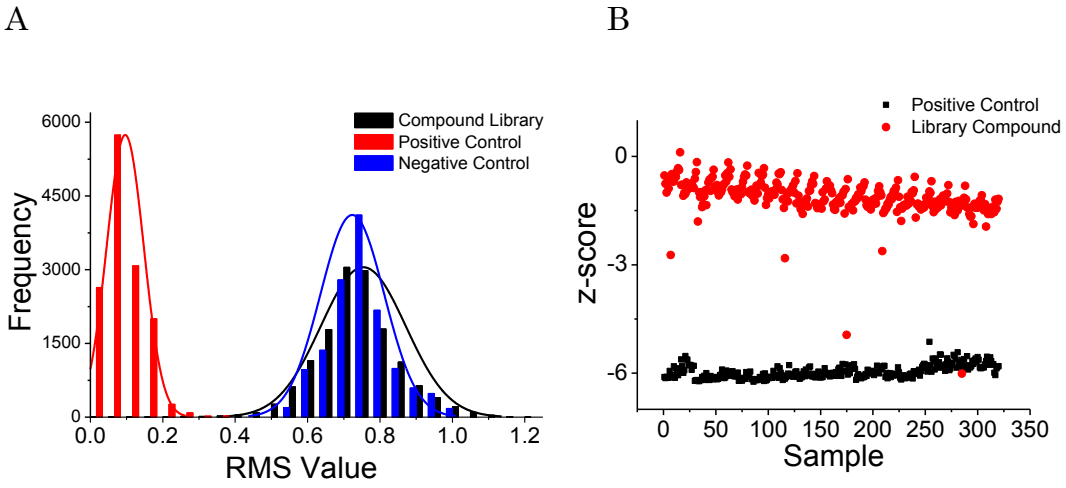

Figure 3-2. TLR8 antagonist screening results: A) Gaussian distribution of the screening results; B) Z-score from a representative plate is shown for both library compounds and positive control.

After the primary screen, the TLR8 HTS data was compared with the TLR5 inhibitor screening (described in Chapter 4) data. By comparing the two sets of data, compounds that exhibit assay interference, toxicity, or nonspecific effects were ruled out. 72 compounds were chosen for further 3-dose (4, 8 and 16 μM) retest confirmation and toxicity test. These 72 compounds were manually picked from the original 10 mM library (a process known as cherry picking). 16 out of 72 were confirmed to decrease TLR8 induced SEAP levels and without obvious cytotoxicity problems up to 16 μM. These 16 compounds were further tested in secondary assays; including more detailed dose dependent tests and specificity tests. Luckily, only 3 compounds fell out of consideration after running the specificity assay. 13 compounds acted in a dose-dependent manner to down regulate TLR8 induced SEAP levels with the IC_{50}s lower than 16 μM and no obvious inhibition on other

TLRs. More interestingly, some compounds contain the same core scaffold (**Figure 3-3**). For example, **40-D4** and **43-H4** share the same pyrazolo[1,5-*a*]pyrimidine core structure; **42-E20** shares the same structural similarity to **54-E6** except that it has a phenol group instead of the carbamate ester; **56-G5**, **169-B11** and **169-E2** all contain 4-phenyl-1,2,4-triazole structure. Due to the fact that the structural similarity between compounds is likely meaning the compounds have bioactivity against the same target and reveals some SAR information. Thus, we selected 6 compounds (3 different scaffold families) to purchase from Maybridge for further evaluation.

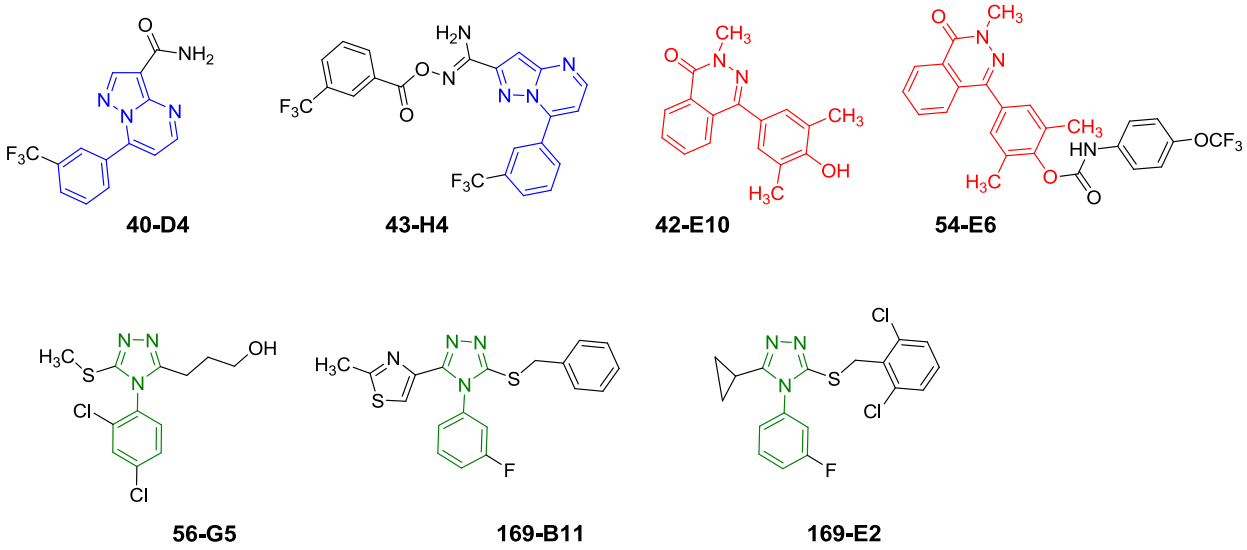

Figure 3-3. Chemical structures of representative hit compounds.

The 6 compounds obtained from Maybridge were assayed for inhibition of TLR8-induced NF-κB, toxicity, and pathway specificity in HEK-Blue cells. **Figure 3-4** represents the data obtained from testing different doses of each compound in the various assays. The IC_{50} values of these compounds were determined to be 130

nM to 1.4 μM. Also, no compounds showed significant inhibitory activities towards other individual TLR signaling, and no cytotoxicity was observed (**Figure 3-5**).

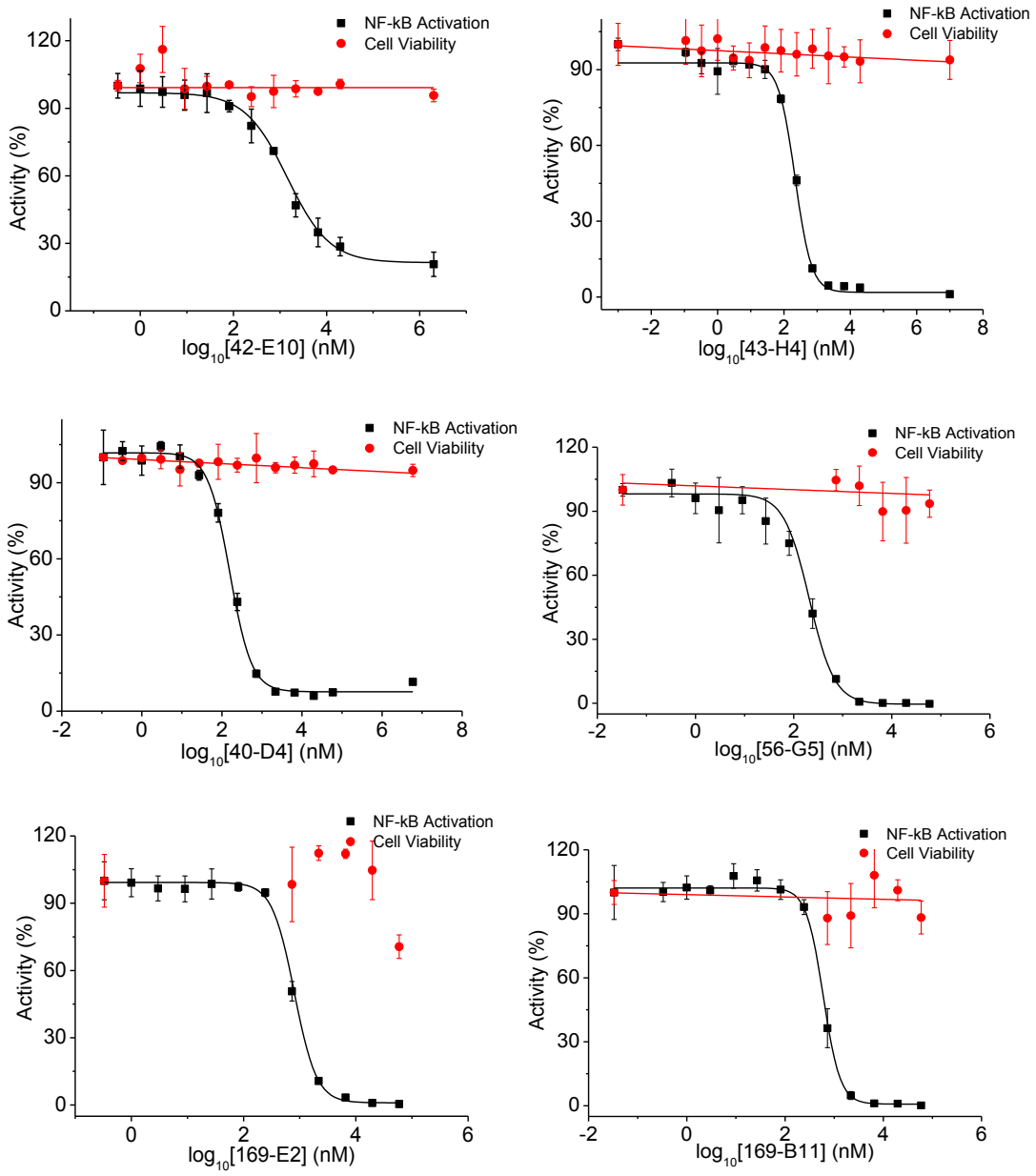

Figure 3-4. TLR8-mediated NF-κB inhibitory activities and cytotoxic effects of purchased hit compounds. Dose-dependent inhibition of R848 induced NF-κB activation in HEK-blue TLR8 cells by purchased hit compounds along with the cytotoxicity test.

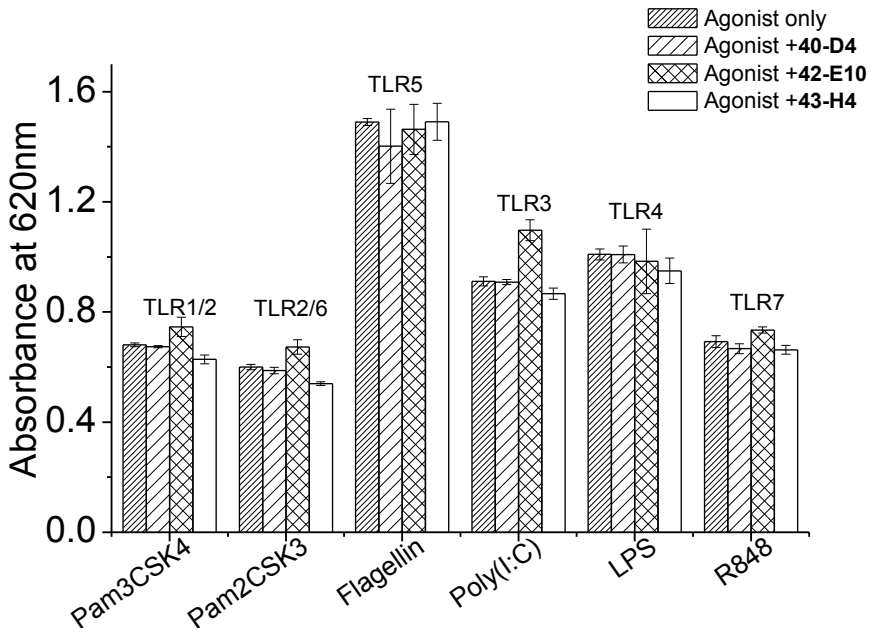

Figure 3-5. Representative specificity test for the purchased hit compounds.

Further evaluation and optimization of these 6 compounds and other hit compounds are ongoing in our laboratory. The following work is mainly focused on the structure-activity relationship study of **40-D4** and **43-H4**, and the effect of pyrazolo[1,5-*a*]pyrimidine derivatives on TLR8 downstream signaling.

3.2.2 Rationale for the design of pyrazolo[1,5-*a*]pyrimidine analogs

40-D4 and **43-H4** have shown very promising specific TLR8 signaling inhibitory activities *in vivo* with no toxic effects. Obviously, **40-D4** bears a similar structure with **43-H4** because both of them share a 7-phenylpyrazolo[1,5-*a*]pyrimidine scaffold. Pyrazolo[1,5-*a*]pyrimidine and derivatives provide a wide spectrum of biological activities and are seen in many bioactive scaffolds as privileged structures.[19-21] Since **40-D4** is slightly more potent than **43-H4**, we

focused on **40-D4** as inspiration for the development of a series of pyrazolo[1,5-*a*]pyrimidine derivatives. In order to identify the key aspects of the structure, 7-phenylpyrazolo[1,5-*a*]pyrimidine scaffold may be conveniently dissected into three regions, as indicated in **Figure 3-6**. Region A, a substituted phenyl moiety, can be modified to explore the impact of electron density, substitution positions and other heterocyclic rings on the potency. Region B can be modified to explore the impact of substitution connectivity to Region A, and other 5,6-bicyclic heterocycles. Region C can be modified to explore various carbonyl substituents, and their effect on potency.

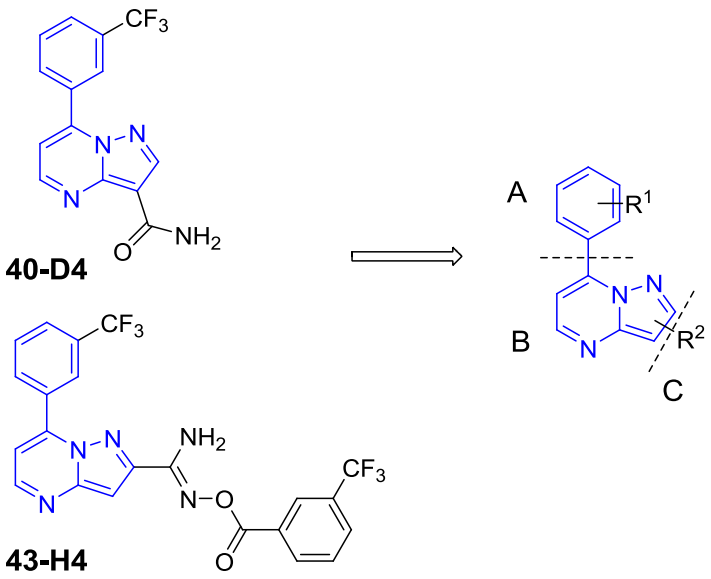

Figure 3-6. Rationale for the design of pyrazolo[1,5-*a*]pyrimidine analogs. The shared core structure divided into three regions that are subjected to structural modification.

3.2.3 Chemical synthesis

For initial SAR studies inspired by **40-D4**, compounds **8a-p** were designed and synthesized. In general, different commercially available aryl methyl ketones were condensed with dimethylformamide dimethylacetal (DMF-DMA) to yield the

enaminones **3a-n**, which react readily with 5-amino-4-ethoxycarbonyl-1H-pyrazole in refluxing glacial acetic acid to give the corresponding ethyl 7-arylpyrazolo[1,5-*a*]pyrimidine-3-carboxylate **4a-n** in good yields, one regioisomer (**5**) of the product was also formed in this step (representative structure is shown in **Table 3-1**). The resultant compounds were converted to the corresponding acid **6a-n** by hydrolysis with sodium hydroxide. Treatment of **6a-n** with thionyl chloride afforded **7a-n**. Then, **7a-n** reacted with appropriate commercially available amines to give **8a-p** (**Scheme 3-1**).

The series of indole scaffold derivatives **14a-c** were prepared as shown in **Scheme 3-2**. 7-Bromo-1*H*-indole reacted with trifluoroacetic anhydride to afford **10**. A subsequent Suzuki coupling was used to attach substituted phenyl substituents at the C-7 position of the indole core **11a-c**. The resultant **11a-c** were hydrolyzed to the corresponding carboxylic acids **12a-c** under basic condition. Then **12a-c** reacted with thionyl chloride to provide **13a-c**. In the final step, target products **14a-c** were synthesized by treating **13a-c** with various commercial available amines.

In order to perform the fluorescent polarization assay to determine if the pyrazolo[1,5-*a*]pyrimidine derivative can disrupt the binding of R848 to TLR8 protein, fluorophore labeled R848 was synthesized in 6 steps (**Scheme 3-3**). The nitration of commercially available 4-quinolinol **14** gave 3-nitro-4-quinolinol (**15**). The conversion of **15** to 3-chloro-4-quinolinol was completed in thionyl chloride, and subsequent treatment with *tert*-butyl-4-aminobutylcarbamate provided **16**. Then **16** underwent catalytic hydrogenation to give **17**. The amine-intermediate **17** was

coupled to ethoxyacetyl chloride, and subsequent with ring closure reaction to give **18**. Treatment of **18** with *meta*-chloroperoxybenzoic acid (*m*CPBA), following by amination to provide *tert*-butyloxycarbonyl (Boc) protected intermediate, then the intermediate underwent deprotection under acidic condition to afford **19**. In the final step, **19** is coupled with commercially available TAMRA, SE to provide the final fluorophore labeled R848. The fluorophore TAMRA is a mixture of two regioisomers. The structures depicted here represent the 5-regioisomer, but the 6-regioisomer is also possible.

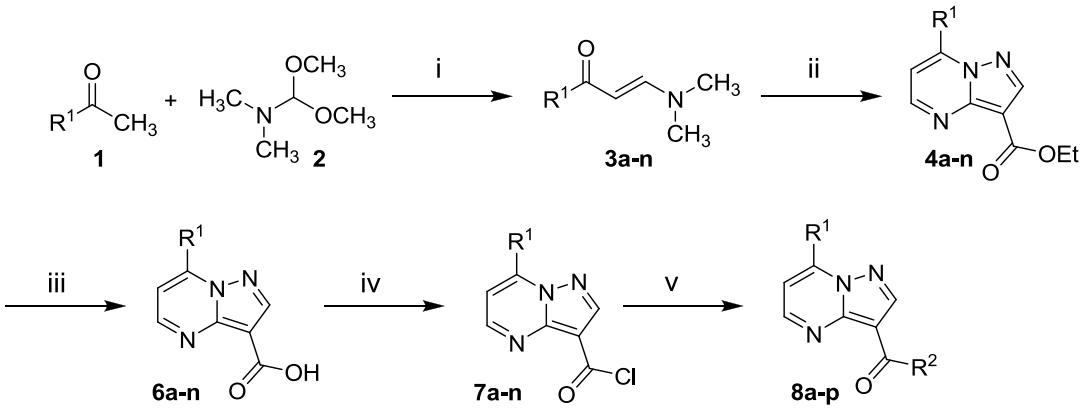

Scheme 3-1. Synthesis of pyrazolo[1,5-*a*]pyrimidine derivative. Reagent and conditions: (i) reflux; (ii) 5-amino-4-ethoxycarbonyl-1*H*- pyrazole, AcOH, reflux; (iii) NaOH, H_2O/EtOH, 80 °C; (iv) $SOCl_2$, reflux; (v) DCM, NH_3 in THF (**8m**), or DCM, methylamine in THF (**8o**), or DCM, diethylamine (**8p**).

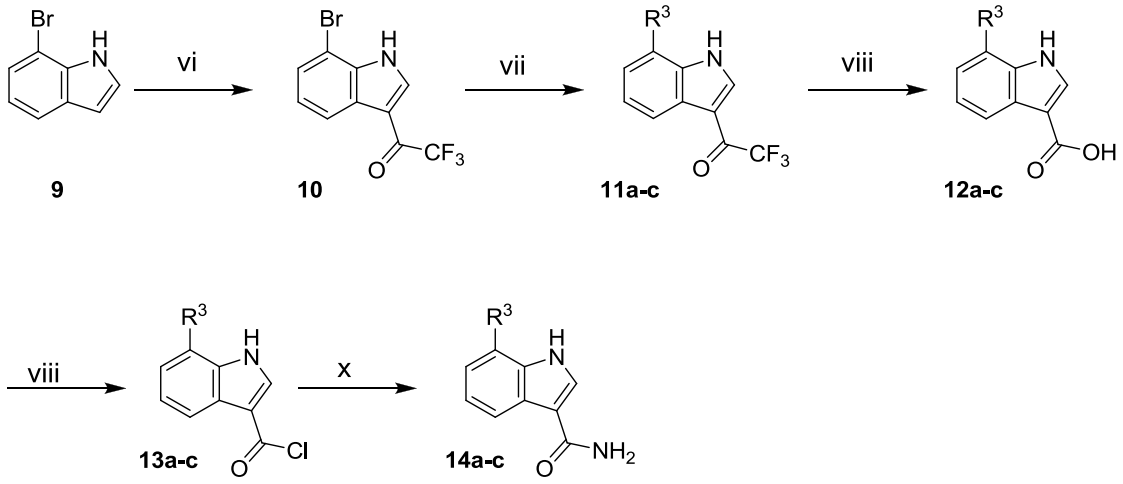

Scheme 3-2. Synthesis of indole derivatives. Reagent and conditions: (vi) trifluoroacetic anhydride, DMF; (vii) R_3-$B(OH)_2$, K_2CO_3, $Pd(PPh_3)_4$, 1,4-dioxane, 80 °C; (viii) in NaOH aq, H_2O/EtOH, 80 °C, then HCl; (viiii) $SOCl_2$, reflux; (x) DCM, NH_3 in THF.

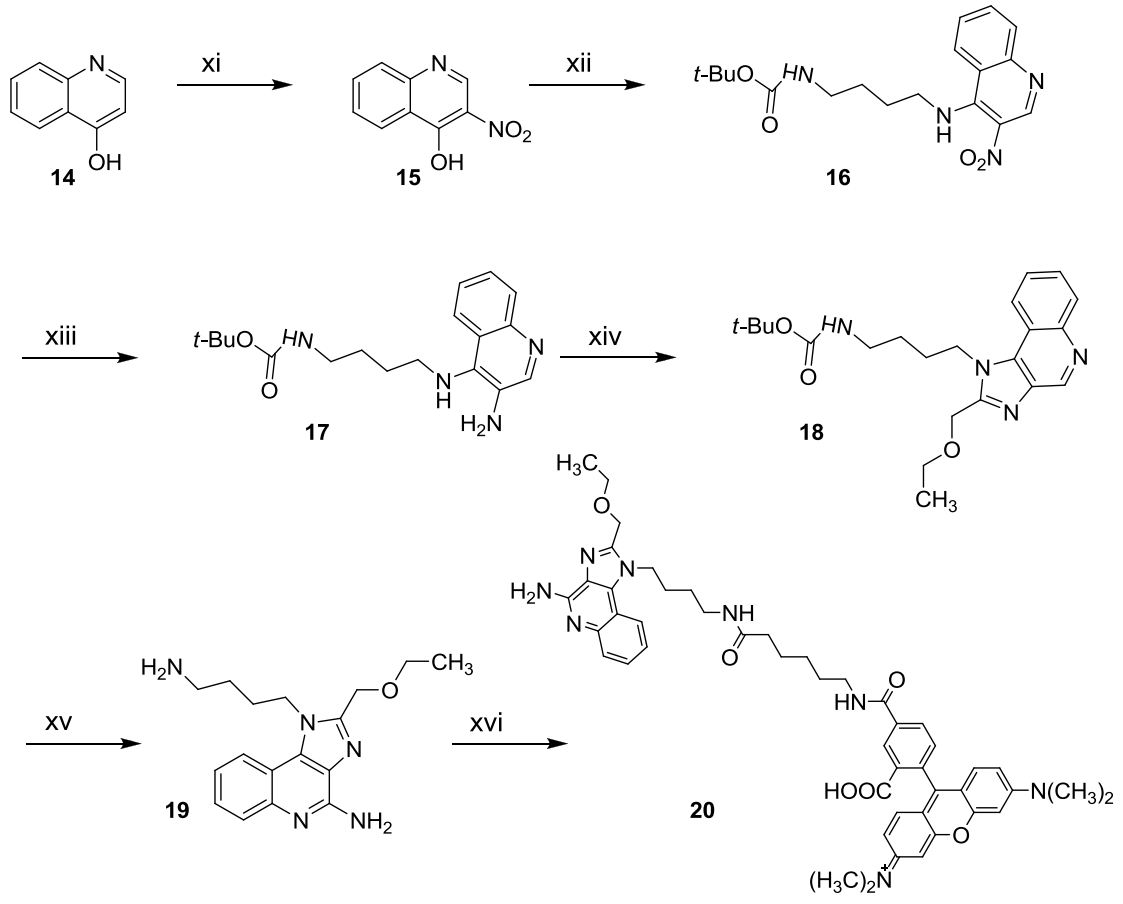

Scheme 3-3. Synthesis of fluorophore-labeled R848. Reagent and conditions: (xi) propionic acid, HNO_3, 125 °C; (xii) (1) $SOCl_2$, CH_2Cl_2, DMF, (2) *tert*-butyl 4-aminobutylcarbamate, Et_3N, CH_2Cl_2; (xiii) H_2, 5% Pd/C, MeOH, EtOAc; (xiv) (1) Ethoxyacetyl chloride, Et_3N, CH_2Cl_2, (2) EtOH, reflux; (xv) (1) *m*CPBA, CH_2Cl_2, (2) *p*-toluenesulfonyl chloride, NH_4OH, CH_2Cl_2, (3) 4M HCl in 1,4-dioxane (4) NaOH, H_2O; (xvi) 5(6)-TAMRA-X, Et_3N, DMSO.

3.2.4 Bioactivity evaluation

All synthesized compounds were tested for inhibitory activity against TLR8 signaling using HEK-Blue TLR8 cells. The same SEAP reporter assay has been used to monitor the R848 induced NF-κB activation. For IC_{50} determination, a range of concentrations of compounds was tested, and the readout value changes in activation versus controls were fitted to inverse sigmoidal curve in Orgin 8.0.

The initial round of **40-D4** modifications aimed at improving inhibitory potency via structural variations at R^1. Different functional groups were attached at different positions of the phenyl ring to affect the electron density, and hydrogen-bond donor/accepter ability of the moiety, thereby determining the role of this group in the binding site.

3-Position substitutions of the phenyl ring seem more active than the 2- and 4- positions. For example, the trifluoromethyl group in 3-position exhibited a higher potency than that of the 2- and 4- positions (**8b**, **8c**). However, by introducing a second trifluoromethyl group in 5-position, the inhibitory activity was similar to that of the **40-D4**. With the absence of any substituent on the phenyl ring (**8d**), the activity decreased by greater than 5-fold. Replacement of the phenyl group with other heterocycles such as pyridine (**8n**) led to loss of the inhibitory activity. For

this reason, **8n** was used as the negative control in the subsequent biological evaluations.

A variety of substituents replacing the trifluoromethyl group in 3-position were synthesized and tested. Substituents with varying electron-withdrawing properties similar to the trifluoromethyl group, such as nitro (**8e**), chloro (**8g**) and fluoro (**8f**) led to less potent compounds. This was also true for substituents with strong electron-donating properties such as methoxy (**8k**, **8l**). Incorporation of three fluoro substitutions on the phenyl ring produces a similarly potent compound **8j**. Interestingly, the introduction of a methyl group on the 3-position (**8m**) increases TLR8 inhibitory potency by 2-fold as compared to the hit compound **40-D4** (**8a**), while the corresponding ethyl ester analog, **4m**, is also slightly more active than the hit. The high potency of **8m** is perhaps due to nonpolar property and the size of the methyl group.

The bioactivity assay was also performed on the ester analogs, due to the desirable physicochemical properties of esters, for instance, better permeability and solubility. Generally, the SAR result of the esters followed the same trend as that of the amide. However comparing with the corresponding amide, the ester is usually less potent (**Table 3-1**). It was also determined that the acid derivatives (**6m**) were less active than the corresponding ester and amide analogs (**8m**). Additionally, the byproduct of the ethyl 7-arylpyrazolo[1,5-*a*]pyrimidine-3-carboxylate formation reaction is also the regioisomer of the desired ester. However the regioisomer (**5**) did not show any inhibitory activity even at 40 μM, which

suggested the substitution position on the pyrazolo[1,5-*a*]pyrimidine is critical for the bioactivity.

Furthermore, introduction of alkyl substitutions on the amide nitrogen atom led to significant reductions of activity. The secondary amide analog (**8o**) showed a 25-fold reduction in potency, while the tertiary amide analog (**8p**) had no significant activity even at 20 μM possibly due to the steric clash between the bulky amide and the binding site. Lastly, we decided to switch the core structure to indole nucleus since indole is also a pyrrole-containing fused aromatic heterocyclic ring and possess interesting biological activities.[22] The three indole containing amide analogs (**14a-c**) showed a complete loss of TLR8 inhibitory activities, suggested that the pyrozolo[1,5-*a*]pyrimide core plays an essential role in their activity.

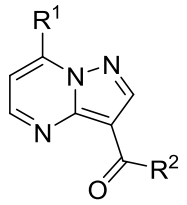

No.	R^1	R^2	IC_{50} [μM][a]
8a	3-CF_3-C_6H_4-	-NH_2	0.13 ± 0.03
8b	2-CF_3-C_6H_4-	-NH_2	0.23 ± 0.14
8c	4-CF_3-C_6H_4-	-NH_2	1.22 ± 0.17
8d	Phenyl	-NH_2	0.76 ± 0.23
8e	3-NO_2-C_6H_4-	-NH_2	0.22 ± 0.07
8f	3-F-C_6H_4-	-NH_2	0.45 ± 0.09
8g	3-Cl- C_6H_4-	-NH_2	0.28 ± 0.11
8h	3-NO_2-4-NHMe-	-NH_2	0.73 ± 0.11
8i	3,5-diCF_3- C_6H_3-	-NH_2	0.25 ± 0.13
8j	2,4,5-triF- C_6H_2-	-NH_2	0.13 ± 0.05
8k	2-OMe- C_6H_4-	-NH_2	2.31± 0.22
8l	3-OMe- C_6H_4-	-NH_2	1.2 ± 0.16

8m	3-Me-C_6H_4-	-NH_2	0.07 ± 0.01
8n	3-Pyridyl	-NH_2	>20
8o	3Me	-NHMe	1.7 ± 0.3
8p	3Me	-NEt_2	>20
4a	3-CF_3-C_6H_4-	-OEt	0.20 ± 0.08
4b	2-CF_3-C_6H_4-	-OEt	0.23 ± 0.12
4c	4-CF_3-C_6H_4-	-OEt	0.70 ± 0.12
4d	Phenyl	-OEt	0.90 ± 0.15
4e	3-NO_2-C_6H_4-	-OEt	0.27 ± 0.08
4f	3-F-C_6H_4-	-OEt	0.60 ± 0.11
4g	3-Cl-C_6H_4-	-OEt	0.37 ± 0.10
4h	3-NO_2-4-NHMe-	-OEt	0.92 ± 0.17
4i	3,5-diCF_3- C_6H_3-	-OEt	0.75 ± 0.09
4j	2,4,5-triF- C_6H_2-	-OEt	0.90 ± 0.15
4k	2-OMe- C_6H_4-	-OEt	1.21 ± 0.22
4l	3-OMe- C_6H_4-	-OEt	1.46 ± 0.12
4m	3-Me-C_6H_4-	-OEt	0.09 ± 0.01
4n	3-Pyridyl	-OEt	> 20
6a	3-CF_3-C_6H_4-	-OH	> 20
6m	3-Me	-OH	> 20
6d	Phenyl	-OH	> 20
5	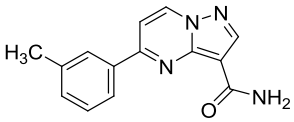		> 40
14a	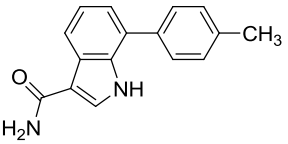		> 20
14b	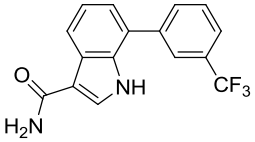		> 20
14c	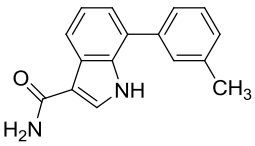		> 20

Table 3-1: Data of the pyrazolo[1,5-*a*]pyrimidine analogs for inhibition of SEAP production in HEK-Blue TLR8 cells.
[a] IC50 values and corresponding standard deviations were determined from at least 3 biological replicates.

Altogether, these results have shown that pyrazolo[1,5-*a*]pyrimidine derivatives present a consistent SAR, the summary of the observed SAR pyrazolo[1,5-*a*]pyrimidine derivatives as TLR8 signaling inhibitor is shown in **Scheme 3-4**. Compound **8m** was found to be the most active compound among all screened pyrazolo[1,5-*a*]pyrimidine derivatives with an IC_{50} of 0.07 ± 0.01 μM, and the corresponding ester analog **4m** (IC_{50} = 0.09 ± 0.01 μM) is also more potent than the hit compound **40-D4** (**8a**). Importantly, **4m** was found to have no significant cytotoxicity up to 60 μM in HEK-Blue TLR8 cells using the established WST-1 cell proliferation assay.

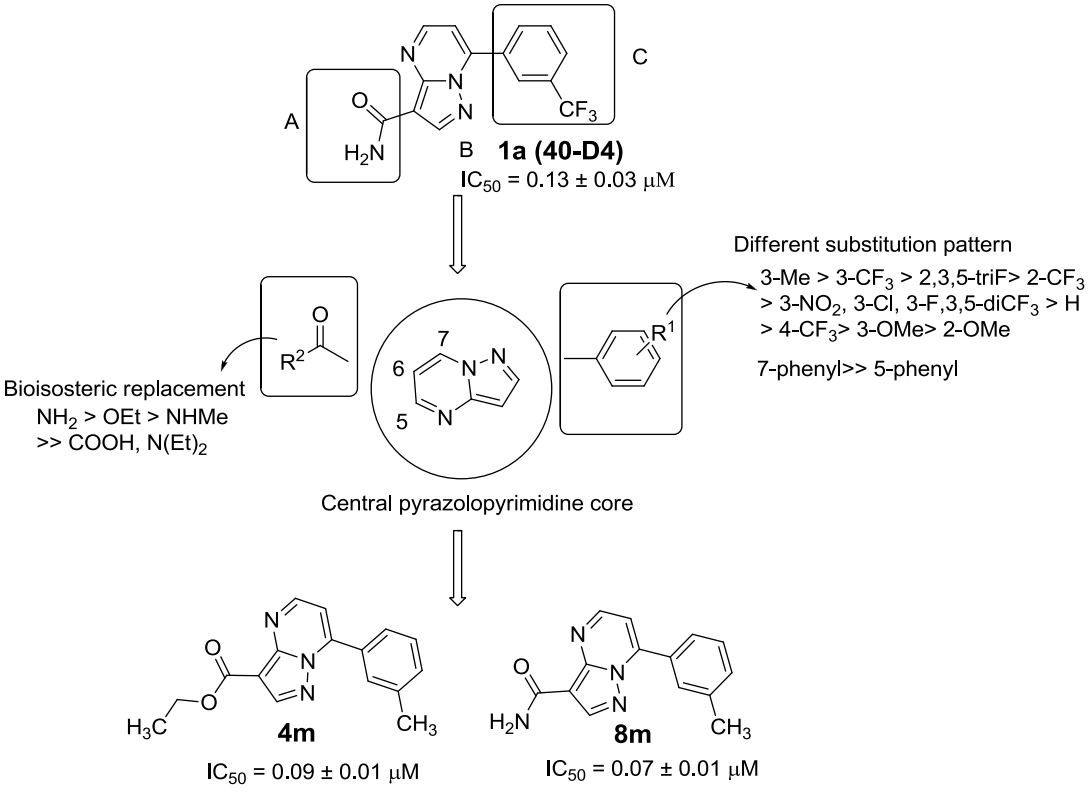

Scheme 3-4. Summary of SAR for the series 7-phenylpyrazolo[1,5-*a*]pyrimidine derivatives as antagonists of TLR8 signaling.

3.2.5 Selectivity and specificity of **8m**

One major challenge for TLR inhibitors development is to engineer specificity for a distinct TLR. In order to determine if **8m** selectively inhibits the TLR8 signaling, the effects of **8m** on other human TLRs were assessed in different HEK-Blue TLR cells including TLR2, TLR3, TLR4, TLR5, and TLR7, using specific ligands to activate particular TLR-mediated NF-κB. We found that at a concentration of 1 μM **8m**, inhibits R848-induced TLR8 signaling without affecting signaling of other TLRs, suggesting that it is highly selective (**Figure 3-7**).

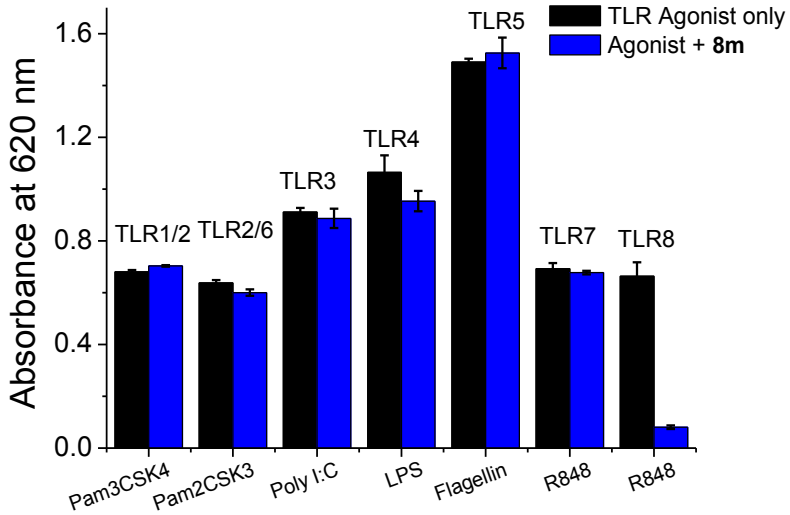

Figure 3-7. Specificity test for **8m** (1 μM) with TLR-specific agonists used to selectively activate distinct HEK-Blue TLR cells: 1. TLR1/2: 100 ng/mL Pam_3CSK_4; 2. TLR2/6 100 ng/mL Pam_2CSK_3; 3. TLR3 5 μg/mL poly (I:C); 4. TLR4: 25 ng/mL LPS; 5. TLR5 50 ng/mL Flagellin; 6. TLR7: 1 μg/mL R848; 7. TLR8: 1 μg/mL R848 were used to selectively activate respective TLRs in the presence or absence of 1 μM

8m. Data present the mean values (± SD) of 3 biological replicates, each performed in triplicate.

3.2.6 Effect of **8m** on TLR8 downstream signaling

R848-induced TLR8 activation results in an increased production of the proinflammatory cytokines, such as TNF-α, IL-6 and IL-8. To further understand the mechanism of TLR8 signaling inhibition by **8m**, we examined its effect on the R848-induced production of TNF-α in THP-1 cells using an ELISA assay. R848 treatment resulted in a significant elevation of the TNF-α production compared to the untreated cells, reaching a maximum of approximately 10-fold after 24 h. **Figure 3-8** demonstrated that **8m** decreases R848-induced TNF-α production in monocyte THP-1 cells in a dose-dependent manner, with an IC_{50} value of 93 ± 12 nM. By contrast, the inactive compound **8n** did not affect the production of TNF-α at 10 μM. The result showed a very similar IC_{50} value as the one determined the SEAP assay, the deviation might due to different cell types and the downstream factors measurement. Thus, **8m** can efficiently block the R848 induced TNF-α production in monocytes, which is consistent with our observations of its activity in NF-κB inhibition in HEK-Blue TLR8 cells.

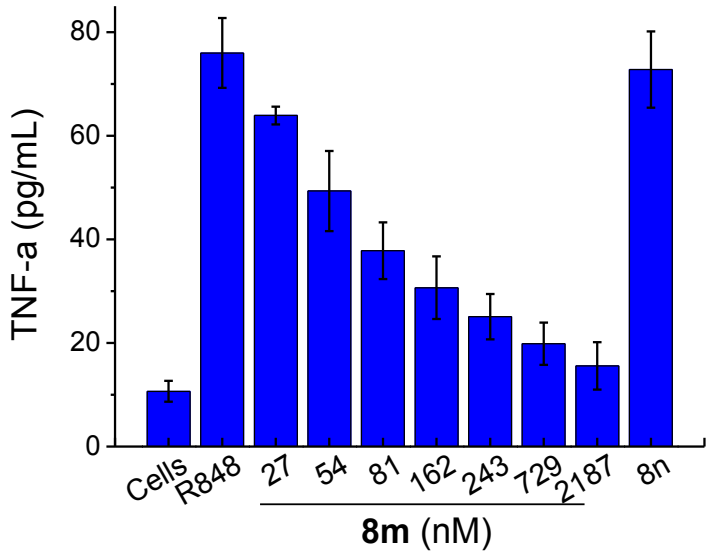

Figure 3-8. Dose-dependence effects of **8m** and negative control **8n** (10 μM) on R848-induced TNF-α production in the THP-1 cells.

Moreover, we investigated the effects of **8m** inhibition on the mRNA expression of proinflammatory cytokines by quantitative real-time polymerase chain reaction (RT-PCR). RT-PCR data was obtained using HEK-Blue TLR8 cells treated with/without R848 and various concentrations of **8a** and **8m**. As shown in **Figure 3-9**, the mRNA levels of TNF-α and IL-8 in HEK-Blue TLR8 cells were increased upon exposure to R848 alone at 21 hours. Treatment with 1μM of **8a** and **8m** significantly inhibited R848-induced mRNA expression of TNF-α and IL-8.

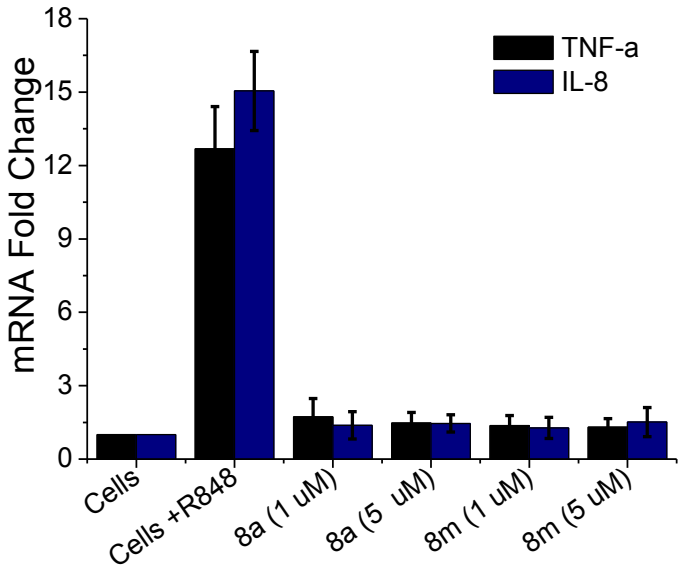

Figure 3-9. Treatment of **8a** and **8m** decreases TNF-α and IL-8 mRNA level in HEK-Blue TLR8 cells. Date shown is the average quantification of two biological replicates, each in technical duplicate.

Altogether, these results corroborate evidence demonstrating that **8m** suppresses TLR8 induced proinflammatory cytokine and cytokine mRNA levels in both HEK-Blue TLR8 cells and THP-1 cells and suggests the pyrazolo[1,5-a]pyrimidine derivatives may provide a therapeutic approach to TLR8 related inflammatory diseases.

3.2.7 Perspective on biophysical assay

Next, we intended to evaluate **8m**'s binding affinity to TLR8 protein by using fluorescence polarization (FP) assays. The FP protein-binding assay used here is based on the finding that certain intrinsically fluorescent small molecules (including ligand and drugs) bind to certain protein in a protein- or site-specific

manner. Theoretically, upon mixing of TLR8 protein and the corresponding small molecule fluorescent probe, the fluorophore, having been engaged into a large molecular weight complex, experiences a slower rotation in solution and consequently exhibits an increased fluorescence anisotropy or polarization. In turn, a test compound (in this case **8m**), which is capable of displacing the probe from the same binding site, will decrease the FP value due to the much faster rotation of the displaced/unbound probe. Anisotropy measurements are ideally suited for measuring the binding affinity of small molecule probes with protein macromolecules.

In order to perform the FP assay, fluorophore labeled ligand is necessary. Since there is no commercially available fluorophore labeled R848, TAMRA labeled R848 was synthesized. Russo and colleagues have reported using TAMRA-R848 to study the localization of the TLR7 in dentric cells.[23] According to the SAR analysis of R848, a tolerant linker site was defined (**Figure 3-10**). A spacer was introduced together with TAMRA, and together they conjugated with R848 at the tolerant linker site. Although, the bioactivity of TAMRA-R848 deceased in HEK-TLR7 cells compared with the unlabeled R848, it still activate the NF-κB signal in HEK-TLR7 cells (EC_{50} = 50 μM) by using luciferase assay. The TAMRA-R848 was successfully synthesized in 7 steps from 4-hydroxyquinoline (**Scheme 3-3**). The next step will be to evaluate the agonistic activity of TAMRA-R848 in HEK-Blue TLR8 cells to ensure that it is retained. Ideally, the TAMRA-R848 would be capable of inducing NF-κB activity in HEK-Blue TLR8 cells with an EC_{50} value similar to R848. Then,

the FP protein-binding assay can be performed to determine the binding affinity of **8m** to TLR8 protein.

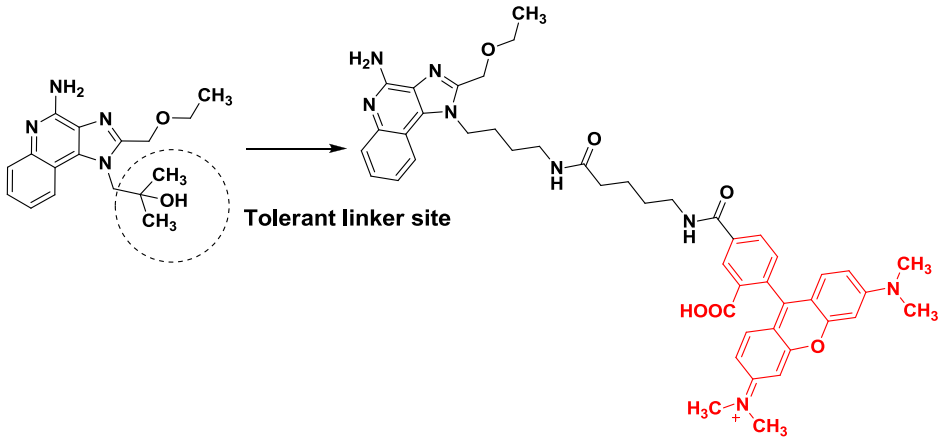

Figure 3-10. R848 was conjugated with a TAMRA (in red) fluorophore at the indicated tolerant linker site.

3.3 Experimental section

3.3.1 General methods and synthesis

General chemistry methods

NMR spectra were acquired on Bruker 400 spectrometer, running at 400 MHz for ^{1}H and 101 MHz for ^{13}C respectively. ^{1}H NMR spectra were recorded at 400 MHz in $CHCl_3$-*d* and $(CH_3)_2SO$-d_6 using residual $CHCl_3$ (7.28 ppm) and DMSO (2.51 ppm) as the internal standard. ^{13}C NMR spectra were recorded at 101 MHz in $CHCl_3$-*d* and DMSO-d_6 using residual $CHCl_3$ (77.16 ppm) and DMSO (39.52 ppm) as internal reference. Thin layer chromatography was performed on Merck Kieselgel 60 Å F254 plates eluting with the solvent indicated, visualized by a 254

nm UV lamp. Compounds were purified using flash chromatography, (Silica gel 60Å, 230-400 mesh, Sorbent Tech.). Mass spectrometry was performed at the mass spectrometry facility of the Department of Chemistry at University of Colorado Boulder on a double focusing high-resolution mass spectrometer. Unless otherwise noted, analytical grade solvents and commercially available reagents were used without further purification. The purity of tested compounds was evaluated via ^{1}H NMR (>95% sample purity).

Synthesis

(*E*)-3-(Dimethylamino)-1-(3-(trifluoromethyl)phenyl)prop-2-en-1-one (**3a**)

3′-(Trifluoromethyl)acetophenone (1.6 mL, 10 mmol) and DMF-DMA) (2.7 mL, 20 mmol) were refluxed overnight until the starting materials were consumed as determined by thin-layer chromatography (TLC), and then the reaction mixture was cooled to room temperature. The precipitate was filtered off and washed with cold hexane followed by cold ethanol to provide 2.1 g (86%) of **3a** as yellow solid. The product was of sufficient purity to be used directly in the next step. ^{1}H NMR (400 MHz, $CDCl_3$) δ 8.15 (td, J = 1.8, 0.9 Hz, 1H), 8.13 – 8.06 (m, 1H), 7.87 (d, J = 12.2 Hz, 1H), 7.72 (ddt, J = 7.8, 1.9, 0.9 Hz, 1H), 7.55 (tt, J = 7.8, 0.8 Hz, 1H), 5.71 (d, J = 12.3 Hz, 1H), 3.20 (s, 3H), 2.97 (s, 3H).

Ethyl 7-(3-(trifluoromethyl)phenyl)pyrazolo[1,5-*a*]pyrimidine-3-carboxylate (**4a**)

5-amino-4-ethoxycarbonyl-1H-pyrazole (216.2 mg, 1.39 mmol) and **3a** (260 mg, 1.27 mmol) were added to acetic acid. The reaction mixture was refluxed while stirring overnight. The progress of the reaction was monitored by TLC, and after completion of the reaction, the mixture was cooled and remove acetic acid by co-evaporation with toluene. The crude product was purified by Biotage column chromatography to yield 330 mg (77.7%) of 7-(3-(trifluoromethyl)phenyl)pyrazolo[1,5-*a*]pyrimidine-3-carboxylate (**4a**) as white solid. ^{1}H NMR (400 MHz, $CDCl_3$) δ 8.88 (d, *J* = 4.4 Hz, 1H), 8.64 (s, 1H), 8.27 (d, *J* = 7.0 Hz, 1H), 7.89 (d, *J* = 8.2 Hz, 1H), 7.77 (d, *J* = 7.0 Hz, 1H), 7.15 (d, *J* = 4.4 Hz, 1H), 4.49 (q, *J* = 7.1 Hz, 1H), 1.46 (t, *J* = 7.1 Hz, 1H).

7-(3-(Trifluoromethyl)phenyl)pyrazolo[1,5-*a*]pyrimidine-3-carboxylic acid (**6a**)

The **4a** (0.2 g, 0.6 mmol) was suspended in ethanol (3 mL) and treated with 7.2 M sodium hydroxide solution (1.1 mL, 7.9 mmol). The mixture was heated to 80 °C and then stirred for 3 h. The mixture was cooled and neutralized to pH 6−7. The slurry was filtered and the solid residue was washed with water and then diethyl ether to obtain 0.12 g (67%) of **6a** as yellow solid. ^{1}H NMR (400 MHz, DMSO-d_6) δ 8.65 (s, 1H), 8.48 (s, 1H), 8.24 (s, 2H), 8.07 – 7.97 (m, 2H), 7.80 (d, *J* = 3.6 Hz, 1H), 7.33 (s, 1H).

7-(3-(Trifluoromethyl)phenyl)pyrazolo[1,5-*a*]pyrimidine-3-carboxamide (**8a**).

A mixture of acid (0.1 g, 0.32 mmol) and thionyl chloride (3 mL) were refluxed in a round bottom flask fitted with calcium chloride guard tube. After the reaction is complete (4 hours), the excess of thionyl chloride was removed by rotary evaporation. The flask was put under high vacuum for 30-60 minutes to complete thionyl chloride removal. The residue was dissolved in anhydrous DCM (3 mL), cooled the solution in ice bath, and then added ammonia (0.5 M in THF) (4 mL, 2 mmol) to the chilled solution. The reaction was seated in ice bath for additional 30 min, then ice bath was removed and the reaction was allowed to stir at room temperature for 3 hours. The crude product was purified by recystalization in DCM and hexane to yield 0.067 g (67.2%) of **8a** as white solid. ^{1}H NMR (400 MHz, DMSO-d_6) δ 8.90 (d, J = 4.5 Hz, 1H), 8.64 (s, 1H), 8.51 (s, 1H), 8.39 (d, J = 7.9 Hz, 1H), 8.03 (d, J = 7.9 Hz, 1H), 7.89 (t, J = 7.9 Hz, 1H), 7.66 – 7.54 (m, 3H). ^{13}C NMR (101 MHz, DMSO-d_6) δ 163.02, 152.50, 147.12, 146.28, 145.97, 134.29, 131.39, 130.31, 129.50, 128.40, 126.95, 125.70, 110.16, 106.10.

Ethyl 7-(2-(trifluoromethyl)phenyl)pyrazolo[1,5-*a*]pyrimidine-3-carboxylate (**4b**)

4b was prepared in a similar manner that described for **4a**. Yield: 76%; ^{1}H NMR (400 MHz, $CDCl_3$) δ 8.87 (dd, J = 4.3, 0.7 Hz, 1H), 8.55 (s, 1H), 7.97 – 7.87 (m, 1H), 7.83 – 7.71 (m, 2H), 7.60 – 7.52 (m, 1H), 7.02 (d, J = 4.2 Hz, 1H), 4.48 (qd, J = 7.1, 0.8 Hz, 2H), 1.44 (td, J = 7.1, 0.8 Hz, 3H).

Ethyl 7-(4-(trifluoromethyl)phenyl)pyrazolo[1,5-*a*]pyrimidine-3-carboxylate (**4c**)

4c was prepared in a similar manner that described for **4a**. Yield 78%; ^{1}H NMR (400 MHz, $CDCl_3$) δ 8.89 (d, *J* = 4.4 Hz, 1H), 8.64 (s, 1H), 8.20 – 8.12 (m, 2H), 7.93 – 7.84 (m, 2H), 7.14 (d, *J* = 4.4 Hz, 1H), 4.50 (q, *J* = 7.1 Hz, 2H), 1.46 (t, *J* = 7.1 Hz, 3H).

Ethyl 7-phenylpyrazolo[1,5-*a*]pyrimidine-3-carboxylate (**4d**)

4d was prepared in a similar manner that described for **4a**. Yield: 73%; ^{1}H NMR (400 MHz, $CDCl_3$) δ 8.84 (d, *J* = 4.4 Hz, 1H), 8.63 (s, 1H), 8.07 – 7.97 (m, 2H), 7.68 – 7.56 (m, 3H), 7.10 (d, *J* = 4.4 Hz, 1H), 4.49 (q, *J* = 7.1 Hz, 2H), 1.45 (t, *J* = 7.1 Hz, 3H).

Ethyl 7-(3-nitrophenyl)pyrazolo[1,5-*a*]pyrimidine-3-carboxylate (**4e**)

4e was prepared in a similar manner that described for **4a**. Yield: 72%; ^{1}H NMR (400 MHz, $CDCl_3$) δ 8.97 – 8.87 (m, 2H), 8.66 (s, 1H), 8.50 (ddd, *J* = 8.3, 2.3, 1.1 Hz, 1H), 8.44 (ddd, *J* = 7.8, 1.8, 1.1 Hz, 1H), 7.84 (ddd, *J* = 8.3, 7.8, 0.5 Hz, 1H), 7.20 (d, *J* = 4.4 Hz, 1H), 4.50 (q, *J* = 7.1 Hz, 2H), 1.47 (t, *J* = 7.1 Hz, 3H).

Ethyl 7-(3-fluorophenyl)pyrazolo[1,5-*a*]pyrimidine-3-carboxylate (**4f**)

4f was prepared in a similar manner that described for **4a**. Yield: 74%; ^{1}H NMR (400 MHz, $CDCl_3$) δ 8.86 (d, *J* = 4.4 Hz, 1H), 8.64 (s, 1H), 7.89 – 7.79 (m, 2H),

7.64 – 7.55 (m, 1H), 7.38 – 7.31 (m, 1H), 7.12 (d, *J* = 4.4 Hz, 1H), 4.49 (q, *J* = 7.1 Hz, 2H), 1.46 (t, *J* = 7.1 Hz, 3H).

Ethyl 7-(3-chlorophenyl)pyrazolo[1,5-*a*]pyrimidine-3-carboxylate (4g)

4g was prepared in a similar manner that described for **4a**. Yield: 73%; ^{1}H NMR (400 MHz, $CDCl_3$) δ 8.86 (d, *J* = 4.4 Hz, 1H), 8.64 (s, 1H), 8.07 – 8.01 (m, 1H), 7.93 (dt, *J* = 7.5, 1.5 Hz, 1H), 7.65 – 7.52 (m, 2H), 7.11 (d, *J* = 4.4 Hz, 1H), 4.49 (q, *J* = 7.1 Hz, 2H), 1.46 (t, *J* = 7.1 Hz, 3H).

Ethyl 7-(4-(methylamino)-3-nitrophenyl)pyrazolo[1,5-*a*]pyrimidine-3-carboxylate (4h)

4h was prepared in a similar manner that described for **4a**. Yield: 63%; ^{1}H NMR (400 MHz, $CDCl_3$) δ 8.86 (d, *J* = 4.4 Hz, 1H), 8.67 (d, *J* = 2.2 Hz, 1H), 8.64 (s, 1H), 8.40 (dd, *J* = 8.9, 2.4 Hz, 1H), 7.33 (d, *J* = 8.9 Hz, 1H), 7.15 (d, *J* = 4.4 Hz, 1H), 4.49 (q, *J* = 7.1 Hz, 2H), 4.11 (s, 3H), 1.46 (t, *J* = 7.1 Hz, 3H).

Ethyl 7-(3,5-bis(trifluoromethyl)phenyl)pyrazolo[1,5-*a*]pyrimidine-3-carboxylate (4i)

4i was prepared in a similar manner that described for **4a**. Yield: 73%; ^{1}H NMR (400 MHz, $CDCl_3$) δ 8.92 (d, *J* = 4.4 Hz, 1H), 8.66 (s, 1H), 8.54 (dd, *J* = 1.1, 0.5 Hz, 2H), 8.23 – 8.04 (m, 1H), 7.20 (d, *J* = 4.3 Hz, 1H), 4.50 (d, *J* = 7.1 Hz, 2H), 1.46 (t, *J* = 7.1 Hz, 3H).

Ethyl 7-(2,4,5-trifluorophenyl)pyrazolo[1,5-*a*]pyrimidine-3-carboxylate (**4j**)

4j was prepared in a similar manner that described for **4a**. Yield: 75%; ^{1}H NMR (400 MHz, $CDCl_3$) δ 8.86 (d, *J* = 4.3 Hz, 1H), 8.60 (s, 1H), 7.79 (ddd, *J* = 10.0, 8.5, 6.3 Hz, 1H), 7.20 (td, *J* = 9.6, 6.4 Hz, 1H), 7.13 (dd, *J* = 4.4, 1.5 Hz, 1H), 4.48 (q, *J* = 7.1 Hz, 2H), 1.45 (t, *J* = 7.1 Hz, 3H).

Ethyl 7-(2-methoxyphenyl)pyrazolo[1,5-*a*]pyrimidine-3-carboxylate (**4k**)

4k was prepared in a similar manner that described for **4a**.Yield: 72%; ^{1}H NMR (400 MHz, $CDCl_3$) δ 8.82 (d, *J* = 4.4 Hz, 1H), 8.62 (s, 1H), 7.65 – 7.44 (m, 3H), 7.22 – 7.02 (m, 2H), 4.47 (q, *J* = 7.1 Hz, 2H), 3.89 (s, 3H), 1.44 (t, *J* = 7.1 Hz, 3H).

Ethyl 7-(3-methoxyphenyl)pyrazolo[1,5-*a*]pyrimidine-3-carboxylate (**4l**)

4l was prepared in a similar manner that described for **4a**. Yield: 75%; ^{1}H NMR (400 MHz, DMSO-d_6) δ 8.90 (d, *J* = 4.5 Hz, 1H), 8.64 (s, 1H), 8.51 (s, 1H), 8.39 (d, *J* = 7.9 Hz, 1H), 8.03 (d, *J* = 7.9 Hz, 1H), 7.89 (t, *J* = 7.9 Hz, 1H), 7.66 – 7.54 (m, 3H).

Ethyl 7-m-tolylpyrazolo[1,5-*a*]pyrimidine-3-carboxylate (**4m**)

4m was prepared in a similar manner that described for **4a**. Yield: 73%; ^{1}H NMR (400 MHz, $CDCl_3$) ^{1}H NMR (400 MHz, $CDCl_3$) δ 8.83 (d, *J* = 4.4 Hz, 1H), 8.63 (s, 1H), 7.60 – 7.47 (m, 3H), 7.19 – 7.07 (m, 2H), 4.48 (q, *J* = 7.1 Hz, 2H), 3.90 (s, 3H),

1.45 (t, J = 7.1 Hz, 3H). ^{13}C NMR (101 MHz, $CDCl_3$) δ 162.57, 159.64, 152.32, 148.94, 147.82, 147.46, 131.38, 129.98, 121.68, 117.13, 115.07, 109.14, 103.16, 60.43, 55.51, 14.61.

Ethyl 7-(pyridin-3-yl)pyrazolo[1,5-*a*]pyrimidine-3-carboxylate (**4n**)

4n was prepared in a similar manner that described for **4a**. Yield: 68%; ^{1}H NMR (400 MHz, $CDCl_3$) δ 9.17 (d, J = 2.2 Hz, 1H), 8.86 (dd, J = 12.5, 4.0 Hz, 2H), 8.63 (s, 1H), 8.51 (ddd, J = 8.0, 2.3, 1.7 Hz, 1H), 7.56 (ddd, J = 8.1, 4.9, 0.9 Hz, 1H), 7.16 (d, J = 4.4 Hz, 1H), 4.48 (q, J = 7.1 Hz, 2H), 1.45 (t, J = 7.1 Hz, 3H).

7-Phenylpyrazolo[1,5-*a*]pyrimidine-3-carboxylic acid (**6d**)

6d was prepared in a similar manner that described for **6a**. Yield: 59%.^{1}H NMR (400 MHz, DMSO-d_6) δ 12.43 (s, 1H), 8.86 (dd, J = 4.6, 0.8 Hz, 1H), 8.63 (s, 1H), 8.14 – 8.05 (m, 2H), 7.70 – 7.58 (m, 3H), 7.46 (dd, J = 4.5, 1.2 Hz, 1H).

7-(3-(Trifluoromethyl)phenyl)pyrazolo[1,5-*a*]pyrimidine-3-carboxylic acid (**6m**)

6m was prepared in a similar manner that described for **6a**.Yield: 67%.^{1}H NMR (400 MHz, DMSO-d_6) δ 8.75 (d, J = 4.5 Hz, 1H), 8.53 (s, 1H), 7.88 – 7.81 (m, 2H), 7.54 – 7.41 (m, 2H), 7.32 (s, 1H), 2.41 (s, 3H).

7-(2-(Trifluoromethyl)phenyl)pyrazolo[1,5-*a*]pyrimidine-3-carboxamide (**8b**)

8b was prepared in a similar manner that described for **8a.** Yield: 64%; ^{1}H NMR (400 MHz, DMSO-d_6) δ 8.86 (d, J = 4.2 Hz, 1H), 8.54 (s, 1H), 8.12 – 8.05 (m, 1H), 7.94 – 7.85 (m, 2H), 7.60 – 7.50 (m, 1H), 7.42 (s, 2H). 7.02 (d, J = 4.2 Hz, 1H).

7-(4-(Trifluoromethyl)phenyl)pyrazolo[1,5-*a*]pyrimidine-3-carboxamide(8c)

8c was prepared in a similar manner that described for **8a**. Yield: 76%; ^{1}H NMR (400 MHz, DMSO-d_6) δ 8.91 (d, J = 4.5 Hz, 1H), 8.63 (s, 1H), 8.33 (d, J = 8.1 Hz, 2H), 8.02 (d, J = 8.2 Hz, 2H), 7.61 (s, 2H), 7.56 (d, J = 4.5 Hz, 1H). ^{13}C NMR (101 MHz, DMSO-d_6) δ 163.00, 152.55, 147.09, 146.26, 134.37, 131.27, 131.18, 125.92, 125.88, 111.68, 110.22, 106.14.

7-Phenylpyrazolo[1,5-*a*]pyrimidine-3-carboxamide (8d)

8d was prepared in a similar manner that described for **8a**. Yield: 81%. ^{1}H NMR (400 MHz, DMSO-d_6) δ 8.86 (d, J = 4.4 Hz, 1H), 8.63 (s, 1H), 8.15 – 8.04 (m, 2H), 7.64 (s, 1H), 7.71 – 7.58 (m, 2H), 7.47 (d, J = 4.4 Hz, 1H). ^{13}C NMR (101 MHz, DMSO-d_6) δ 163.63, 153.17, 148.72, 147.66, 147.33, 131.80, 130.54, 130.19, 129.00, 110.14.

7-(3-Nitrophenyl)pyrazolo[1,5-*a*]pyrimidine-3-carboxamide (8e)

8e was prepared in a similar manner that described for **8a**. Yield: 72%; ^{1}H NMR (400 MHz, DMSO-d_6) δ 9.04 – 9.01 (m, 1H), 8.92 (d, J = 4.5 Hz, 1H), 8.66 (s, 1H), 8.55 – 8.49 (m, 2H), 7.98 – 7.92 (m, 1H), 7.66 – 7.59 (m, 3H). ^{13}C NMR (101

MHz, DMSO-d_6) δ 152.53, 148.06, 147.11, 146.31, 145.27, 136.62, 131.97, 131.81, 130.77, 126.45, 125.19, 110.25, 106.25.

7-(3-Fluorophenyl)pyrazolo[1,5-a]pyrimidine-3-carboxamide (**8f**)

8f was prepared in a similar manner that described for **8a**. Yield: 72%. ^{1}H NMR (400 MHz, DMSO-d_6) δ 8.88 (d, J = 4.5 Hz, 1H), 8.63 (s, 1H), 8.04 (ddd, J = 10.2, 2.4, 1.6 Hz, 1H), 7.98 (ddd, J = 7.8, 1.6, 1.0 Hz, 1H), 7.69 (td, J = 8.1, 6.1 Hz, 1H), 7.60 (d, J = 7.5 Hz, 2H), 7.57 – 7.49 (m, 2H). ^{13}C NMR (101 MHz, DMSO-d_6) δ 163.31, 163.01, 160.89, 152.40, 147.17, 146.25, 132.36, 131.23, 126.45, 118.86, 117.19, 109.86, 106.04.

7-(3-Chlorophenyl)pyrazolo[1,5-*a*]pyrimidine-3-carboxamide(**8g**)

8g was prepared in a similar manner that described for **8a**. Yield: 79%; ^{1}H NMR (400 MHz, DMSO-d_6) δ 8.87 (d, J = 4.5 Hz, 1H), 8.64 (s, 1H), 8.24 (t, J = 1.9 Hz, 1H), 8.11 – 8.03 (m, 1H), 7.74 (ddd, J = 8.1, 2.2, 1.1 Hz, 1H), 7.67 (t, J = 7.9 Hz, 1H), 7.63 – 7.51 (m, 3H). ^{13}C NMR (101 MHz, DMSO-d_6) δ 163.01, 152.42, 147.14, 146.26, 146.02, 133.59, 132.30, 131.73, 130.99, 129.89, 128.94, 109.92, 106.06.

7-(4-(Methylamino)-3-nitrophenyl)pyrazolo[1,5-*a*]pyrimidine-3-carboxamide (**8h**)

8h was prepared in a similar manner that described for **8a**. Yield: 59%. ^{1}H NMR (400 MHz, $CDCl_3$) δ 8.87 (d, J = 4.4 Hz, 1H), 8.67 (d, J = 2.2 Hz, 1H), 8.65 (s,

1H), 8.49 (m, 1H), 7.51 (d, J = 8.7 Hz, 1H),7.32 (s, 2H), 7.22 (d, J = 4.3 Hz, 1H), 4.11 (s, 3H).

7-(3,5-Bis(trifluoromethyl)phenyl)pyrazolo[1,5-*a*]pyrimidine-3-carboxamide (**8i**)

8i was prepared in a similar manner that described for **8a**. Yield: 61%; ^{1}H NMR (400 MHz, $CDCl_3$) δ 8.91 (d, J = 4.4 Hz, 1H), 8.67 (s, 1H), 8.61 – 8.63 (m, 2H), 8.29 – 8.23 (m, 1H), 7.38 (s, 2H), 7.20 (d, J = 4.3 Hz, 1H).

7-(2,4,5-Trifluorophenyl)pyrazolo[1,5-*a*]pyrimidine-3-carboxamide (**8j**)

8j as prepared in a similar manner that described for **8a**. Yield: 73%; ^{1}H NMR (400 MHz, DMSO-d_6) δ 8.91 (d, J = 4.4 Hz, 1H), 8.60 (s, 1H), 8.24 – 8.05 (m, 1H), 7.86 – 7.82 (m, 1H), 7.66 – 7.54 (m, 4H).

7-(2-Methoxyphenyl)pyrazolo[1,5-*a*]pyrimidine-3-carboxamide (**8k**)

8k was prepared in a similar manner that described for **8a.** Yield: 66%; ^{1}H NMR (400 MHz, DMSO-d_6) δ 8.83 (d, J = 4.3 Hz, 1H), 8.57 (s, 1H), 7.81 – 7.72 (m, 4H), 7.31 – 7.23 (m, 2H), 7.06 (m, J = 4.3 Hz, 1H), 3.77 (s, 3H).

7-(3-Methoxyphenyl)pyrazolo[1,5-*a*]pyrimidine-3-carboxamide (**8l**)

8l was prepared in a similar manner that described for **8a.** Yield: 62%; ^{1}H NMR (400 MHz, DMSO-d_6) δ 8.83 (d, J = 4.4 Hz, 1H), 8.63 (s, 1H), 7.71 – 7.59 (m, 3H), 7.33 – 7.18 (m, 2H), 7.12 (s, 2H) 3.90 (s, 3H).

7-*m*-Tolylpyrazolo[1,5-*a*]pyrimidine-3-carboxamide (**8m**)

8m was prepared in a similar manner that described for **8a**. Yield: 76%. ^{1}H NMR (400 MHz, DMSO-d_6) δ 8.82 (d, J = 4.6 Hz, 1H), 8.59 (s, 1H), 7.88 (d, J = 8.8 Hz, 2H), 7.72 (s, 1H), 7.55 – 7.45 (m, 3H), 7.41 (d, J = 4.6 Hz, 1H), 2.41 (s, 3H). ^{13}C NMR (101 MHz, DMSO-d_6) δ 163.12, 152.38, 147.77, 147.24, 146.20, 138.37, 132.60, 130.48, 130.32, 128.95, 127.37, 109.56, 105.79, 21.48.

7-(Pyridin-3-yl)pyrazolo[1,5-*a*]pyrimidine-3-carboxamide(**8n**)

8n as prepared in a similar manner that described for **8a**. Yield: 73%; ^{1}H NMR (400 MHz, DMSO-d_6) δ 9.25 (dd, J = 2.3, 0.8 Hz, 1H), 8.90 (d, J = 4.5 Hz, 1H), 8.82 (dd, J = 4.8, 1.6 Hz, 1H), 8.63 (s, 1H), 8.56 (ddd, J = 8.0, 2.3, 1.7 Hz, 1H), 7.70 – 7.65 (m, 1H), 7.40 (s, 2H). ^{13}C NMR (101 MHz, DMSO-d_6) δ 163.01, 152.48, 152.35, 150.35, 147.05, 146.23, 145.14, 137.91, 126.71, 123.87, 109.90, 106.11.

N-methyl-7-m-tolylpyrazolo[1,5-*a*]pyrimidine-3-carboxamide (**8o**)

8o was prepared in a similar manner that described for **8a**. Yield: 86%; ^{1}H NMR (400 MHz, $CDCl_3$) δ 8.76 (s, 1H), 8.71 (d, J = 4.4 Hz, 1H), 8.34 (d, J = 7.9 Hz,

1H), 8.31 – 8.24 (m, 1H), 8.02 (s, 1H), 7.93 – 7.86 (m, 1H), 7.83 – 7.73 (m, 1H), 7.13 (d, *J* = 4.4 Hz, 1H), 3.12 (d, *J* = 4.9 Hz, 3H), 2.45 (s, 3H),

N, N-diethyl-7-m-tolylpyrazolo[1,5-*a*]pyrimidine-3-carboxamide (8p)

8p was prepared in a similar manner that described for **8a**. Yield: 83%; ^{1}H NMR (400 MHz, $CDCl_3$) δ 8.70 (d, *J* = 4.3 Hz, 1H), 8.38 (s, 1H), 8.32 – 8.24 (m, 2H), 7.88 (d, *J* = 7.9 Hz, 1H), 7.81 – 7.72 (m, 1H), 7.04 (d, *J* = 4.3 Hz, 1H), 3.63 (s, 4H), 2.53 (s, 3H), 1.26 (s, 6H).

1-(7-Bromo-1*H*-indol-3-yl)-2,2,2-trifluoroethanone (10)

A stirred, ice-cooled solution of 7-bromoindole (0.5 g, 2.6 mmol) in DMF (2 mL) was treated, dropwise, with trifluoroacetic anhydride (0.43 mL, 3.1 mmol). This solution was allowed to warm to room temperature over 2 hours, and then poured into a solution of saturated aqueous $NaHCO_3$ solution. The title compound precipitated as a white solid and was filtered off, washed with water and dried (0.66 g, 89%). ^{1}H NMR (400 MHz, $CDCl_3$) δ 9.17 (s, 1H), 8.38 (dd, *J* = 8.0, 0.9 Hz, 1H), 8.14 (dd, *J* = 3.0, 1.6 Hz, 1H), 7.64 – 7.52 (m, 1H), 7.32 – 7.27 (m, 2H).

2,2,2-Trifluoro-1-(7-*p*-tolyl-1*H*-indol-3-yl)ethanone (11a)

A mixture of 10 (0.12 g, 0.41 mmol), 4-methylphenylboronic acid (0.024 g, 0.84 mmol), $Pd(PPh_3)_4$ (0.048 g, 0.041 mmol), and K_2CO_3 (0.13 g, 0.82 mmol) in 1,4-dioxane (5mL) was degassed and backfilled with nitrogen gas (3×), and then heated

at 80 °C for 12 hours. After this time, the entire reaction mixture was filtered, and the filtrate was concentrated to dryness to give a residue which was purified via flash column chromatography to give **14a** as white solid (0.081 g, 65%). ^{1}H NMR (400 MHz, $CDCl_3$) δ 8.81 (s, 1H), 8.20 (m, 1H), 7.95 (d, J = 3.0 Hz, 1H), 7.54 – 7.49 (m, 2H), 7.41 – 7.33 (m, 3H), 7.32 – 7.29 (m, 1H), 2.46 (s, 3H).

7-p-tolyl-1*H*-indole-3-carboxylic acid (**12a**)

11a (0.1 g, 0.33 mmol) was dissolved in 20% aqueous NaOH solution (3 mL) and heated at reflux for 1 h, then cooled, diluted with water (3 mL) and washed with EtOAc (5 ml). The aqueous phase was separated and acidified to pH 1 with 5M aqueous HCl solution. The title compound (**12a**) precipitated as a white solid and was filtered off, washed with water and dried under vacuum (0.072 g, 87%). ^{1}H NMR (400 MHz, DMSO-d_6) δ 12.23 (s, 1H), 12.12 (s, 1H), 8.23 – 7.80 (m, 2H), 7.62 (d, J = 8.0 Hz, 1H), 7.43 (m, 3H), 7.12 (t, J = 7.8 Hz, 1H), 2.45 (s, 3H).

7-*p*-Tolyl-1*H*-indole-3-carboxamide (**14a**)

A mixture of **12a** (0.063g, 0.25 mmol) and thionyl chloride (3 mL) were refluxed in a 10 mL round bottom flask fitted with calcium chloride guard tube. After the reaction is complete (4 hours), the excess of thionyl chloride was removed by rotary evaporation. The flask was put under high vacuum for 30-60 minutes to complete thionyl chloride removal. The residue was dissolved in anhydrous DCM (2 mL), cooled the solution in ice bath, and then added ammonia (0.5 M in THF) (3 mL,

1.5 mmol) to the chilled solution. The reaction was kept in ice bath for additional 30 min, then ice bath was removed and the reaction was allowed to stir at room temperature for 3 hours. The crude product was purified by recystalization in DCM and hexane to yield **14a** (0.042g, 67%). ^{1}H NMR (400 MHz, DMSO-d_6) δ 8.85 (s, 1H), 8.23 – 7.80 (m, 2H), 7.47 (s, 2H), 7.39 (d, J = 7.7 Hz, 2H), 7.32 – 7.29 (m, 2H), 7.13 (d, J = 7.8 Hz, 2H), 2.43 (s, 3H).

7-(3-(Trifluoromethyl)phenyl)-1*H*-indole-3-carboxamide(14b)

14b was prepared in a similar manner that described for **14a**. ^{1}H NMR (400 MHz, DMSO-d_6) δ 8.87 (s, 1H), 8.28 – 7.93 (m, 3H), 7.82 (s, 1H), 7.45 (s, 2H), 7.32 – 7.29 (m, 1H), 2.45 (s, 3H).

7-*m*-Tolyl-1*H*-indole-3-carboxamide (14c)

14c was prepared in a similar manner that described for **14a**. ^{1}H NMR (400 MHz, DMSO-d_6) δ 8.81 (s, 1H), 8.05 – 7.85 (m, 2H), 7.57– 7.47 (m, 3H), 7.42 (d, J = 4.3 Hz, 1H), 7.29 – 7.24 (m, 1H), 2.44 (s, 3H), 2.38 (s, 3H).

3-Nitro-4-quinolinol (15)

A mixture of 4-quinolinol (**14**) (3 g, 20.7 mmol) in propionic acid (29 mL) was heated to 125 °C with stirring. Nitric acid (70%, 3.3 mL, 52 mol) was added dropwise to the stirred solution while maintaining the reaction mixture temperature at 125 °C. The product began to precipitate before the addition of nitric

acid was completed, and the reaction mixture became quite thick. When addition was complete, the mixture was stirred at 125 °C for 30 min and cooled to room temperature. The mixture was diluted with ethanol, and the solid was collected by vacuum filtration. The solid was washed successively with ethanol, water, and ethanol. The resulting light-yellow solid was heated in refluxing ethanol and filtered from the hot mixture to give 3.1 g (80%) of product as a light-yellow solid (**2**). ^{1}H NMR (400 MHz, DMSO-d_6) δ 13.03 (br, 1H), 9.21 (s, 1H), 8.27 (ddd, J = 8.1, 1.5 Hz, 1H), 7.81 (ddd, J = 8.4, 7.0, 1.5 Hz, 1H), 7.74 (ddd, J = 8.3, 1.2, 0.6 Hz, 1H), 7.54 (ddd, J = 8.2, 7.0, 1.2 Hz, 1H).

***tert*-Butyl 4-(3-nitroquinolin-4-ylamino)butylcarbamate (16)**

The intermediate (15) (1.9 g, 10 mmol) was suspended in 15 mL dichloromethane. Thionyl chloride (2 mL, 27 mmol), and N,N-dimethylformamide (1 mL) were added dropwise over 10 min and then heated at 40 ℃ for 2 hours. The reaction mixture was then poured in ice. The organic layer was washed with saturated sodium bicarbonate solution, water and brine. Then the organic layer was dried over Na_2SO_4, filtered, concentrated and dried in vacuo. The solid residue 1.7 g (82%) 3-nitrolquinolin-4-ol was used for next step without any further purification. 3-nitrolquinolin-4-ol (1.3 g, 6.2 mmol) was added to a stirred solution of tert-butyl 4-aminobutylcarbamate (1.41g, 7.5 mmol) and triethylamine (4 mL) in DCM (20 mL) at 0 ℃. The reaction was monitored by thin layer chromatography. When all of the starting material was gone, the reaction mixture was washed with water, the

organic layer was dried over anhydrous Na_2SO_4, filtered and then concentrated under vacuum to provide 1.64 g (73%) of *tert*-butyl 4-(3-nitroquinolin-4-ylamino)butylcarbamate (**16**) as a yellow solid. ^{1}H NMR (400 MHz, $CDCl_3$) δ 9.73 (s, 1H), 9.39 (s, 1H), 8.32 (dd, *J* = 8.6, 0.8 Hz, 1H), 8.01 (dd, *J* = 8.3, 1.0 Hz, 1H), 7.79 (ddd, *J* = 8.3, 7.0, 1.3 Hz, 1H), 7.51 (ddd, *J* = 8.4, 7.0, 1.4 Hz, 1H), 4.64 (s, 1H), 4.01 (td, *J* = 7.0, 5.0 Hz, 2H), 3.23 (d, *J* = 6.4 Hz, 2H), 1.90 (dd, *J* = 9.0, 6.1 Hz, 2H), 1.74 – 1.67 (m, 2H), 1.46 (s, 9H).

***tert*-Butyl 4-(3-aminoquinolin-4-ylamino)butylcarbamate (17)**

1.6 g (4.4 mmol) of **16** was dissolved to a mixed solvent of 27 mL of methanol and 9 mL of ethyl acetate. Degas with vacuum/nitrogen a few times, 0.9 g 5% palladium-carbon was added to the solution. Then degas with vacuum/hydrogen and the mixture was stirred overnight under hydrogen atmosphere. The mixture was filtered through celite and the filtrate was concentrated by using rotary evaporator. The residue was purified by Biotage column chromatography (5% methanol in DCM to 10 % methanol in DCM gradient) to obtain tert-butyl 4-(3-aminoquinolin-4-ylamino)butylcarbamate (**17**) (1.1g, 75%). ^{1}H NMR (400 MHz, $CDCl_3$) δ 8.50 (s, 1H), 8.04 – 7.94 (m, 1H), 7.89 – 7.79 (m, 1H), 7.53 – 7.41 (m, 2H), 4.65 (s, 1H), 3.83 (s, 2H), 3.46 – 3.04 (m, 5H), 1.71 – 1.59 (m, 4H), 1.46 (s, 9H).

***tert*-Butyl 4-(2-(ethoxymethyl)-1*H*-imidazo[4,5-*c*]quinolin-1-yl)butylcarbamate (18)**

Ethoxyacetyl chloride (134 mg, 1.9 mmol) was added dropwise to a stirred solution of **17** (0.4 g, 1.21 mmol) in dichloromethane (15 mL). After 1 hour, the solution was concentrated under reduced pressure. The residue was dissolved in ethanol (5 mL) and triethylamine (170 µL, 1.2 mmol) and the solution was heated at reflux overnight, then was allowed to cool to room temperature and was concentrated under reduced pressure. The residue was dissolved in DCM and washed with water and brine. The organic layer was dried over anhydrous Na_2SO_4, filtered, and concentrated under reduced pressure. The residue purified by Biotage column chromatography (3% methanol in DCM to 10 % methanol in DCM gradient)) to obtain 0.36 g (75%) of *tert*-butyl 4-(2-(ethoxymethyl)-1*H*-imidazo[4,5-*c*]quinolin-1-yl)butylcarbamate (**18**) as a yellow foamy solid. ^{1}H NMR (400 MHz, $CDCl_3$) δ 9.29 (s, 1H), 8.28 (dd, *J* = 7.8, 0.9 Hz, 1H), 8.13 (d, *J* = 7.8 Hz, 1H), 7.73 – 7.61 (m, 2H), 4.87 (s, 2H), 4.79 (s, 1H), 4.69 – 4.60 (m, 2H), 3.62 (q, *J* = 7.0 Hz, 1H), 3.28 – 3.17 (m, 2H), 2.10 – 1.98 (m, 2H), 1.78 – 1.67 (m, 2H), 1.42 (s, 9H), 1.25 (t, *J* = 7.0 Hz, 2H).

1-(4-Aminobutyl)-2-(ethoxymethyl)-1*H*-imidazo[4,5-*c*]quinolin-4-amine (**19**)

3-chloroperoxybenzoic acid (0.28 g of approximately 77% purity) was added to a solution of **18** (0.32g, 0.8 mmol) in DCM (10 mL). The reaction was allowed to stir overnight and was washed with saturated sodium bicarbonate solution (20 mL). The aqueous layer was extracted with DCM (2×15 mL), and the combined organic layer was dried over anhydrous Na_2SO_4, filtered and concentrated. Then dissolve the residue in DCM (5 mL), then p-toluenesulfonyl chloride (175 mg, 0.92 mmol),

NH_4OH (0.5 mL of 30%) was added, stirred the reaction mixture vigorously. After15 hours, the reaction mixture was diluted with DCM and washed with saturated sodium bicarbonate solution. The aqueous layer was extracted with DCM (2×15 mL), the combined organic layer was washed with brine, died with anhydrous Na_2SO_4, filtered and concentrated. The residue purified by Biotage column chromatography (3% methanol in DCM to 10 % methanol in DCM gradient) to obtain 0.24 g (72%) of *tert*-butyl4-(4-amino-2-(ethoxymethyl)-1*H*-imidazo[4,5-*c*]quinolin-1-yl)butylcarbamate. ^{1}H NMR (400 MHz, $CDCl_3$) δ 7.85 (d, *J* = 7.5 Hz, 1H), 7.82 – 7.73 (m, 1H), 7.49 (t, *J* = 7.3 Hz, 1H), 7.35 – 7.25 (m, 1H), 5.85 (s, 2H), 4.77 (d, *J* = 12.0 Hz, 2H), 4.67 – 4.23 (m, 2H), 3.58 (q, *J* = 7.0 Hz, 2H), 3.48 (s, 1H), 3.19 (d, *J* = 6.3 Hz, 2H), 1.95 (dq, *J* = 12.1, 7.9 Hz, 2H), 1.77 – 1.58 (m, 2H), 1.42 (s, 9H), 1.23 (t, *J* = 7.0 Hz, 3H). HCl (2mL of a 4M solution in 1,4-dioxane) was added to *tert*-butyl4-(4-amino-2-(ethoxymethyl)-1*H*-imidazo[4,5-*c*]quinolin-1-yl)butylcarbamate (0.1 g, 0.24 mmol), and the reaction was stirred for one hour. Then, the reaction solution was adjusted to pH 11 with the addition of NaOH pellets in a small amount of water. DCM (5 mL) was added flowed by saturated sodium bicarbonate. The organic layer was separated, washed with brine, died over anhydrous Na_2SO_4, filtered, and concentrated. The residue purified by Biotage column chromatography (5% methanol in DCM to 10 % methanol in DCM gradient) to obtain 52 mg (69%) of 1-(4-aminobutyl)-2-(ethoxymethyl)-1*H*-imidazo[4,5-*c*]quinolin-4- amine (**19**). ^{1}H NMR (400 MHz, MeOD) δ 7.89 (d, *J* = 8.1 Hz, 1H), 7.67 (d, *J* = 8.3 Hz, 1H), 7.48 (t, *J* = 7.7 Hz, 1H), 7.30 (t, *J* = 7.6 Hz, 1H), 4.95 (s, 4H), 4.75 (s, 2H), 4.56 – 4.30 (m, 2H), 3.61

(q, *J* = 7.0 Hz, 2H), 2.68 (s, 2H), 1.88 (d, *J* = 7.3 Hz, 2H), 1.77 – 1.48 (m, 2H), 1.25 (t, *J* = 7.0 Hz, 3H).^{13}C NMR (101 MHz, MeOD) δ 151.59, 149.44, 144.31, 133.80, 127.31, 125.53, 125.49, 122.19, 120.04, 114.57, 66.06, 64.27, 45.85, 40.70, 29.27, 27.29, 14.04.

R848-TAMRA (20)

A solution of **19** (1.7 mg, 5.4 µmol), amide activated 6-(tetramethylrhodamine-5-(and-6)-carboxamido)hexanoic acid, succinimidyl ester (5(6)-TAMRA-X, SE) (Invitrogen) (3.5 mg, 5.4 µmol) and triethylamine (3.5 µl, 24 µmol) in DMSO (1 ml) was stirred at room temperature for 2 hours. The resulting DMSO solution was purified directly by reverse phase HPLC (eluting with 10 to 90% acetonitrile:water; 0.1% trifluoroacetic acid) giving two regioisomers 3.1 mg (69 %) as product. ^{1}H NMR (400 MHz, DMSO-d_6) δ 8.91 – 8.86 (m, 1H), 8.66 (s, 1H), 8.30 (d, *J* = 8.1 Hz, 1H), 8.20 (d, *J* = 7.6 Hz, 1H), 7.90 – 7.79 (m, 2H), 7.73 (t, *J* = 7.3 Hz, 1H), 7.63 – 7.50 (m, 2H), 7.10 – 6.85 (m, 5H), 4.84 (s, 2H), 4.67 – 4.57 (m, 2H), 3.61 (q, *J* = 7.0 Hz, 2H), 3.34 – 3.16 (m, 12H), 3.14 – 3.03 (m, 3H), 2.55 (s, 1H), 2.08 – 2.01 (m, 2H), 1.88 – 1.79 (m, 2H), 1.65 – 1.56 (m, 2H), 1.55 – 1.47 (m, 3H), 1.34 – 1.23 (m, 3H), 1.18 (t, *J* = 7.0 Hz, 3H).

3.3.2 Biological assays

Cell Cultures of HEK-Blue TLR cells and THP-1 cells

All cultured cells were grown at 37 °C in a humidified incubator containing 5% CO_2. Human embryonic kidney (HEK)-Blue TLR cells were cultured in complete

culture medium: Dulbecco's modified Eagle's medium, 10% (v/v) of fetal bovine serum (FBS), 50 U/ml penicillin, 50 mg/ml streptomycin, 100 mg/ml Normocin, and 2 mM L-glutamine. Human monocytic cell line THP-1 were cultured in Roswell Park Memorial Institute (RPMI) 1640 medium supplemented with 10%(v/v) FBS, 2mM L-glutamine, 100µg/ml streptomycin and 100 U/ml penicillin and 0.05 mM 2-mercaptoethanol.

High-Throughput Screening for inhibitors of TLR8 signaling

The Maybridge HitFinder library of 14,400 small molecules was chosen to screen for small-molecule inhibitors of TLR8 signaling. HEK-Blue TLR8 cells were suspended in test medium (DMEM, 10% (v/v) FBS (deactivated phosphatases), Pen-Strep (50 U/ml–50 µg/ml), 100 µg/ml Normocin™ and 2 mM L-glutamine) at 400,000/mL and added corresponding amount of R848 to make final concentration of 1 µg /mL. Then seeded in 50 µL of medium containing 20,000 cells per well into clear 384-well tissue culture plates (Nunc, Rochester, NY) using using the BioTek MicroFlo Select dispenser. 200 nL of compound solutions were pin transferred from stock 384-well plates into the 384-well assay plates containing cells using CyBi-Well robotic system, resulting in 4 µM final concentration for the library compounds. The compound library was screened in two replicates. Both positive and negative control wells were employed: 16 triptolide treated wells were present on each compound assay plate screened, and 16 wells were treated with DMSO alone. QUANTI-Blue was added 24 hours after compound addition (50 µL). Plates were incubated for 30

min at 37 °C with shaking. Absorbance at 600 nm was determined with plate reader (Perkin Elmer Envision 2102).

Establishment of TLR stable cell lines

Stable TLR3, TLR5, TLR7 and TLR8 overexpressed HEK-Blue cells were prepared by lentiviral infection of HEK-Blue Null1 cells. HEK-Blue Null1 cells (Invivogen) are permanently transfected with an NF-κB and AP-1-sensitive promoter-driven alkaline phosphatase. NF-κB and AP-1 binds to the promoter upon nuclear translocation, and NF-κB activation induces the expression of alkaline phosphatase that can be assessed by measuring SEAP activity using QUANTI-Blue (Invivogen). For lentiviral infection, HEK-Blue Null1 cells were incubated with recombinant lentiviral particles expressing a distinct TLR (multiplicity of infection) in the presence of hexadimethrine bromide 4 µg/mL to enhance transfection efficiency. Forty-eight hours later, transduced cells were extensively washed and subjected to antibody selection with 100 µg/mL hygromycin B (Invitrogen).

SEAP reporter assay

HEK-Blue TLR8 cells were plated at 350,000 cells/mL in a tissue culture treated 96-well plate in test medium (DMEM, 10% (v/v) FBS (deactivated phosphatases). Then cells were treated with 1 µg/mL R848 (Invivogen) and varying concentrations of appropriate compound. Cells were incubated with compound and R848 at 37 °C. After 20-24 hours of incubation, 20 µL of culture media was removed and placed in a new 96-well plate. 180 µL of Quanti-Blue (Invivogen) was added to the media, and the plate incubated at 37 °C until color change was observed (30

min-1 hour). Plates were then quantified on a Beckman-Coulter DTX 880 Multimode Detector by measuring absorbance at 620 nm. Data was normalized as readout of ligand treated cells is 100% activation, and untreated cells are 0% activation. Experiment was conducted with a minimum of three biological replicates, in triplicate.

TLR selectivity assay

The selectivity of compounds against the TLR family were examined HEK-Blue cells overexpressing a specific TLR and accessory proteins. The assay was performed in the same was "SEAP reporter assay". Except polyriboinosinic:polyribocytidylic acid (Poly(I:C)) (5 µg/mL), LPS (lipopolysaccharide) (20 ng/mL), Pam_3CSK_4 (N-palmitoyl-S-[2,3-bis(palmitoyloxy)-(2RS)-propyl]-[R]-cysteinyl-[S]-seryl-[S]-lysyl-[S]-lysyl-[S]-lysyl-[S]-lysine·3HCl) (100 ng/mL), Pam_2CSK_4 (S-[2,3-bis(palmitoyloxy)-(2RS)-propyl]-[R]-cysteinyl-[S]-seryl-[S]-lysyl-[S]-lysyl-[S]-lysyl-[S]-lysine x 3 CF_3COOH) (100 ng/mL), Flagellin (50 ng/mL), R848 (2 µg/mL) were used to selectively activate HEK-Blue hTLR3, hTLR4, hTLR1/2, hTLR2/6, hTLR5, hTLR1/2, and hTLR7 cells, respectively.

WST-1 cell proliferation assay

HEK-Blue TLR8 cells were prepared as described above for SEAP reporter assay. After 100 µL of supernatant was removed, 1:10 dilution of WST-1 reagent (Roche) was added to the cells. Cells were incubated at 37 °C until a color change was observed (30 min-1.5 hours). Absorbance was read in a Beckman-Coulter DTX

880 Multimode Detector at 450 nm. Data was normalized untreated cells are 100% survival. Experiment was conducted with three biological replicates, in triplicate.

Enzyme-linked immunosorbent assay (ELISA)

ELISA was performed to measure TNF-α expression levels. THP-1 cells with phorbol-12-myristate-13-acetate (PMA) (20 ng/mL) treatment were seeded at 2×10^6 per well in 2 mL supplemented RPMI medium (10%(v/v) FBS, 2mM L-glutamine, 100µg/ml streptomycin and 100 U/ml penicillin and 0.05 mM 2-mercaptoethanol) in 6-well tissue-culture plates and incubated at 37°C in humidified 5% CO2 atmosphere. After 24 hours, the cells were adhered to the surface of the dish. The medium was replaced with unsupplemented RPMI, and the cells were treated with or without R848 (1ug mL) and various concentrations of compounds. After 24 hours, supernatants of the culture media were collected, and the levels of TNF-α were determined using human TNF-α OptEIA ELISA kit (BD Biosciences), according to the manufacturer's instructions. Experiment was conducted with a minimum of two biological replicates, in triplicates.

RT-PCR analysis of IL-8 and TNF-a mRNA expression

HEK-Blue TLR8 cells were seeded at a density of 1×10^6 cells per well of a 6-well plate. After 24 hours incubation, the medium was replaced by serum free medium, and then the cells were treated with or without R848 (1 µg/mL) and various concentrations of compound for 24 h at 37°C.Then, cells were scraped and resuspended in PBS. RNA was extracted using the E.Z.N.A. total RNA Kit from OMEGA. Reverse transcription was performed using the Qiagen RT First Strand

Kit per manufacturer instructions. Reverse transcription was performed using a BioRad T100 thermalcycler. qPCR was performed using soAdvanced™ SYBR® Green Supermix from BioRad. RT² qPCR IL-8 and TNF-α primers were obtained from QIAGEN. GAPDH primers were obtained from SABiosceinces. Data was analysized using the ΔΔCt method with GADPH as a housekeeping gene, normalised to time at 0 hours Individual PCR experiments were conducted with a minimum of two biological replicates, in triplicate.

3.4 Reference

1. Panter, G.; Kuznik, A.; Jerala, R., Therapeutic applications of nucleic acids as ligands for Toll-like receptors. *Curr. Opin. Mol. Ther.* **2009,** *11* (2), 133-45.
2. Barrat, F. J.; Meeker, T.; Gregorio, J.; Chan, J. H.; Uematsu, S.; Akira, S.; Chang, B.; Duramad, O.; Coffman, R. L., Nucleic acids of mammalian origin can act as endogenous ligands for Toll-like receptors and may promote systemic lupus erythematosus. *J. Exp. Med.* **2005,** *202* (8), 1131-9.
3. Marshak-Rothstein, A., Toll-like receptors in systemic autoimmune disease. *Nat. Rev. Immunol.* **2006,** *6* (11), 823-35.
4. Kuznik, A.; Bencina, M.; Svajger, U.; Jeras, M.; Rozman, B.; Jerala, R., Mechanism of endosomal TLR inhibition by antimalarial drugs and imidazoquinolines. *J. Immunol.* **2011,** *186* (8), 4794-804.
5. Yin, S.; Gao, B., Toll-like receptor 3 in liver diseases. *Gastroenterol. Res. Pract.* **2010,** *2010*.
6. Tanaka, H.; Imaizumi, T., Inflammatory Chemokine Expression via Toll-Like Receptor 3 Signaling in Normal Human Mesangial Cells. *Clin. Dev. Immunol.* **2013,** *2013*, 984708.
7. Sun, S.; Rao, N. L.; Venable, J.; Thurmond, R.; Karlsson, L., TLR7/9 antagonists as therapeutics for immune-mediated inflammatory disorders. *Inflammation & allergy drug targets* **2007,** *6* (4), 223-35.
8. Janke, M.; Poth, J.; Wimmenauer, V.; Giese, T.; Coch, C.; Barchet, W.; Schlee, M.; Hartmann, G., Selective and direct activation of human neutrophils but not eosinophils by Toll-like receptor 8. *J. Allergy Clin. Immunol.* **2009,** *123* (5), 1026-33.
9. Forsbach, A.; Nemorin, J. G.; Montino, C.; Muller, C.; Samulowitz, U.; Vicari, A. P.; Jurk, M.; Mutwiri, G. K.; Krieg, A. M.; Lipford, G. B.; Vollmer, J., Identification of RNA sequence motifs stimulating sequence-specific TLR8-dependent immune responses. *J. Immunol.* **2008,** *180* (6), 3729-38.

10. Sarvestani, S. T.; Williams, B. R.; Gantier, M. P., Human Toll-like receptor 8 can be cool too: implications for foreign RNA sensing. *J. Interferon Cytokine Res.* **2012,** *32* (8), 350-61.
11. Tanji, H.; Ohto, U.; Shibata, T.; Miyake, K.; Shimizu, T., Structural reorganization of the Toll-like receptor 8 dimer induced by agonistic ligands. *Science* **2013,** *339* (6126), 1426-9.
12. Guiducci, C.; Gong, M.; Cepika, A. M.; Xu, Z.; Tripodo, C.; Bennett, L.; Crain, C.; Quartier, P.; Cush, J. J.; Pascual, V.; Coffman, R. L.; Barrat, F. J., RNA recognition by human TLR8 can lead to autoimmune inflammation. *J. Exp. Med.* **2013,** *210* (13), 2903-19.
13. Sacre, S. M.; Lo, A.; Gregory, B.; Simmonds, R. E.; Williams, L.; Feldmann, M.; Brennan, F. M.; Foxwell, B. M., Inhibitors of TLR8 reduce TNF production from human rheumatoid synovial membrane cultures. *J. Immunol.* **2008,** *181* (11), 8002-9.
14. Doring, Y.; Hurst, J.; Lorenz, M.; Prinz, N.; Clemens, N.; Drechsler, M. D.; Bauer, S.; Chapman, J.; Shoenfeld, Y.; Blank, M.; Lackner, K. J.; von Landenberg, P., Human antiphospholipid antibodies induce TNFalpha in monocytes via Toll-like receptor 8. *Immunobiology* **2010,** *215* (3), 230-41.
15. Prinz, N.; Clemens, N.; Strand, D.; Putz, I.; Lorenz, M.; Daiber, A.; Stein, P.; Degreif, A.; Radsak, M.; Schild, H.; Bauer, S.; von Landenberg, P.; Lackner, K. J., Antiphospholipid antibodies induce translocation of TLR7 and TLR8 to the endosome in human monocytes and plasmacytoid dendritic cells. *Blood* **2011,** *118* (8), 2322-32.
16. Lipinski, C. A.; Lombardo, F.; Dominy, B. W.; Feeney, P. J., Experimental and computational approaches to estimate solubility and permeability in drug discovery and development settings. *Adv. Drug Deliv. Rev.* **2001,** *46* (1-3), 3-26.
17. Zhu, W.; Ou, Y.; Li, Y.; Xiao, R.; Shu, M.; Zhou, Y.; Xie, J.; He, S.; Qiu, P.; Yan, G., A small-molecule triptolide suppresses angiogenesis and invasion of human anaplastic thyroid carcinoma cells via down-regulation of the nuclear factor-kappa B pathway. *Mol. Pharmacol.* **2009,** *75* (4), 812-9.
18. Zhang, J. H.; Chung, T. D.; Oldenburg, K. R., A Simple Statistical Parameter for Use in Evaluation and Validation of High Throughput Screening Assays. *J. Biomol. Screening* **1999,** *4* (2), 67-73.
19. Dowling, J. E.; Alimzhanov, M.; Bao, L.; Block, M. H.; Chuaqui, C.; Cooke, E. L.; Denz, C. R.; Hird, A.; Huang, S.; Larsen, N. A.; Peng, B.; Pontz, T. W.; Rivard-Costa, C.; Saeh, J. C.; Thakur, K.; Ye, Q.; Zhang, T.; Lyne, P. D., Structure and Property Based Design of Pyrazolo[1,5-a]pyrimidine Inhibitors of CK2 Kinase with Activity in Vivo. *ACS Med. Chem. Lett.* **2013,** *4* (8), 800-5.
20. Wang, X.; Magnuson, S.; Pastor, R.; Fan, E.; Hu, H.; Tsui, V.; Deng, W.; Murray, J.; Steffek, M.; Wallweber, H.; Moffat, J.; Drummond, J.; Chan, G.; Harstad, E.; Ebens, A. J., Discovery of novel pyrazolo[1,5-a]pyrimidines as potent pan-Pim inhibitors by structure- and property-based drug design. *Bioorg. Med. Chem. Lett.* **2013,** *23* (11), 3149-53.

21. Almansa, C.; de Arriba, A. F.; Cavalcanti, F. L.; Gomez, L. A.; Miralles, A.; Merlos, M.; Garcia-Rafanell, J.; Forn, J., Synthesis and SAR of a new series of COX-2-selective inhibitors: pyrazolo[1,5-a]pyrimidines. *J. Med. Chem*. **2001,** *44* (3), 350-61.
22. Sharma, V.; Kumar, P.; Pathak, D., Biological importance of the indole nucleus in recent years: A comprehensive review. *J. Heterocycl. Chem*. **2010,** *47* (3), 491-502.
23. Russo, C.; Cornella-Taracido, I.; Galli-Stampino, L.; Jain, R.; Harrington, E.; Isome, Y.; Tavarini, S.; Sammicheli, C.; Nuti, S.; Mbow, M. L.; Valiante, N. M.; Tallarico, J.; De Gregorio, E.; Soldaini, E., Small molecule Toll-like receptor 7 agonists localize to the MHC class II loading compartment of human plasmacytoid dendritic cells. *Blood* **2011,** *117* (21), 5683-91.

CHAPTER 4

Identification of TLR5 signaling agonists and antagonists

4.1 Introduction

Toll-like receptors play an important role in the early recognition of invading microbial pathogens and the activation of subsequent immune responses against them. Individual TLRs recognize distinct PAMPs, initiating signaling cascades that promote the immune response. Pathogen-encoded TLR ligands are divided into three broad categories: lipids and lipopeptides (TLR1/2, TLR4 and TLR2/6), proteins (TLR5, TLR11), and nucleic acids (TLR3, TLR7, TLR8 and TLR9). Upon activation by PAMPs, TLRs initiate a cascade of intracellular signaling pathways in innate immune cells, leading to the induction of inflammatory and innate immune responses, which in turn stimulate the development of long lasting adaptive responses to eliminate the pathogens. Regarding the crucial role of TLRs in activation of innate immunity and initiation of inflammatory responses, both TLR agonists and antagonists are considered as effective immune regulators, suggesting that these reagents have potential therapeutic values in inflammatory diseases and cancers.

TLR5, one member of the TLR family, is localized at the plasma membrane. It is mainly expressed on antigen presenting cells (APCs), as well as on normal epithelia and various cancer cells. TLR5 recognizes flagellin, the protein component of bacterial flagella expressed by Gram-positive and Gram-negative bacteria

including *Salmonella*, *Listeria*, and *Peseudomonas*.[1] TLR5 signaling involves a MyD88-dependent cascade that induces NF-κB activation, proinflammatory cytokine production, and increased co-stimulatory molecules on APCs.

Numerous studies have shown that TLR5 is a potential therapeutic target due to its important role in multiple inflammatory diseases and cancer. It is reported that flagellin induced TLR5 signaling in breast cancer cells inhibits cell proliferation and anchorage-independent growth, and thus provides antitumor activity.[2] This suggests a TLR5 agonist has the potential to be used as an effective adjuvant for vaccines and for cancer radiotherapy. Entolimod (known as CBLB502), a highly purified cGMP grade flagellin variant, is a potent TLR5 agonist currently under development as both a radiation countermeasure and an anticancer agent.[3] TLR5 agonists can also be used in the treatment of degenerative diseases and myocardial infarction.[4]

The activation of TLR5 has also been found to have negative effects on certain inflammatory diseases. Shiva Shahrara and her colleagues found that activation of TLR5 causes abnormal blood vessel formation in the joints of rheumatoid arthritis patients, recruits circulating myeloid cells into the joint, and further facilitates their differentiation into mature osteoclasts.[5,6] It has also been demonstrated that TLR5 plays a quintessential role in microbial recognition in intestinal epithelial cells. Disregulation of TLR5 signaling leads to intestinal inflammation through excess recognition of flagellin. Significantly elevated flagellin levels were observed in the serum samples of patients with Crohn's disease.[7]

Taken together, both selective TLR5 agonists and antagonists have therapeutic potential for cancer and inflammatory diseases. To date, no small molecule agonists or antagonists have been discovered specifically for TLR5 signaling. Owing to the fact that targeting protein-protein interactions with small molecules is challenging, we performed both cell-based high-throughput screening

and *in silico* screening to discover agonists and antagonists of TLR5 signaling. In this chapter, cell-based HTS and virtual screening studies aimed at identifying TLR5 agonists and antagonists are presented. Only one potential inhibitor from cell-based HTS showed inhibition of TLR5 induced NF-κB activation suggesting it is worthy of further evaluation.

4.2 *In silico* screening for TLR5-Flagellin inhibitor

4.2.1 Glide software

Schrödinger's Glide (Grid-Based Ligand Docking with Energetics) is currently one of the most successful and widely used molecular docking program.[8] It is designed to investigate the multiple conformations of a ligand, identify conformations best matching the receptor binding site, and rank-order them with a parameterized scoring function. This makes it an efficient way to screen large-scale virtual compound libraries by docking flexible ligands to a rigid receptor. Glide is designed to perform an exhaustive search of the positional, orientational, and conformational space for the ligand in the protein active site.[9] The software provides three different levels of docking procedure: HTVS (high-throughput virtual screening) mode for efficiently enriching large million-compound libraries, SP (standard precision) mode for reliably docking tens to hundreds of thousands of ligands with high accuracy, and XP (extra precision) mode for further elimination of false positives by more extensive sampling and advanced scoring.

4.2.2 Protein and Grid preparation

The crystal structure of the zebrafish TLR5-*Samonella* flagellin complex, known as 3V47, was retrieved from the Protein Data Bank (PDB). The complex consists of two copies of the 1:1 sTLR5-flagellin complex; only one copy was retained for further process. The protein is prepared using the Schrödinger protein preparation wizard by adding missing hydrogen, assigning proper bond orders and deleting water and sulphate molecules. Finally the protein structure was minimized to the default root mean square deviation (RMSD) value of 0.30 Å. Then a 20 × 20 Å grid was defined that covers all the important residues located on the Flic-TLR5 major binding site (**Figure 4-1A**). Van der Waals radii were not scaled in the receptor grid generation. Following the grid generation, the flagellin protein was removed from the binding groove.

4.2.3 Ligand library preparation

The Enamine library, which includs 1.3 million small-molecule compounds, was processed with the Schrödinger LigPrep wizard to assign the appropriate protonation states at physiological pH=7.2 ± 0.2 and the conformation generation was carried out using the Optimization Potential for Ligand Simulation 2005 (OPLS_2005) force field. Finally, 10 conformations for each ligand were generated and ready for docking.

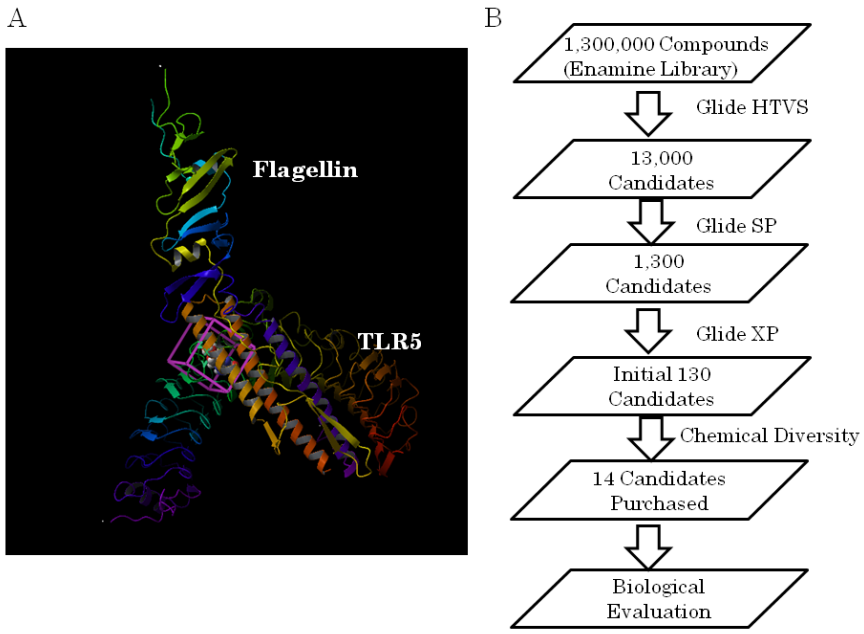

Figure 4-1. Schematic depiction of HTVS procedure: A) Simulation Region in TLR5 and Flagellin binding site highlighted by the magenta box; B) Schematic representation of the HTVS.

4.2.4 Virtual screening of Enamine library

The prepared Enamine library was subjected to Glide docking. Since each compound has 10 conformations, each conformation was first screened through Glide's HTVS mode, from which the top 10% were subjected to the Glide SP mode. The top 10% outcomes from SP were redocked using Glide XP for higher precision. Finally, we selected the ligands ranked in the top 10% according to the predicted binding energy (Glide score) for further evaluation (**Figure 4-1B**).

The selection of the candidate molecules was based on the following criteria: 1) predicted binding energy value and favorable spatial complementarity; 2) reasonable chemical structure, acceptable protonated state and tautomeric form; 3)

existence of at least one hydrogen bond between the compound and one of the Flagellin binding residues on the TLR5 surface (eg. Tyr267, Gly270 and Ser271); 4) consideration of both scaffold structural diversity and the compounds with the same core scaffold. As a result, 17 out of 130 compounds were selected and purchased from Enamine for biological evaluation (**Figure 4-2**).

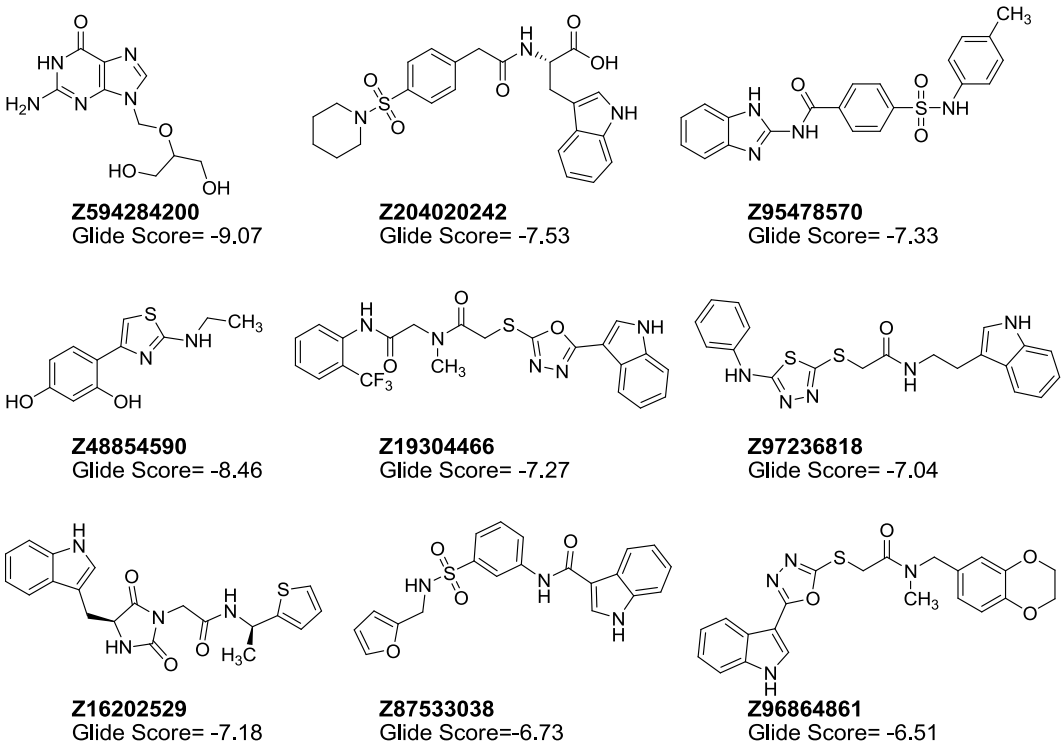

Figure 4-2. Chemical structures and the Glide scores of representative hit compounds.

4.2.5 Validation through biochemical assays: inhibition, toxicity and specificity studies

These initial 17 hits were first evaluated using previously established cell-based assay that monitor TLR5 activation. Flagellin from *B. subtilis*, was employed to selectively activate TLR5 signaling, resulting in the activation of NF-κB in TLR5

overexpressing HEK-Blue cells. We monitored the SEAP level as an indicator of Flagellin-induced TLR5 activation to evaluate the compounds' inhibitory activity. The compounds with inhibitory activity on TLR5 signaling were further tested for their cytotoxic effect on the HEK-Blue TLR5 cells using WST-1 assay. To our great disappointment, most compounds when tested in cell-based assays showed no or low inhibition of TLR5-induced SEAP activity even up to 50 μM. Only 5 inhibitors showed any inhibition of NF-κB in a dose-responsive manner. But the toxicity assay revealed that inhibitory activities observed for the 5 compounds were due solely to toxic effects. We decided to abandon this method to identify TLR5 inhibitors, and instead planned to perform an unbiased cell-based screening.

In conclusion, the *in silico* screening method failed to identify potent small molecules targeting the TLR5-Flagellin binding site. There are several possible reasons for the failure. First, while the compounds showed good predicted binding energy to the TLR5 protein, docking does not eliminate the possibility that small molecules might have multiple targets or exhibit cytotoxicity *in vivo*. This is also considered as the major disadvantage of *in silico* screening methods. Secondly, the zebrafish TLR5 crystal structure was used for the *in silico* docking study (human TLR5 crystal structure has not been solved yet), but the human TLR5 signaling pathway was employed for hits validation. Although the TLR5 protein is conserved in vertebrates from fish to mammals, the differences in the Flagellin binding site on the protein might still exist.

4.3 Cell-based high throughput screening for agonists and antagonists of TLR5 signaling

As previously described in Chapter 3, the SEAP assay using TLR expressed HEK-Blue cells is a robust assay for HTS. The TLR5 agonist and antagonist screenings were implemented using a stable HEK-Blue cell line that expressed TLR5. In the TLR5 agonist screening, flagellin (50 ng/mL) was used as positive control, and 0.4% DMSO (final concentration) served as negative control. For the TLR5 antagonist screening, triptolide (20 nM) was used for positive control, and 0.4% DMSO served as negative control. The Z' factor for the HTS assay (used to measure SEAP levels in HEK-Blue TLR5 cells) in a 384-well plate format was 0.68, indicating that the assay is ready for HTS. The Maybridge Hitfinder library was used for both agonist and antagonist screenings.

4.3.1 TLR5 agonist screening result

In the primary HTS, compounds were identified as active if they increase the SEAP levels as indicated by an increase in absorbance at 600 nm. The positive control flagellin increased the SEAP level by 30-fold on average and was used to perform the data analysis. The data for each library compound was converted into a root mean square (RMS) value, and the Z-score of each library compound was calculated based on the distribution of the RMS (**Figure 4-3**). We performed hit selection based on the rank of the compounds' Z-scores. The top 60 compounds in the Z-score ranking were considered hits and chosen for confirmation in further studies.

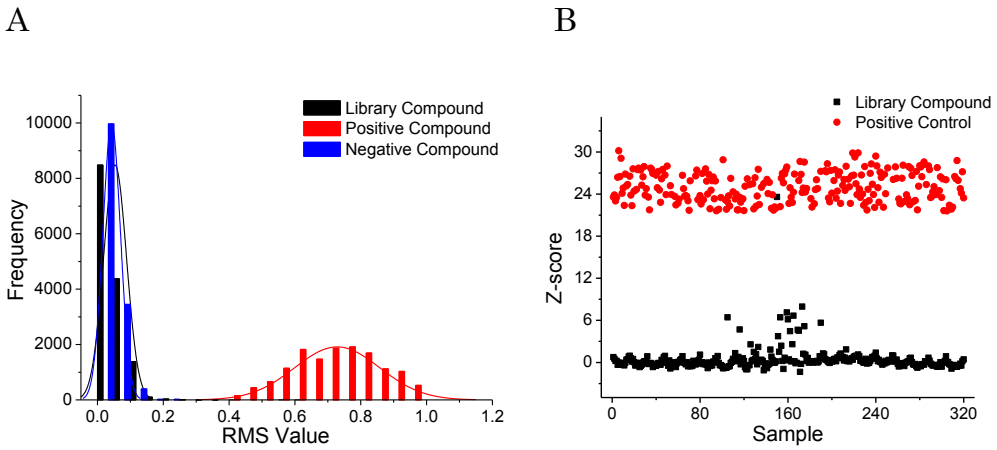

Figure 4-3. TLR5 agonist screening results: A) Gaussian distribution of the screening results; B) Z-score from a representative plate is shown for both library compounds and positive control.

As this was the first time that the HTS SEAP assay was employed in our lab for identification of TLR agonists and antagonists, there was no prior screening data available for comparison. Therefore, all 60 compounds were manually picked from the original 10 mM library for further 3-dose (4, 8, and 16 μM) testing of hit confirmation, specificity and toxicity. Of the 60 compounds tested, 55 compounds were inactive. Only 5 compounds displayed NF-κB activation at 16 μM in HEK-Blue TLR5 cells. However the activation potency of these five compounds was significantly lower than flagellin. The result of the toxicity assay revealed that all five compounds showed obvious toxic effects at 20 μM, which means the observed NF-κB activation might due to toxicity-induced cell stress response.

In summary, no potential TLR5 agonist was identified from the Maybridge library screening. This result is consistent with a recent TLR2 agonists screening in our laboratory using the same Maybridge library. A possible cause for the failure is that TLR5 recognizes bacteria flagellin and the polypeptide Entolimod, which causes dimerization and initiates the signaling cascade. Compared to a 30-60 kD protein, it might be challenging for a small molecule to induce the TLR5

dimerization. Therefore, a larger small molecule library or peptide library might be needed for TLR5 agonist identification.

4.3.2 TLR5 antagonist screening result

In the primary HTS, compounds were identified as active if they decrease the SEAP levels, as indicated by a decrease in absorbance at 600 nm. The positive control, triptolide, decreased flagellin induced SEAP level by 90% at 25 nM and was used to perform the data analysis. The top 60 compounds based on Z-score rankings were considered hits and chosen for confirmation in further studies (**Figure 4-4**).

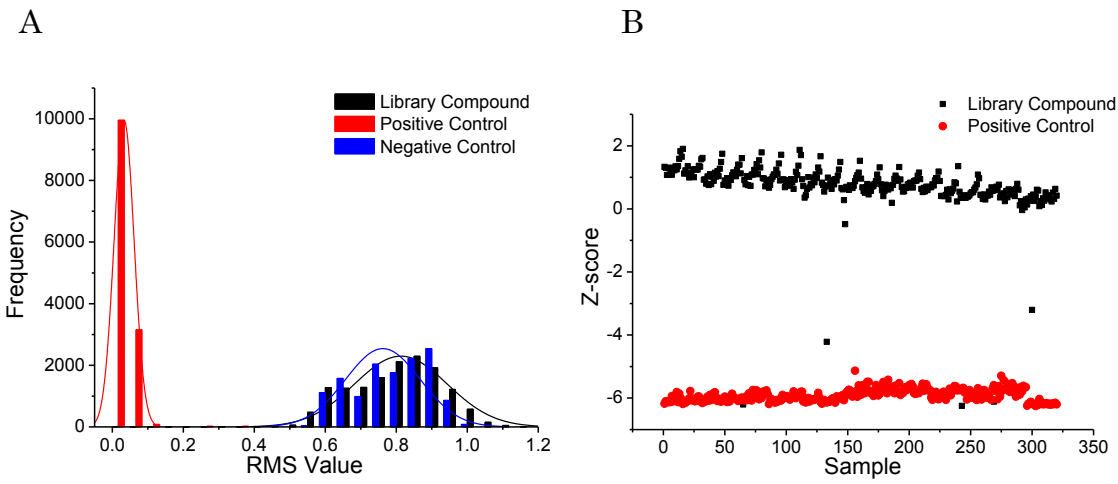

Figure 4-4. TLR5 antagonist screening results: A) Gaussian distribution of the screening results; B) Z-score from a representative plate is shown for both library compounds and positive control.

The 60 compounds from the original 10 mM library were subjected to further 3-dose (4, 8, and 16 μM) testing of hit confirmation and toxicity. Fifty-seven out of 60 were inactive or exhibited cytotoxicity in the validation process. Only three compounds displayed NF-κB inhibition without an obvious toxicity effect. Then we purchased these three compounds from Maybridge for further evaluation using 1)

inhibition of TLR5 induced NF-κB in HEK-Blue TLR5 cells, 2) toxicity effects and 3) pathway specificity. All three purchased compounds showed toxic effects at 8 μM. The data from assays performed using the original the 10 mM library was significantly different from those obtained from the freshly prepared compound solution. These inconsistencies might be due to multiple freeze-thaw cycles that further diluted the compound we picked from the 10 mM compound library.

The TLR5 inhibitor screening data were compared with those obtained from a later obtained from a TLR8 inhibitor screening. By comparing the results of the TLR5 inhibitor screening to similar screenings performed using TLR8 receptors, most of the non-specific and toxic inhibitors were eliminated. By lowering the hit-threshold, 28 compounds were selected as potential hits that inhibit TLR5 singling but did not affect TLR8 signaling. Then these 28 compounds were picked from the 10 mM compound library for further validation. Because of the low threshold, most compounds did not show inhibitory activity on TLR5 signaling up to 8 μM. Only two compounds, **157-H7** and **167-B2** exhibited inhibitory active with estimated IC_{50}s lower than 10 μM and no observable toxicity problem. These two compounds were subjected to further selectivity tests in various HEK-Blue TLR cells. The preliminary results showed that at 16 μM, **167-B2** inhibited TLR8, TLR5 and TLR2 signaling, whereas **157-H7** only specifically inhibited TLR5 signaling and did not affect other TLR signaling (**Figure 4-5**), suggesting that **157-H7** is TLR5 specific. Due to the inconsistency problem we have met before, further evaluation of the purchased **157-H7** is ongoing.

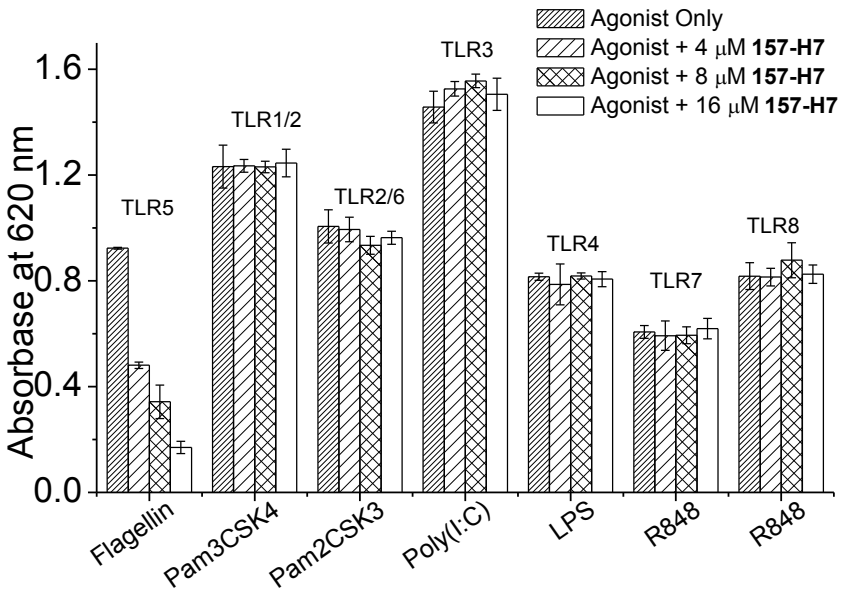

Figure 4-5. Preliminary result of specificity test for **157-H7** with specific agonists used to selectively activate HEK-Blue TLR cells.

4.4 Reference

1. Letran, S. E.; Lee, S. J.; Atif, S. M.; Uematsu, S.; Akira, S.; McSorley, S. J., TLR5 functions as an endocytic receptor to enhance flagellin-specific adaptive immunity. *Eur. J. Immunol.* **2011,** *41* (1), 29-38.
2. Cai, Z.; Sanchez, A.; Shi, Z.; Zhang, T.; Liu, M.; Zhang, D., Activation of Toll-like receptor 5 on breast cancer cells by flagellin suppresses cell proliferation and tumor growth. *Cancer Res.* **2011,** *71* (7), 2466-75.
3. Kojouharov, B. M.; Brackett, C. M.; Veith, J. M.; Johnson, C. P.; Gitlin, II; Toshkov, I. A.; Gleiberman, A. S.; Gudkov, A. V.; Burdelya, L. G., Toll-like receptor-5 agonist Entolimod broadens the therapeutic window of 5-fluorouracil by reducing its toxicity to normal tissues in mice. *Oncotarget* **2014,** *5* (3), 802-14.
4. Savva, A.; Roger, T., Targeting toll-like receptors: promising therapeutic strategies for the management of sepsis-associated pathology and infectious diseases. *Front.in Immunol.* **2013,** *4*, 387.
5. Kim, S. J.; Chen, Z.; Chamberlain, N. D.; Essani, A. B.; Volin, M. V.; Amin, M. A.; Volkov, S.; Gravallese, E. M.; Arami, S.; Swedler, W.; Lane, N. E.; Mehta, A.; Sweiss, N.; Shahrara, S., Ligation of TLR5 Promotes Myeloid Cell Infiltration and Differentiation into Mature Osteoclasts in Rheumatoid Arthritis and Experimental Arthritis. *J. Immunol.* **2014,** *193* (8), 3902-13.
6. Chamberlain, N. D.; Vila, O. M.; Volin, M. V.; Volkov, S.; Pope, R. M.; Swedler, W.; Mandelin, A. M., 2nd; Shahrara, S., TLR5, a novel and unidentified

inflammatory mediator in rheumatoid arthritis that correlates with disease activity score and joint TNF-alpha levels. *J. Immunol.* **2012,** *189* (1), 475-83.
7. Sitaraman, S. V.; Klapproth, J. M.; Moore, D. A., 3rd; Landers, C.; Targan, S.; Williams, I. R.; Gewirtz, A. T., Elevated flagellin-specific immunoglobulins in Crohn's disease. *Am. J. Physiol.* **2005,** *288* (2), G403-6.
8. Li, Y. Z.; Shen, J.; Sun, X. G.; Li, W. H.; Liu, G. X.; Tang, Y., Accuracy Assessment of Protein-Based Docking Programs against RNA Targets. *J. Chem. Inf. Model* **2010,** *50* (6), 1134-1146.
9. Friesner, R. A.; Banks, J. L.; Murphy, R. B.; Halgren, T. A.; Klicic, J. J.; Mainz, D. T.; Repasky, M. P.; Knoll, E. H.; Shelley, M.; Perry, J. K.; Shaw, D. E.; Francis, P.; Shenkin, P. S., Glide: a new approach for rapid, accurate docking and scoring. 1. Method and assessment of docking accuracy. *J. Med. Chem.* **2004,** *47* (7), 1739-49.

CHAPTER 5

General conclusions and future prospects

5.1 Conclusions

Toll-like receptors are pattern recognition receptors that play crucial roles in innate immunity, by detecting and responding to pathogens. The significance of TLRs action is emphasized by the fact that any deviation from their normal modus operandi can result in inflammatory diseases and cancer. Both TLR agonists and antagonists have potential therapeutic value in the treatment of innate immunity associated diseases. For the past few years, our laboratory has been involved in efforts aimed at identifying and characterizing new small molecule inhibitors and activators of distinct TLR signaling.[1-3] These inhibitors and activators could serve as starting points for the development of therapeutic drugs and additionally be useful as probes to improve the understanding of TLR signaling. This dissertation focused on the development of novel small molecule agents for TLR signaling by using moderate to high throughput screening methods. A structure-activity based approach was utilized, mainly centering on hits **NCI126224** (targets TLR4 signaling) and **40-D4** (targets TLR8 signaling). Further mechanistic studies were

performed to better understand the 'lead' compounds we identified. This chapter will summarize the major findings of the dissertation, and explore future research directions.

High-throughput screening

In this work, both *in silico* and cell-base screening approaches were performed to identify distinct TLR agonists and antagonist. Both approaches possess benefits and limitations. *In silico* screening is an efficient and more economic way to screen millions of compounds on a particular protein. The limitations are the desired effects of the hits might not be observed in the *in vivo* test, or the hits might have off-target or toxic effects. The biggest advantage of cell-base screen is the ability to perform pathway and phenotypic screens; the results could have a broad range of applications in solving greater biological questions. However, false positive rates are higher, due to off-target effects, and need further validation.[4] The results in this thesis suggest that compared to an *in silico* screen, cell-based screen is a more effective way to identify agents that targeting TLR.

Cell-based HTS is a straightforward, repetitive procedure once the steps for the screening are well developed. However, it requires a fair amount of initial work before a fully feasible screen is ready to launch. Every step in the screen was carefully planned and multiple times of test, and a pilot screen were performed prior to the full screen. The first two screens we did were aimed towards the discovery of TLR5 agonists and antagonists. The SEAP assay had a decent Z'-factor

value of 0.68, which makes it a very robust assay for HTS. The screens were performed using 4 μM of the screening compound from the Maybridge Hitfinder library (14,400 compounds). After the primary screens, 60 compounds for each screen were considered hits (hit rate is 0.42%) and were picked for validation. This seemed to be an acceptable hit rate until all 120 compounds failed to duplicate the desired activities on TLR5 signaling due to toxicity problems. This experience highlights that the major drawback of the screen was the high incidence of false-positives from cytotoxic chemicals. It would have been advantageous to perform multiple TLR screens using the same library and comparing the results. By comparing the results of different screenings, we would be weed out compounds with toxicity observed across all TLRs and it would also provide some information about the compounds' specificity.

HTS for TLR8 signaling inhibitor was performed using the same Maybridge Hitfinder library. This time we compared the results with the TLR5 inhibitor screen data and ruled out the false-positives and non-specific compounds. After further validation, 13 potential hits were found to exhibit specific inhibitory activities against TLR8 signaling. Additionally, we reexamined the TLR5 inhibitor HTS data. By comparing the TLR8 HTS data and lowering the hit-threshold, 28 more compounds were picked for validation, and 1 potential TLR5 inhibitor was identified.

TLR4 inhibitors

Chapter 2 of this thesis presents the identification of a group of new TLR4 signaling inhibitors by screening an NCI chemical library. The objective of the screening was to identify potent TLR4 antagonists. The screen of 1,368 compounds identified only one TLR4 inhibitor, **NCI126224**. Structure-activity relationship studies were performed on the initial hit 2-(2-nitrobenzylidene) malonate (**NCI126224**) to identify the key components of the structure and improve the potency. Therefore, a series of TLR4 inhibitors derived from arylidene malontates were synthesized and their effects were assessed on TLR4-mediated NO production in RAW 264.7 cells. The result of the SAR studies revealed that small modifications of the arylidene malontate core significantly affected its inhibitory potency, and suggesting a near optimal recognition of its potential target. Further biological evaluation indicates that **NCI126224** suppressed LPS-induced NF-κB activation and the cytokine production of IL-1ß and TNF-α. A possible mechanism of **NCI126224** targeting the TLR4-MD-2 interface was also proposed.

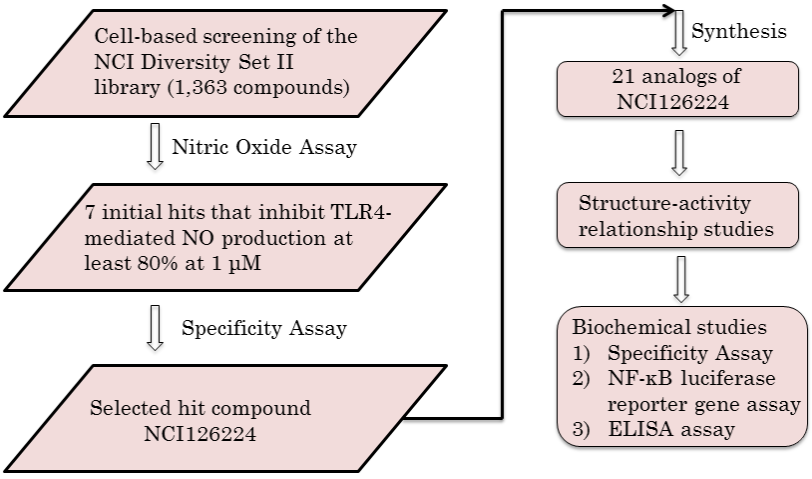

Figure 5-1. Flow chart illustrating identification of TLR4 signaling inhibitors.

TLR8 inhibitors

Thirteen potential TLR8 inhibitors were identified through high throughput screening of the Maybridge Hitfinder library, with some of the hits containing same scaffold. My work mainly focused on SAR investigation and biological evaluation of pyrazolo[1,5-*a*]pyrimidine scaffold. Through the systematic SAR studies, I have been able to synthesize two compounds with improved TLR8 signaling inhibitory activity when compared to the original hit compound **40-D4**. We have made a series of small molecules analogs which are systematically varied in 3 specified regions of **40-D4** structure individually, the pyrazolo[1,5-*a*]pyrimidine core, the substititution on the 3-position phenyl group, and bioisosteric replacement of functional groups at 3-position. We found that modifications to the substituent on the phenyl ring is well tolerated, however, the smaller substituent on the *meta*-position of the phenyl is the most favored. Different substitution positions on the pyrazolo[1,5-*a*]pyrimidine core and replacement of pyrazolo[1,5-*a*]pyrimidine with an indole moiety essentially abolished activity. Additionally, we found that modification of the primary amide to an ethyl ester is tolerated. Two compounds, **8m** and **4m**, show increased TLR8 singling inhibition when compared to **40-D4** with nanomolar potencies. Further biological evaluation indicates that **8m** specifically inhibits TLR8 signaling without affecting other TLRs. **8m** also suppresses TLR8 induced proinflammatory cytokine and cytokine mRNA levels. These finding suggests that these compounds may have therapeutic application in the treatment of TLR8 related inflammatory diseases.

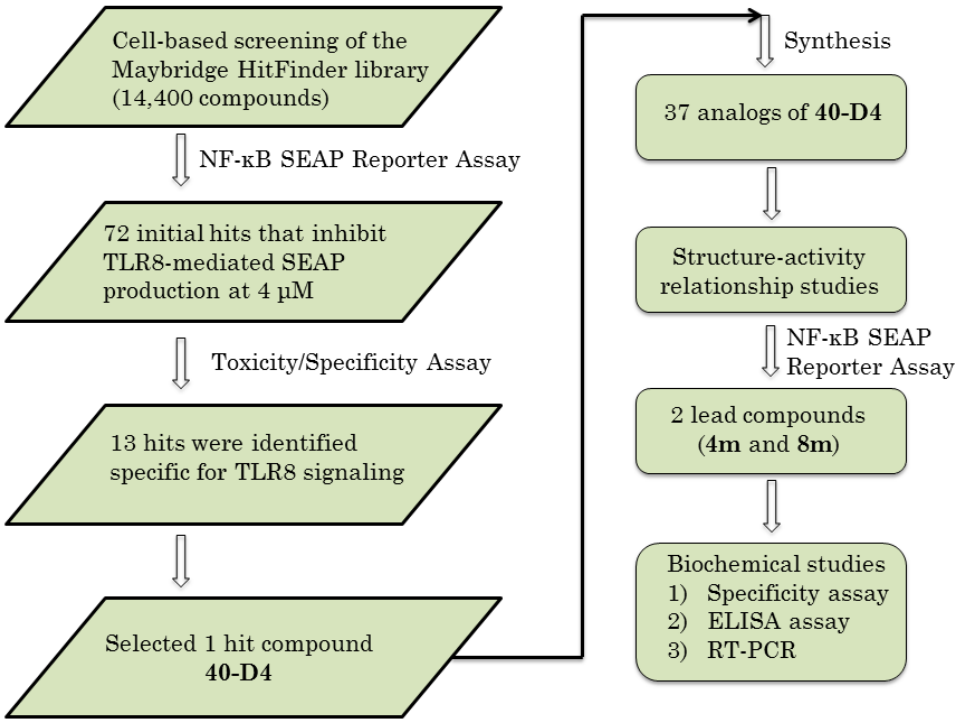

Figure 5-2. Flow chart illustrating the identification of TLR8 signaling inhibitors.

5.2 Future Directions

Based on the findings in this thesis, recommendations for future study are listed below.

1) The human TLR family contains 13 members. Some of them share the same adaptor proteins and downstream signaling pathway. Therefore, from a therapeutic and mechanistic point of view, it is important for an inhibitor to exhibit specificity in binding a distinct TLR without affecting the other TLRs. The present study supported the notation that **8m** is a specific inhibitor of TLR8 signaling, based on the cell-based assays described. It remains unclear whether **8m** directly bind to TLR8. The protein target of **8m** needs to be determined by biophysical assays. So the future direction of this project

should be focused on the identification of the inhibitors' target. A fluorophore labeled R848 (TAMRA-R848) has been synthesized and characterized for the purpose of an FP protein binding assay. It is also reported that short synthetic single-stranded Uracil-rich RNAs are effective TLR8 agonists.[5-6] An alternative plan is to use a fluorophore labeled, Uracil-rich RNA sequence as an agonist, in the competitive binding study of **8m** to TLR8 protein. The result of this study would provide more insight into the role of this inhibitor in TLR8 signaling. The microscale thermophresis and pull-down assays are also options for the target identification of **8m**.

2) Ideally, if the biophysical assays proved that **8m** binds to TLR8 protein, the co-crystallization of **8m** with TLR8 would be the next endeavor. This could be achieved through collaboration with the Shimizu group (solved the unliganded and liganded forms of TLR8 structures).[7] The co-crystal structure might provide more information about the binding interactions between the TLR8 and **8m**. More potent compounds might emerge from structure-based optimization. Another thing we need keep in mind is that R848 is an unnatural ligand for TLR8 signaling; the mechanisms of viral RNA recognition and R848 by TLR8 might be different. The *in vivo* therapeutic effectiveness of **8m** (or the best compound to emerge from optimization) has to be determined before we can ascertain that it has potential for use in human therapy. In other words, we will need to show that the efficacy of **8m**

against viral RNA-induced TLR8 activity is as good as R848-induced TLR8 activity.

3) This study also identified a potential TLR5 signaling inhibitor, **157-H7**. Future efforts on this project should be focused on the validation of potency and specificity. Then, SAR analysis can be performed to provide guidance for the design of more potent analogs. Further biological evaluation will be performed after the lead compound identified.

5.3 Reference

1. Cheng, K.; Wang, X.; Zhang, S.; Yin, H., Discovery of small-molecule inhibitors of the TLR1/TLR2 complex. *Angew. Chem.* **2012,** *51* (49), 12246-9.
2. Cheng, K.; Wang, X.; Yin, H., Small-molecule inhibitors of the TLR3/dsRNA complex. *J. Am. Chem. Soc.* **2011,** *133* (11), 3764-7.
3. Chavez, S. A.; Martinko, A. J.; Lau, C.; Pham, M. N.; Cheng, K.; Bevan, D. E.; Mollnes, T. E.; Yin, H., Development of beta-amino alcohol derivatives that inhibit Toll-like receptor 4 mediated inflammatory response as potential antiseptics. *J. Med. Chem.* **2011,** *54* (13), 4659-69.
4. Zaman, G. J., Cell-based screening. *Chem. High Throughput Screening* **2008,** *11* (7), 494.
5. Lan, T.; Kandimalla, E. R.; Yu, D.; Bhagat, L.; Li, Y. K.; Wang, D. Q.; Zhu, F. G.; Tang, J. X.; Putta, M. R.; Cong, Y. P.; Trombino, A. F.; Sullivan, T.; Agrawal, S., Stabilized immune modulatory RNA compounds as agonists of Toll-like receptors 7 and 8. *Proc. Natl. Acad. Sci. U. S. A.* **2007,** *104* (34), 13750-13755.
6. Bernard, M. A.; Han, X. B.; Inderbitzin, S.; Agbim, I.; Zhao, H.; Koziel, H.; Tachado, S. D., HIV-Derived ssRNA Binds to TLR8 to Induce Inflammation-Driven Macrophage Foam Cell Formation. *PloS one* **2014,** *9* (8).
7. Tanji, H.; Ohto, U.; Shibata, T.; Miyake, K.; Shimizu, T., Structural Reorganization of the Toll-Like Receptor 8 Dimer Induced by Agonistic Ligands. *Science* **2013,** *339* (6126), 1426-1429.